

การศึกษาปฏิกิริยาที่เกี่ยวข้องกับการผลิตไบโอดีเซล
โดยใช้ตัวเร่งปฏิกิริยาของแข็งที่มีความเป็นกรด



นางสาวกนกวรรณ จ้าวสุวรรณ

วิทยานิพนธ์นี้เป็นส่วนหนึ่งของการศึกษาตามหลักสูตรปริญญาวิศวกรรมศาสตรดุษฎีบัณฑิต
สาขาวิชาวิศวกรรมเคมี ภาควิชาวิศวกรรมเคมี
คณะวิศวกรรมศาสตร์ จุฬาลงกรณ์มหาวิทยาลัย

ปีการศึกษา 2552

ลิขสิทธิ์ของจุฬาลงกรณ์มหาวิทยาลัย

**STUDY OF RELATED REACTIONS FOR PRODUCTION OF
BIODIESEL USING SOLID ACID CATALYSTS**

Miss Kanokwan Ngaosuwan

A Dissertation Submitted in Partial Fulfillment of the Requirements
for the Degree of Doctor of Engineering Program in Chemical

Engineering

Department of Chemical Engineering

Faculty of Engineering

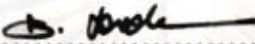
Chulalongkorn University

Academic year 2009

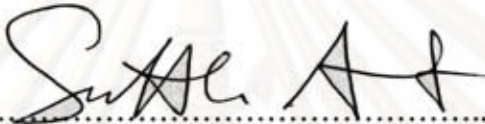
Copyright of Chulalongkorn University

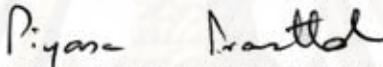
Thesis Title STUDY OF RELATED REACTIONS FOR
 PRODUCTION OF BIODIESEL USING SOLID ACID
 CATALYSTS
By Miss Kanokwan Ngaosuwan
Field of Study Chemical Engineering
Thesis Advisor Professor Piyasan Praserttham, Dr.Ing.
Thesis Co-Advisor Professor James G. Goodwin Jr., Ph.D.


Accepted by the Faculty of Engineering, Chulalongkorn University
in Partial Fulfillment of the Requirements for the Doctoral Degree

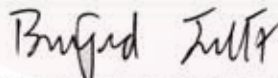
 Dean of the Faculty of Engineering
(Associate Professor Boonsom Lerthirunwong, Dr.Ing.)


THESIS COMMITTEE


 Chairman
(Professor Suttichai Assabumrungrat, Ph.D.)

 Thesis Advisor
(Professor Piyasan Praserttham, Dr.Ing.)

 Thesis Co-Advisor
(Professor James G. Goodwin Jr., Ph.D.)

 Examiner
(Associate Professor Bunjerd Jongsomjit, Ph.D.)

 Examiner
(Associate Professor Muenduen Phisalaphong, Ph.D.)

 External Examiner
(Assistant Professor Waraporn Tanakulrungsank, Ph.D.)

กนกวรรณ จ้าวสุวรรณ : การศึกษาปฏิกิริยาที่เกี่ยวข้องกับการผลิตไบโอดีเซลโดยใช้ตัวเร่งปฏิกิริยาของแข็งที่มีความเป็นกรด. (STUDY OF RELATED REACTIONS FOR PRODUCTION OF BIODIESEL USING SOLID ACID CATALYSTS) อ. ที่ปรึกษาวิทยานิพนธ์หลัก : ศาสตราจารย์ ดร. ปิยะสาร ประเสริฐธรรม อ. ที่ปรึกษาวิทยานิพนธ์ร่วม Professor James G. Goodwin Jr., Ph.D., 118 หน้า.

งานวิจัยนี้มุ่งเน้นการสร้างความรู้พื้นฐานของการใช้ตัวเร่งปฏิกิริยาวิวพิคซ์ในปฏิกิริยาที่เกี่ยวข้องกับการผลิตไบโอดีเซลเพื่อใช้ในการออกแบบตัวเร่งปฏิกิริยาที่มีประสิทธิภาพสูงและมีเสถียรภาพเพื่อให้เหมาะสมกับกระบวนการสังเคราะห์ไบโอดีเซล เริ่มจากการศึกษาการใช้ตัวเร่งปฏิกิริยาวิวพิคซ์ในปฏิกิริยาไฮโดรไลซิสของน้ำมันและไขมันในการผลิตกรดไขมันอิสระซึ่งเป็นวัตถุดิบพื้นฐานในอุตสาหกรรมโพลิเอทิลีนไกล และ การสังเคราะห์ไบโอดีเซลแบบสองขั้นตอน (ปฏิกิริยาไฮโดรไลซิส-ปฏิกิริยาเอสเทอริฟิเคชัน) โดยใช้วัตถุดิบราคาถูกซึ่งมีปริมาณกรดไขมันอิสระมากกว่าร้อยละ 5-15 ทั้งสแตบเบนเซอร์โคเนีย และ แชค-13 ใช้ในการเร่งปฏิกิริยาไฮโดรไลซิสของไตรกลีเซอไรด์ที่อุณหภูมิ 110-150 องศาเซลเซียส ในเครื่องปฏิกรณ์แบบกึ่งต่อเนื่อง โดยป้อนน้ำที่อัตราการไหลต่ำ พบว่าลักษณะของตัวเร่งปฏิกิริยามีบทบาทสำคัญต่อการเลือกเกิดผลิตภัณฑ์ ค่าพลังงานกระตุ้น และการเสื่อมสภาพของตัวเร่งปฏิกิริยา และพบว่าปฏิกิริยาไฮโดรไลซิสและปฏิกิริยาทรานเอสเทอริฟิเคชันเกิดขึ้นได้พร้อมกันสำหรับการสังเคราะห์ไบโอดีเซลที่อุณหภูมิ 110-150 องศาเซลเซียส และความดัน 120-180 psi และสามารถใช้แบบจำลองฮิลล์รีเคิลในการอธิบายกลไกการเกิดได้ทั้งปฏิกิริยาไฮโดรไลซิสและปฏิกิริยาทรานเอสเทอริฟิเคชัน โดยเริ่มจากไตรกลีเซอไรด์ที่ดูดซับบนผิวทำปฏิกิริยากับน้ำหรือเมทานอลที่อยู่ในวัฏภาคของเหลว นอกจากนี้งานวิจัยนี้ยังแสดงให้เห็นถึงบทบาทของพื้นผิวของตัวรองรับเซอร์โคเนียที่มีต่อประสิทธิภาพการเร่งปฏิกิริยา การเตรียมตัวรองรับเซอร์โคเนียแบบโซลโวลเทอรัมอลจะทำให้เกิดพันธะเซอร์โคเนียกับกลุ่มไฮดรอกซิลบนพื้นผิว เป็นผลให้เกิดเฮเทอโรโพลีเอซิดของเซอร์โคเนีย แสดงความเป็นกรดรุนแรงแบบบรอนสเตด ช่วยเพิ่มประสิทธิภาพในการเกิดปฏิกิริยาเอสเทอริฟิเคชันของกรดอะซิติก เจือจางกับเฮพทานอล

ภาควิชา..... วิศวกรรมเคมี
สาขาวิชา..... วิศวกรรมเคมี
ปีการศึกษา..... 2552

ลายมือชื่อนิสิต..... พนภรณ์ อัครสุวรรณ
ลายมือชื่ออ.ที่ปรึกษาวิทยานิพนธ์หลัก..... Jan M
ลายมือชื่อ อ.ที่ปรึกษาวิทยานิพนธ์ร่วม..... J. Goodwin

4971801021 : MAJOR CHEMICAL ENGINEERING
 KEYWORDS : BIODIESEL SYNTHESIS / HYDROLYSIS /
 TRANSESTERIFICATION / ESTERIFICATION / SOLID ACID CATALYST /
 TUNGSTATED ZIRCONIA (WZ) / SAC-13/ SOLVOTHERMAL / Zr-
 HETEROPOLYACID / BRØNTEED ACID SITES

KANOKWAN NGAOSUWAN : STUDY OF RELATED REACTIONS
 FOR PRODUCTION OF BIODIESEL USING SOLID ACID
 CATALYSTS. THESIS ADVISOR : PROFESSOR PIYASAN
 PRASERTHDAM, D.Ing., THESIS CO-ADVISOR : PROFESSOR
 JAMES G. GOODWIN Jr., Ph.D. 118 pp.

The focus of this research was to establish a better fundamental insight into heterogeneous catalysis for the reactions related to biodiesel production, in an attempt to design the catalyst systems more proficient and durable for applications concerning biodiesel synthesis. This research was to explore the viability of heterogeneous catalyzed hydrolysis of oils and fats for the synthesis of free fatty acids (FFAs), a platform reaction of the oleochemical industry and a possible reaction in a novel 2-step (hydrolysis-esterification) biodiesel synthesis process using low cost feedstocks containing > 5–15% FFAs. Using tungstated zirconia (WZ) and SAC-13 as catalysts, the hydrolysis of tricaprylin (TCp) was carried out at 110–150°C in a semi-batch reactor with continuous addition of water at low flow rates. The characteristics of the catalysts played an important role in reaction selectivity, apparent activation energy, and deactivation. Hydrolysis and transesterification are two reactions that can occur during the synthesis of biodiesel. Investigations of the mechanistic pathways in hydrolysis and transesterification were carried out at 100–130°C and 120–180 psi. Using a reaction model discrimination procedure, it was found that both hydrolysis and transesterification on WZ could be successfully described by an Eley-Rideal single site mechanism with adsorbed TCp reacting with bulk phase water or methanol. This research also proved that the surface nature of zirconia can play a crucial role in determining the catalytic activity of WZ catalysts. The solvothermal method for preparation of crystalline zirconia support can result in the formation of Zr-OH bond on its surface. These surface species, related to the Zr-heteropolyacid, act as strong Brønsted acid sites. They consequently affect the catalytic activity for esterification of dilute acetic acid and 1-heptanol.

Department : Chemical Engineering Student's Signature Kanokwan Ngaosuwana
 Field of Study : Chemical Engineering Advisor's Signature Piyasan Praserttham
 Academic Year : 2009 Co-Advisor's Signature James G. Goodwin Jr.

ACKNOWLEDGEMENTS

The author would like to express my heartfelt thanks to all those individuals whose wisdom, support, and encouragement made my journey possible. Special thanks extended to Professor Dr. Piyasan Praserttham, my advisor and Professor Dr. James G. Goodwin Jr., my co-advisor, who guided me through hurdles, and provided constant support that made my journey completed lot easier than it would have been. Despite their busy schedules, they would always find the time to discuss anything from intriguing experimental results to an issue of surviving in the scientific world. I am also grateful to thank Professor Dr. Suttichai Assabumrungrat, as a chairman, Associate Professor Dr. Muenduen Phisalaphong, Associate Professor Dr. Bunjerd Jongsomjit, and Assistant Professor Dr. Waraporn Tanakulrungsank, as the members of thesis committee.

Dr. Edgar Lotero, my academic mentor, inspired the series of experiments described in this dissertation. My deepest gratitude also goes to Dr. Xunhua Mo and Dr. Kaewta Suwannakarn who has not only been my academic mentor but also my wonderful friend. Their helpful ideas, suggestions, and discussions have significantly contributed to the remarkable success achieved in this work.

Many thanks for kind suggestions and useful help to Dr. Sujaree Kaewkun, Dr. Nattaporn Lohitharn, Miss Kittiya hongsirikarn, Dr. Monica Veca, and Dr. Dora Lopez from Clemson University and Mr. Watcharapong Khaodee, Miss Peangpit Wongmaneenil, Mr. Thongchai Glinrun, Miss Chantamanee Poonjarernsilp, and many friends in the Center of Excellence on Catalysis and Catalytic Reaction Engineering (CECC) from Chulalongkorn University who always provided the encouragement and co-operate along the thesis study.

Most of all, I would like to express my greatest gratitude to my parents and my family who always gave me suggestions, support and encouragement.

Finally, I gratefully acknowledge financial supports from the Commission on Higher Education of the Thai, Ministry of Education and U.S. Department of Agriculture and from the Animal Co-Products Research & Education Center (ACREC) at Clemson University. I also would like to thank Magnesium Electron for providing the WZ catalysts.

CONTENT

	Page
ABSTRACT (IN THAI).....	iv
ABSTRACT (IN ENGLISH).....	v
ACKNOWLEDGEMENT.....	vi
CONTENT.....	vii
LIST OF FIGURES.....	x
LIST OF TABLE.....	xiii
NOMENCLATURE.....	xiv
 CHAPTER	
I	
INTRODUCTION.....	1
II	
BACKGROUND.....	4
2.1 Lipid.....	4
2.2 Feedstocks for biodiesel synthesis.....	5
2.3 Biodiesel facts.....	6
2.4 Lipid conversion reaction occurring during biodiesel synthesis.....	9
2.4.1 Hydrolysis (fat splitting process)	9
2.4.2 Transesterification (Alcoholysis)	10
2.4.3 Esterification.....	11
2.4.3 Thermal cracking (pyrolysis)	12
2.5 Catalysis reactions.....	12
2.5.1 Homogeneous catalysis.....	12
2.5.2 Heterogeneous catalysis.....	15
III	
EXPERIMENTAL.....	21
3.1 Material and Chemicals.....	21
3.2 Pretreatment for the commercially available catalysts and catalyst preparation.....	22

3.2.1	Pretreatment for the commercially available catalyst.....	22
3.2.2	Catalyst preparation.....	23
3.3	Catalyst characterization technique.....	23
3.4	Reaction procedure and sample analysis.....	26
3.4.1	3-Phase reaction system in a semi-batch reactor.....	26
3.4.2	Batch reaction system in a Parr reactor.....	27
3.4.3	Batch reaction system in a three neck round bottom flask reactor.....	29
IV	RESULTS AND DISCUSSION.....	30
4.1	Solid acid catalyzed hydrolysis of TCp in a semi-batch reactor.....	30
4.1.1	Catalyst characterization.....	31
4.1.2	The exclusion of mass transfer limitations.....	32
4.1.3	Effect of water flow rate on TCp hydrolysis.....	33
4.1.4	Temperature effect on TCp hydrolysis.....	38
4.1.5	Activation energy of TCp hydrolysis.....	42
4.1.6	Kinetic study of TCp hydrolysis.....	44
4.1.7	Catalyst deactivation and regeneration.....	49
4.2	Reaction kinetics and mechanisms for hydrolysis and transesterification of TCp on WZ catalyst.....	57
4.2.1	Catalyst characterization.....	57
4.2.2	Influence of solvents on the kinetics of hydrolysis and of transesterification for TCp.....	58
4.2.3	Exclusion of mass transport effects for both hydrolysis and transesterification.....	58
4.2.4	Catalytic activity of WZ for hydrolysis and transesterification.....	62
4.2.5	Influence of reaction temperature on WZ catalyzed hydrolysis and transesterification.....	64
4.2.6	Concentration effects on the initial rate of reaction for WZ catalyzed hydrolysis and transesterification at 130°C.....	67

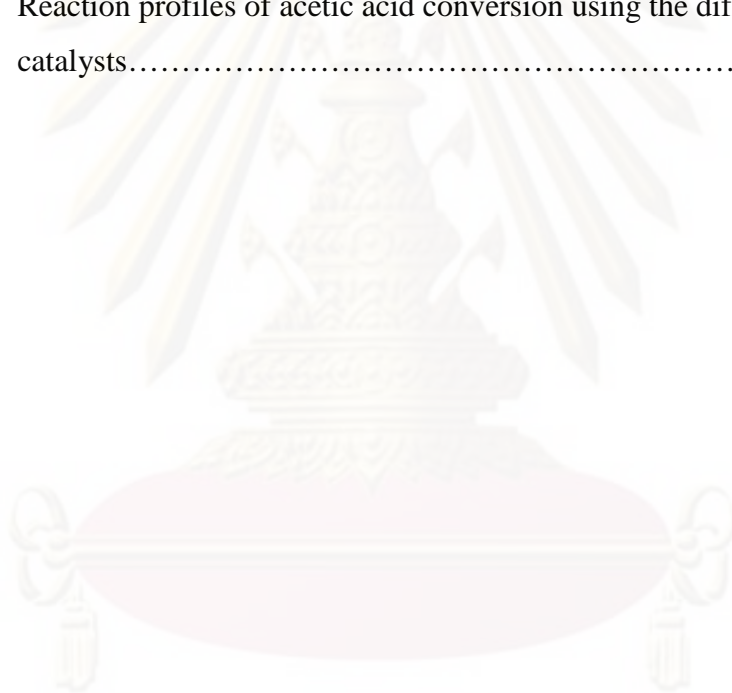
4.2.7	Apparent reaction orders for WZ catalyzed hydrolysis and transesterification at 130°C	71
4.2.8	Selective poisoning of WZ acid sites for hydrolysis and transesterification.....	73
4.2.9	Proposed mechanisms for WZ catalyzed hydrolysis and transesterification at 130°C.....	74
4.2.10	Comparison of hydrolysis and transesterification.....	79
4.3	The role of zirconia surface on catalytic activity of tungstated zirconia via two-phase esterification of acetic acid and 1-heptanol.....	80
4.3.1	Catalyst characterization.....	80
4.3.2	Proposed the active species of tungstated zirconia.....	86
4.3.3	Catalytic activity for 2-phase esterification of dilute acetic acid and 1-heptanol.....	87
V	CONCLUSIONS AND RECOMMENDATIONS.....	89
5.1	Conclusions.....	89
5.2	Recommendations.....	91
	REFERENCES.....	93
	APPENDICES.....	105
	APPENDIX A : PREPARATION OF ZIRCONIA SUPPORT.....	106
	APPENDIX B : CALCULATION FOR CATALYST PREPARATION.....	108
	APPENDIX C : CALCULATION FOR CRYSTALLITE SIZE.....	109
	APPENDIX D : CONDITION OF GAS CHROMATROGRAPHY.....	110
	APPENDIX E : CALCULATION FOR CATALYTIC PERFORMANCE...	112
	APPENDIX F : CALIBRATION CURVE.....	113
	APPENDIX G : LIST OF PUBLICATIONS.....	117
	VITAE.....	118

LIST OF FIGURES

FIGURE	Page
2.1	Chemical structures of vegetable oils and animal fats..... 5
2.2	TG hydrolysis..... 9
2.3	TG transesterification..... 10
2.4	Carboxylic acid esterification..... 11
2.5	Acid-catalyzed reaction mechanism for carboxylic acid esterification..... 13
3.1	Schematic semi-batch reaction system used..... 27
4.1	The exclusion of internal mass transport effects during WZ catalyzed hydrolysis of TCp at 140°C with water flow rate of 5 μL/min..... 33
4.2	Water concentration in the reaction liquid with time-on-stream at different water flow rates (5, 10 and 20 μL/min) in the absence of a catalyst at 130°C..... 34
4.3	Effect of water flow rate on the catalytic activity for TCp hydrolysis of : (a) WZ and (b) SAC-13 [T = 130°C, P = 1 atm, water flow rate (5, 10 and 20 μL/min)]. 36
4.4	Effect of temperature on the catalytic activity in the hydrolysis of TCp at a water flow rate of 5 μL/min using: (a) WZ and (b) SAC- 13..... 40
4.5	Influence of reaction temperature on the extent of TCp hydrolysis to HCp at a water flow rate 5 μL/min: (a) WZ and (b) SAC-13..... 41
4.6	Arrhenius plot of the hydrolysis of TCp to DCp in the temperature range of 110-to-150°C: (a) WZ and (b) SAC-13..... 43
4.7	GL and DCp yields in WZ and SAC-13 catalyzed TCp hydrolysis as a function of TCp conversion..... 46
4.8	HCp yield in WZ and SAC-13 catalyzed TCp hydrolysis as a function of TCp conversion..... 47
4.9	Catalytic activity during multiple hydrolysis of TCp cycles with catalyst reuse and regeneration: (a) WZ and (b) SAC-13..... 50

FIGURE	Page
4.10 IR spectra of the fresh, regenerated and used (after TCp hydrolysis for 2 h at 130°C) catalyst samples: (a) WZ and (b) SAC-13.....	52
4.11 Thermogravimetric analysis (TGA) of the fresh, regenerated and used catalyst samples after TCp hydrolysis for consecutive 2 h reaction cycles: (a) WZ and (b) SAC-13.....	53
4.12 Reaction profiles for experiments to exclude mass transport effects on hydrolysis (130°C, 32% v/v of solvent/total reaction volume, H ₂ O:TCp = 1:1 and WZ loading of 0.06g/mL): (a) various stirring speeds (1790-2385 rpm) and (b) various WZ particle sizes (0.104-0.251 mm and non-sieved WZ).....	60
4.13 Reaction profiles for experiments to exclude mass transport effects on transesterification (130°C, 32% v/v of solvent/total reaction volume, MeOH:TCp = 1:1 and WZ loading of 0.06g/mL): (a) various stirring speeds (1790-2385 rpm) and (b) various WZ particle sizes (0.104-0.251 mm and non-sieved WZ).....	61
4.14 Selectivity for DCp, MCp and glycerol on WZ after 1 h of reaction for hydrolysis (H ₂ O:TCp = 1:1) and transesterification (MeOH:TCp = 1:1) at 130°C with a loading of WZ of 0.06 g/mL....	64
4.15 Arrhenius plots in the temperature range of 100-130°C with 32% v/v of solvent/total reaction volume using a WZ loading of 0.06g/mL: (a) hydrolysis (H ₂ O:TCp = 1:1) and (b) transesterification (MeOH:TCp = 1:1).....	66
4.16 Effect of reactant concentration on the initial reaction rate for TCp hydrolysis at 130°C: (a) $C_{TCp,0} = 1.25$ mol/L and (b) $C_{W,0} = 1.25$ mol/L.....	69
4.17. Effect of reactant concentration on the initial reaction rate for TCp transesterification with methanol 130°C: (a) $C_{TCp,0} = 1.25$ mol/L and (b) $C_{M,0} = 1.25$ mol/L.....	70

FIGURE	Page	
4.18	Selective poisoning of the acid sites on WZ catalyst using pyridine adsorption (Reaction conditions: $C_{TCP,0} = 1.25$, $C_{W,0}$ and $C_{M,0} = 1.25$ mol/L at 130°C with 0.06g/mL of WZ).....	74
4.19	XRD patterns for ZrO ₂ supports and WZ catalysts.....	81
4.20	ESR spectra of ZrO ₂ supports and WZ catalysts.....	83
4.21	FT-IR spectra of ZrO ₂ supports.....	84
4.22	Raman spectra of WZ-NT and WZ-H ₂ catalysts.....	85
4.23	Schematic for proposed catalytic active species presented in (a) WZ-NT and (b) WZ-H ₂ catalyst.....	87
4.24	Reaction profiles of acetic acid conversion using the different WZ catalysts.....	88



ศูนย์วิทยทรัพยากร
จุฬาลงกรณ์มหาวิทยาลัย

LIST OF TABLE

TABLE		Page
2.1	Lipid feedstocks pricing and impact on biodiesel production cost.....	7
2.2	American Society for Testing and Materials (ASTM) Standard of maximum allowed quantities in diesel and biodiesel.....	8
4.1	Pretreatment conditions and characterization results for WZ and SAC-13.....	32
4.2	The catalytic activity, selectivity, and absolute amount of water on the catalyst after 2 h TOS at different water flow rates for both WZ and SAC-13.....	37
4.3	Comparison of catalyst activities in the three-phase reaction system for WZ and SAC-13 (TCp hydrolysis at 130°C with TCp = 2.03 mol/L, H ₂ O flow rate = 5 μL/min, and 7 wt.% catalyst loading based on TCp)	45
4.4	Thermogravimetric and elemental analysis for fresh, spent, and regenerated catalysts (WZ and SAC-13).....	55
4.5	Comparison of WZ catalyzed hydrolysis of TCp (H ₂ O:TCp = 1:1) ^a and transesterification of TCp with methanol (MeOH:TCp = 1:1) ^a ...	63
4.6	Orders of reaction for WZ catalyzed hydrolysis of TCp and transesterification of TCp with methanol at 130°C for various reactant molar ratios.....	67
4.7	Surface area, theoretical W surface density, surface acidity, crystallite size and XRD phases for ZrO ₂ support and WZ samples...	82

ศูนย์วิจัยทรัพยากร

จุฬาลงกรณ์มหาวิทยาลัย

NOMENCLATURE

Chemicals

HCp	Caprylic acid
DCp	Dicaprylin
DG	Diglyceride
HLa	Dodecanoic acid or lauric acid
E	Ester product (MeCp)
FFA	Free fatty acid
GL	Glycerol
M	Methanol
MeCp	Methyl caprylate
MCp	Monocaprylin
MG	Monoglyceride
W	Water
TG	Triglyceride
TCp	Tricaprylin or glyceryl trioctanoate

Catalysts

WZ	Tungstated zirconia (commercially available catalyst)
SAC-13	Fluorosulfonic acid Nafion [®] polymer on amorphous silica
WZ-NT	Synthesized tungstated on non-treated zirconia
WZ-H ₂	Synthesized tungstated on H ₂ treated zirconia surface

Reactions

		Unit
LH	Langmuir-Hinshelwood	
RDS	Rate determining step	-
TOF	Turnover frequency	min ⁻¹
TON	Turnover number of catalyst	h ⁻¹
TOS	Time on stream	

	Reactions	Unit
C_{TCp}	Concentration of TCp and methanol	
C_M	Concentration of methanol	
C_W	Concentrations of TCp and water	
E_{app}	Apparent activation energy	kJ/mol
k_R	Reaction rate constant	
k_{TCp}	Rate constant for TCp adsorption	
K_{TCp}	Adsorption equilibrium constants for adsorption of TCp	
K_M	Adsorption equilibrium constants for adsorption of methanol	
K_W	Adsorption equilibrium constant for water	
r_0	Initial rate of reaction	mmol/g-cat- min
S	Vacant acid site on the catalyst surface	
Greek letter		
α	Apparent TCp order of reaction	
β	Apparent water or methanol order of reaction for hydrolysis or transesterification.	

CHAPTER I

INTRODUCTION

Fats and oils are in lipids as an extensive family of chemicals. They are a large and diverse group of naturally occurring organic compounds that are related by their solubility in nonpolar organic solvents (e.g. ether, chloroform, acetone and benzene) and general insolubility in water. Nowadays, the use of fats and oils as a raw material receives increasing attention for biodiesel production which is made up of mono alkyl esters of long chain fatty acids. The most reputed advantages of using biodiesel as an alternative fuel are its renewability, cleaner emission of exhaust gas, biodegradability and null greenhouse effect given the photosynthetic origin of the fats and oils feedstocks.

In the transesterification for commercialization of biodiesel, refined vegetable oil as a raw material (in the USA, soybean oil; in Europe, rapeseed oil) reacts with low molecular weight alcohol (methanol, MeOH) and uses homogeneous alkali catalysts (NaOH, KOH, NaOCH₃) to enhance the reaction rate and improve the produced fuel's features. The end costs of biodiesel production from refined vegetable oil mostly depend on the price of feedstocks. These days, the unit price of biodiesel is much higher (1.5-3 times) than that of diesel fuel derived from crude oil due to the cost of feedstocks. For this reason, low cost feedstocks (feedstocks with high free fatty acids; FFAs) such as frying oils, animal fat, yellow grease (FFAs less than 15%) and brown grease (FFAs more than 15%) are attractive choices to replace refined vegetable oil [1-3]. As a result of high amount of FFAs contained in these raw materials, the saponification reaction of FFAs reacted with alkali catalyst to form soap and water will decrease the ester yield and prevent the phase separation of ester, glycerol (GL).

The simultaneous transesterification of triglycerides (TGs) and esterification of FFAs from low cost feedstocks using acid catalysis in a particular reactor have to be carefully integrated into the process to make biodiesel economically favorable [4-

7]. However, based on TG conversion resulting from two routes during the solid acid catalyzed esterification of FFAs and transesterification of TGs using methanol [7], water formation from acid catalyzed esterification can further react with TGs in hydrolysis [7-10]. Hydrolysis of TGs can be applied in a novel 2-step (hydrolysis-esterification) biodiesel synthesis process using low cost feedstocks containing > 5-15% FFAs. Since the esterification of FFAs is faster than transesterification of triglycerides on acid catalysts, there could be a possibility to construct a more efficient biodiesel synthesis process around the use of 2-step hydrolysis-esterification on solid acids rather than what is now done with 3-step pre-esterification (homogeneous acid catalyzed)–separation (removal of acid and water)–transesterification (homogeneous base catalyzed) [11].

In parallel, the replacement of liquid homogeneous catalysts with solid heterogeneous catalysts, which are non-corrosive, separable and recyclable, would enable the design of more economical continuous processes and greatly solve problems such as expensive separation/purification protocols and neutralization steps encountered with the former and facilitate continuous operation. Despite the great importance of heterogeneous acid catalysis in biodiesel forming reactions, many relevant fundamental issues remain poorly understood and hamper the accurate adoption, efficient use and specific alteration of solid catalysts and process optimization. Therefore, the outlook for the applications of solid catalysts for conversion of fats and oils feedstocks via hydrolysis, transesterification, and esterification is promising.

The main objective of this research has been to study the heterogeneous catalysis of the related biodiesel forming reaction. Using model compound, important fundamental issues including the production of FFAs by TGs hydrolysis, and transesterification and hydrolysis mechanisms have been studied. Potential solid acid catalysts such as WZ (tungstated zirconia) and SAC-13 (Nafion[®] SAC-13) have been compared, characterized and evaluated for TGs hydrolysis using model compound in the 3-phase reaction system. Particular attentions have been paid to catalyst activity, selectivity, deactivation and reusability to better discern the suitability of solid acid catalysts for hydrolysis of TGs. The mechanistic correlations between hydrolysis and transesterification of TGs using solid acid catalyst have been investigated and

elaborately analyzed at relatively high temperature. To provide explanation for the findings previously described for WZ catalysts and especially its benefit for 2-phase reaction system in the presence of water, the influence of surface characteristics of zirconia support under different thermal treatment atmosphere on the catalytic activity of WZ were determined via 2-phase esterification (high water content). The scope of the research presented is given below,

1. Using tricaprylin (TCp) as a model compound for larger TGs and for mixtures (as are typical in fats and oils) in order to facilitate the kinetic study for hydrolysis and transesterification.
2. Characterization of the catalysts using X- ray diffraction (XRD), BET surface area, Thermogravimetric analysis (TGA), Inductive Coupled Plasma Spectroscopy (ICP) and Fourier Transform Infrared (FTIR) Spectroscopy, Raman Spectroscopy, and Electron Spin Resonance (ESR).
3. Study the kinetics of SAC-13 and WZ catalyzed hydrolysis of TGs at atmospheric pressure in the 3-phase reaction system for a temperature range of 110-150°C.
4. Study the reusability, deactivation and regeneration of SAC-13 and WZ catalyzed hydrolysis of TCp in a 3-phase reaction system.
5. Study the kinetics and mechanisms of TCp hydrolysis compared to transesterification using a WZ catalyst at a relatively high temperature (130°C) in a batch reactor.
6. Study the influence of surface characteristic of zirconia support under different thermal treatment atmosphere on the catalytic activity of WZ via 2-phase esterification (high water content) at atmospheric pressure.

ศูนย์วิจัยทรัพยากร

จุฬาลงกรณ์มหาวิทยาลัย

CHAPTER II

BACKGROUND

Lipids are an important renewable raw material to produce an alternative (to petroleum) fuel such as biodiesel. The most common lipids for biodiesel synthesis are vegetable oils and animal fats which are converted by a two step process of transesterification of TGs and esterification of FFAs, a 2-step process of hydrolysis of TGs following by esterification of FFAs, or the simultaneous esterification of FFAs and transesterification of TGs.

2.1 Lipids

Lipids are a large and diverse group of organic compounds occurring naturally. Lipids may either be solid or liquid at room temperature, depending on their structure and composition. Normally, “oil” refers to a lipid that is liquid at room temperature, while “fat” refers to a lipid that is solid or semi-solid at room temperature. Fats and oils primarily consist of glycerol (a backbone of carbon) being mono-, di-, and TGs and low moderate contents of FFAs (carboxylic acids at each end) as shown in Figure 2.1. Other compounds such as phospholipids, polypeptides, sterols, water, odorants and other impurities can be found in crude oils and fats. In addition to TGs, oils and fats usually contain some fatty acids in their free form as a result of the spontaneous hydrolysis of the parent TG molecules. The FFA contents vary among different lipid sources and also depend on the treatments and storage conditions. Other compounds, such as phospholipids, glycolipids, sterols, water, 5 long chain alcohols, carbohydrates and vitamins, can be found in oils and fats in minor concentrations [12].

Food-grade vegetable oils, containing low FFA level, are currently used for a commercial biodiesel production. Although waste greases such as yellow grease and brown grease, containing FFA level of 15% and 33% respectively, they are considered as attractive feedstocks for biodiesel synthesis because of their wide availability and low cost compared to the food-grade vegetable oils [13].

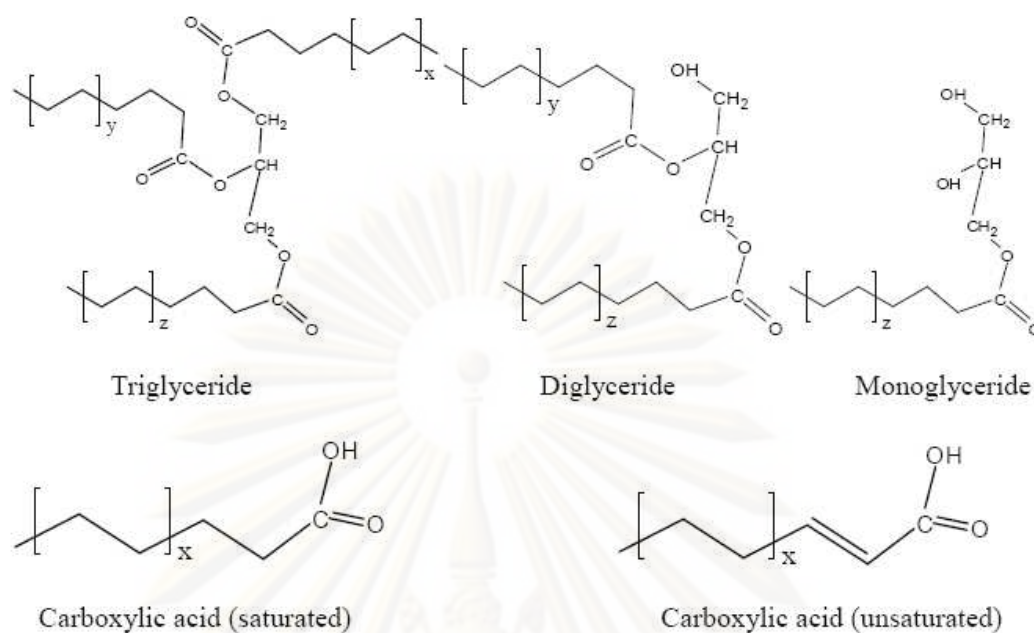


Figure 2.1 Chemical structures of vegetable oils and animal fats.

2.2 Feedstocks for biodiesel synthesis

Basically, any lipid source such as vegetable oil, animal fat and waste restaurant grease can be used for biodiesel formation with small alcohols via base/acid catalysts. But from the standpoint of chemical reaction, refined oil with low impurity and low fatty acid content is the desired feedstock for biodiesel production. In such case, homogeneous alkali catalyst can be used to provide considerable catalytic efficiency for lipid transformation. For instance, only a relatively short duration of 30–60 min is required to drive the conversion of TGs to completion at 60°C. However, alkaline catalysis is very sensitive to the purity of reactants. It suffers from saponification and neutralization in the presence of free fatty acids or moisture. Thus, strict feedstock specification must be satisfied (as for instance, FFA <0.5 wt%; water <0.1–0.3 wt%) for base catalysis [14]. Otherwise, soap production would seriously hinder productivity and complicate product separation by formation of gel and increased viscosity. Also, the alcohol and catalyst must be essentially anhydrous (0.1–0.3 wt% or less) complying with rigorous specifications. Such demanding feedstock specifications, consequently, translate into a high overall production cost of

biodiesel because the high expense if refined oil has to be used. According to NREL (National Renewable Energy Laboratory, USA), the raw material contributes 60~70% of final manufacture cost for biodiesel made from refined soybean oil. The usage of expensive feedstocks has been attributed to be mainly responsible for the lack of economical competitiveness of biodiesel as compared to fossil fuel and has consequently retarded its commercial expansion. As a matter of fact, there is a large quantity of high FFAs and moisture-rich lipid materials readily available at low price in a wide variety of forms. For instance, in United States alone, there are nearly 2.75 billion pounds of waste recyclable restaurant grease annually. Yellow grease is obtained from restaurant waste oil and sells for only \$0.09- 0.20/lb, on the average cheaper than refined vegetable oil by 50%. Brown grease which is mainly collected from traps installed in commercial, municipal or industrial sewage facilities, is another cheap feedstock priced at \$0.01-0.07/lb. Other than the greases, inedible animal fats such as poultry fat (2.2 billion lb/yr), tallow (3.9 billion lb/yr) and lard (1.3 billion lb/yr), also constitute important sources of inexpensive feedstocks for biodiesel. The traditional use of inedible animal fats has been as an animal feed ingredient. This use, however, has been seriously challenged with emerging concerns that this practice facilitates the transmission of potential infectious diseases from one animal species to another. Thus, alternatively, the synthesis of biodiesel from inedible fat provides a way for using more efficiently and environmentally friendly a renewable resource to produce an important value-added product. As can be expected, use of ample and low cost feedstocks would significantly lower the production cost, making biodiesel more accessible and inexpensive in the near future (Table 2.1).

2.3 Biodiesel facts

Biodiesel is defined as fuel comprised of a mixture of mono alkyl esters of long chain fatty acids derived from vegetable oils or animal fats which conforms to the requirements set by ASTM D6751. Biodiesel exhibits properties and characteristics that are comparable to conventional diesel (Table 2.2). Consequently, it can be used either as a substitute for diesel fuel or more commonly in fuel blends. In addition, biodiesel offers the advantages over petroleum-based diesel such as 1) a higher cetane number and a higher flash point, meaning better and safer performance, 2) higher

lubricity which prolongs engine life and reduces the frequency of engine part replacement, and 3) the presence of oxygen in biodiesel (~10%) improves combustion and reduces CO and hydrocarbon emissions. Blends of biodiesel and petroleum diesel are designated by a “B” followed by the volume percentage of biodiesel fuel in the blend, i.e., B20 represents 20 vol% of biodiesel and 80 vol% petroleum diesel. B5 and B20, the most common blends, can be used in unmodified diesel engines.

Table 2.1 Lipid feedstocks pricing and impact on biodiesel production cost [1].

Feedstocks type	Biodiesel prices (US\$/L)	Year
Soybean, canola, sunflower, rapeseed	0.54-0.62	1999
Waste grease	0.34-0.42	1999
Soybean	0.428	2001
Yellow grease	0.324	2001
Brown grease	0.246	2001
Canola	0.72	2003
Waste cooking oil	0.54-0.74	2003
Soybean	0.53	2005
Edible and inedible beef tallow	0.22-0.63	2006

ศูนย์วิทยทรัพยากร

จุฬาลงกรณ์มหาวิทยาลัย

Table 2.2 American Society for Testing and Materials (ASTM) Standard of maximum allowed quantities in diesel and biodiesel [8, 15].

Property	Diesel	Biodiesel
Standard	ASTM D975	ASTM D6751
Composition	HC ^a (C10-21)	FAME ^b (C12-22)
Kinematic viscosity (mm ² /s at 40°C)	1.9-4.1	1.9-6.0
Boiling point (°C)	188-343	182-338
Flash point (°C)	60-80	100-170
Cloud point (°C)	-15 to 5	-3 to 12
Pour point (°C)	-35 to -15	-15 to 16
Water (vol %)	0.05	0.05
Carbon (wt %)	87	77
Hydrogen (wt %)	13	12
Oxygen (wt %)	0	11
Sulfur (wt %)	0.05	0.05
Cetane number (ignition quality)	40-55	48-60
Stoichiometric air/fuel ratio (AFR)	15	13.8
HFRR ^c (μm)	685	314
BOCLEd scuff (g)	3600	>7000
Life-cycle energy balance (energy units produced per unit energy consumed)	0.83/1	3.2/1

^aHydrocarbons. ^bFatty Acid Methyl Esters. ^cHigh Frequency Reciprocating Rig. ^dBall-on-Cylinder Lubricity Evaluator.

2.4 Lipid conversion reaction occurring during biodiesel synthesis

There are four primary reactions involving biodiesel from fats and oils.

2.4.1 Hydrolysis (fat splitting process)

TGs as main components of vegetable oils and fats can be hydrolyzed with water/steam to produce three moles of FFAs and one mole of glycerol by the following consecutive reactions as can be seen in Figure 2.2.

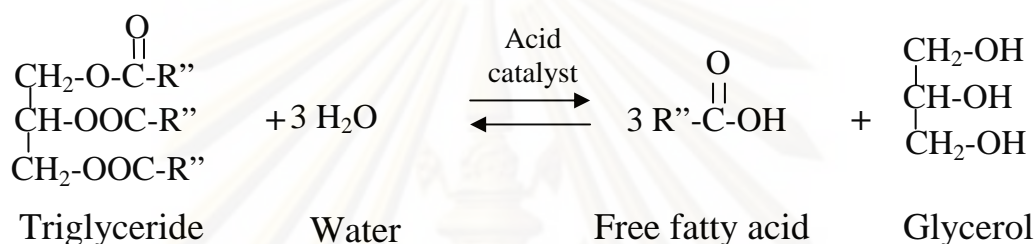


Figure 2.2 TG hydrolysis.

Hydrolysis of TGs is essentially a homogeneous reaction that proceeds in stages. The fatty acid radicals are displaced from the TG one at a time from tri to di to mono. An incomplete hydrolysis will thus contain MGs and DGs as well as TGs. During the initial stage, the reaction proceeds slowly, limited by the low solubility of the water in the oil phase. In the second stage, the reaction proceeds fairly rapidly brought about by the greater solubility of water in the FFAs. The final stage is characterized by a diminishing reaction rate as the fatty acids liberated and the GL byproduct reach equilibrium conditions. This is called fat splitting process. Hydrolysis of TGs is a reversible reaction. At the point of equilibrium, the rates of hydrolysis and re-esterification are equal. The GL byproduct must be withdrawn continuously to force the reaction to completion. Increasing the temperature and pressure accelerates the reaction because of the increased solubility of the water in the oil phase and to its higher activation energy. As oils and water are immiscible, the hydrolysis of oils can be hindered by solubility issues. However, conducting the reaction at high temperatures increases the solubility of water in the oil phase minimizing this limitation. Temperature, in particular, exerts a significant effect. An increase in temperature from 150 to 220°C increases water solubility by two to three

times [16]. The use of high temperature not only affects the solubility of water in the oil, but also improves the kinetics of the process. The presence of small amounts of mineral acids, such as sulfuric acid or certain metal oxides, such as zinc or magnesium oxide, accelerates the hydrolysis. These metal oxides are true catalysts. They also assist in the formation of emulsions.

2.4.2 Transesterification (Alcoholysis)

Transesterification consists of a number of consecutive reversible steps. For manufacturing biodiesel, transesterification is performed to lower the viscosity of vegetable oils. When the methanol (the lowest molecular weight of alcohol) reacted with 1 mole of TG (primary compound in vegetable oils and fats) is converted sequentially to DG, MG, and finally GL, and 3 mole of fatty acid methyl ester (FAME). The transesterification reaction for biodiesel synthesis is shown in Figure 2.3.

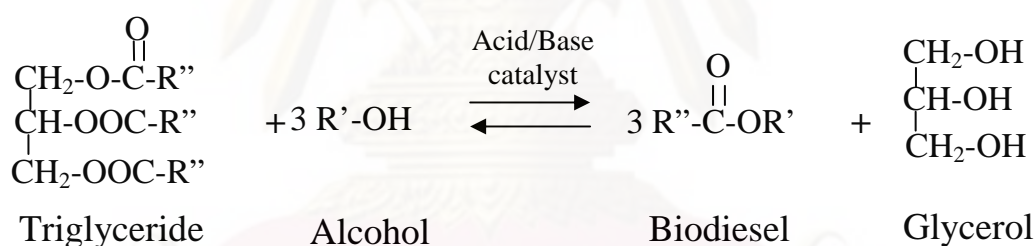


Figure 2.3 TG transesterification.

Due to the transesterification process being a reversible reaction, alcohols are generally used in excess to assist in a fast reaction rate and guarantee a complete conversion. Methanol and ethanol are commonly used, especially methanol because of its low cost. The rate of the reaction can be significantly improved by the presence of acid or basic catalysts. In general, the use of basic catalysts is more desirable since it provides the satisfactory conversion within a short time. Among the mentioned methodologies, transesterification is considered as the best current process. Most of the conventional biodiesel production is performed by the alkali-catalyzed transesterification, since it can be operated under mild conditions to achieve

significant conversion with minimal side reactions and reaction time. However, standard biodiesel production suffers from the presence of water and FFAs in feedstocks. On one hand, water favors the formation of FFAs by hydrolysis of TGs and esters products (biodiesel). Formation of FFA in presence of basic homogeneous catalysts gives rise to soap, creating serious problems for product separation, and ultimately hindering catalytic activity. As a result, highly refined vegetable oils are required for the process; otherwise, the pretreatment steps are necessitated for the feedstocks to reduce the acid and water concentrations below an optimum threshold limit, i.e., FFAs < 1 wt% and water < 0.5 wt% [17].

2.4.3 Esterification

Esterification of FFA with low molecular weight alcohols is another method to produce biodiesel and can be used as a pretreatment for basic transesterification to convert the FFA into ester product (biodiesel) and avoid saponification especially when FFA content is higher than 1 wt%. Esterification is a reversible reaction between carboxylic acids and alcohols in the presence of strong acid catalyst, resulting in the formation of water and at least one ester product (Figure 2.4).

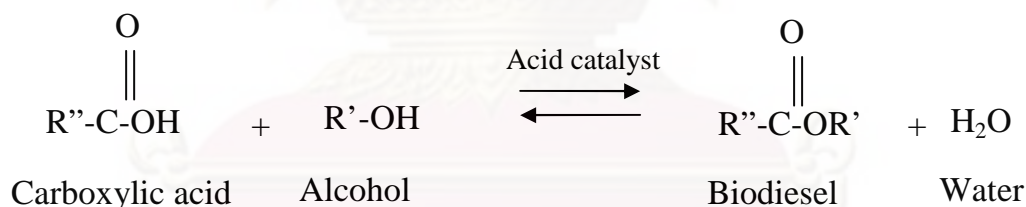


Figure 2.4 Carboxylic acid esterification.

The mechanism of homogeneous catalyzed esterification has long been established; a protonated carboxylic acid is nucleophilically attacked by an alcohol molecule from the bulk phase yielding an ester and water. Esterification can be carried out by a catalyst free method, enzymatic method, or use of homogeneous and heterogeneous acid catalysts. Non-catalytic esterification is normally performed under supercritical conditions for alcohol i.e., the critical temperature and pressure of methanol are 239°C and 8.09 MPa. Under such reaction conditions, the alcohol itself starts acting as a catalyst [9], the degree of alcohol solubility in oil is increased,

thereby favoring the transition from a solubility-limited reaction to a rate-limited reaction [18, 19]. As a result, TG transesterification can be simultaneously performed. Additional benefits from a supercritical alcohol method are the separation of esters and glycerol from reaction mixture becomes much easier since in the presence of water and glycerol will be in the water portion while esters are in the upper portion. Saka and Kusdiana [20] reported a fast and high conversion of rapeseed oil into methyl esters by using supercritical methanol without the aid of any catalyst. However, in this process, high energy intensity is required and additional safety hazards are presented. The use of homogeneous and heterogeneous acid catalysts for FFA esterification has been extensively researched due to the insensitivity to the wide range of feedstocks, high production yields, relatively low cost, and potentially being recovered and reused.

2.4.4 Thermal cracking (pyrolysis)

Pyrolysis is defined as the conversion of one substance into another by means of heat in the absence of air or oxygen with temperatures range from 450 to 850°C or by heat with the aid of a Lewis acid catalyst. Lewis acid catalysts used in this process include zeolites, clay montmorillonite, aluminum chloride, aluminum bromide, ferrous chloride, and ferrous bromide. Nevertheless, the removal of oxygen during the thermal processing also eliminates the environmental benefits associated with using an oxygenated fuel [14]. In addition, fuels are produced more like gasoline rather than diesel.

2.5 Catalysis

2.5.1 Homogeneous catalysis

Simple strong liquid mineral acids, such as sulfuric acid (H_2SO_4), phosphoric acid (H_3PO_4), hydrochloric acid (HCl), and others, are the most frequently used for direct esterification of FFAs with alcohol. They have also been used to catalyze transesterification of TGs to produce biodiesel. However, because of their much lower activity (by 3 orders of magnitude) [21] and much stronger corrosiveness than the base catalysts [17], acid catalysts have never enjoyed the same popularity for

biodiesel synthesis as its counterpart in either the academic and industrial sectors. Only recently, given the versatility of acid catalysis to deal with FFAs, has its use been proposed as an economically viable alternative to base catalysis for biodiesel formation from low cost feedstocks [17]. As the most common way to synthesize organic esters of enormous practical importance, esterification of carboxylic acids with alcohols, indeed, represents a well known category of liquid-phase reactions of considerable industrial interest.

The accepted mechanistic route for the homogeneous acid-catalyzed esterification is illustrated in Figure 2.5. The sequence of steps can be summarized as following: in the first two steps, the catalysts essentially activate the carbonyl carbon on the carboxylic group by protonating the carbonyl oxygen; third, the activated carbonyl group undergoes the nucleophilic attack by an alcohol molecule to form a tetrahedral intermediate; fourth, proton migration gives rise to a good leaving group; fifth, the carbonyl carbon-hydroxyl oxygen bond of the hemiacetal species (tetrahedral intermediate) cleaves yielding a protonated alkyl ester and a water molecule; finally, the catalyst regenerates by the deprotonation of the ester product.

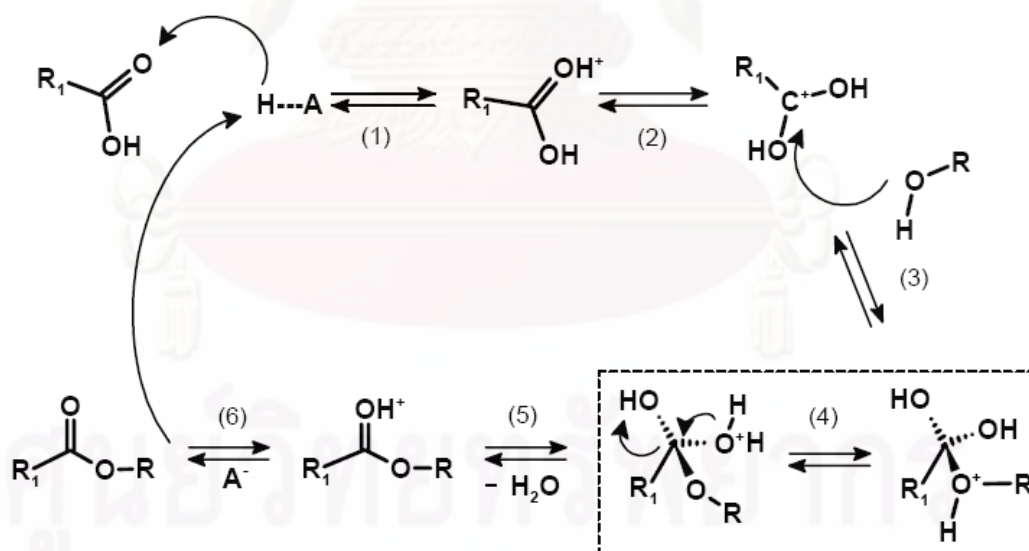


Figure 2.5 Acid-catalyzed reaction mechanism for carboxylic acid esterification [22].

Simple Brønsted acid catalysts such as H_2SO_4 , HCl , H_3PO_4 and arylsulfonic acid, are generally known to be effective for the direct esterification. In a few cases involving substrates with either high sterical hindrance or aromatic moieties, several

alternative Brønsted acids have been suggested such as a combination of H_2SO_4 and H_3BO_3 and trifluorobenzeneboronic acid [23].

Liquid Lewis acid catalysts, i.e., BF_3 , TiCl_4 , $\text{HfCl}_4 \cdot 2\text{THF}$, $\text{Sc}(\text{OTf})_3$, and others, are capable to efficiently esterify the carboxylic acid, and more beneficial than Brønsted acids since the parallel undesired side reaction i.e., alcohol dehydration can be suppressed [23-26]. Water produced from either direct esterification or side reaction (i.e., alcohol dehydration) was reported to show the negative effect on retarding the reaction rate due to thermodynamic limitation and lowering the catalyst performance by strongly binding to the active species (H^+) in the solution, giving rise to weaker acids.

Recently, given their non-corrosiveness and reusability, acidic ionic liquids have been proposed as catalysts to offer a new and environmental benign approach for alkyl ester synthesis. Ionic liquids have the potential as dual solvent-catalysts in organic synthesis such as SO_3H - and R_3NH -functional Brønsted-acidic ionic liquids. However, they are generally less acidic than strong mineral acids, requiring either higher amounts of catalysts or reaction temperatures to achieve comparable ester yields as the latter.

There is relatively limited information regarding acid-catalyzed esterification of long chain fatty acids in the presence of TGs as the situation requires in biodiesel synthesis. In most cases, related studies focus on the impacts of reaction parameters on the final free acidity of lipid feedstock without paying much attention to the reaction kinetics. Mainly using H_2SO_4 as catalyst, the pre-esterification of different lipid feedstocks with high FFA contents have been investigated. In accordance, oils with initial FFA contents up to 19% can be easily reduced to 1% or lower using 1-step reaction at 60°C after short reaction time, regardless the origins of oils. The specific efficiency of a process is adjustable by varying operation parameters. For instance, the use of larger amounts of catalysts speeds up esterification rate therefore substantially shortening the necessitated reaction time. Typically, catalyst concentration has ranged between 1 and 2 wt% (with respect to oil) in academic studies using H_2SO_4 .

In general, homogeneous catalysis is more active than heterogeneous catalysis since the active sites in liquid phase are capable to move freely in the reagents. Meanwhile, the active sites of solid catalysts are confined on the surface, making the reactions could be limited by the effect of internal mass transfer resistance. However, it has been reported that on a site basis, solid acid catalysts show the same capacity as liquid ones for performing the reactions [27]. In addition, industrial processes prefer the use of solid catalysts to carry out chemical transformations due to their ease in separation from any reaction mixture. Solid catalysts can potentially be regenerated, and they are environmentally benign since they can be used over and over releasing little waste to the environment.

2.5.2 Heterogeneous catalysis

A number of research studies have been directed towards the use of solid acids as heterogeneous catalysts for biodiesel synthesis via esterification of FFAs and transesterification of TGs. Biodiesel production has commercially been performed by using liquid catalysts, such as NaOH, KOH, and H₂SO₄ but these require an additional pretreatment step for base catalysts or toxic, corrosive and often hard to remove from reaction solution for acid catalysts. Thus it is desirable to use solid acid catalysts, because the solid acids are less toxic and are reported in the literature to be active for esterification [7, 8, 28-33] and transesterification [7, 27, 34-38].

Esterification can be catalyzed by the catalysts having a medium acid strength; hence, ion-exchange resins such as Amberlyst-15 and Nafion® (having high acidity density of medium acid strength) show promise as the active catalysts for esterification [28, 39-41]. Although, Amberlyst-15 and Nafion contain highly acidic sites, in the reaction of carboxylic acids with long chain hydrocarbon moieties, they show less activity due to diffusion limitations [41]. The catalyst activity strongly depends on the swelling of this material which controls the accessibility of the acid sites. The adsorption effect must be taken into account in the reaction, because more than 95% of the protons are inside the micro-spheres and are only accessible to chemical species which are able to diffuse into the polymer matrix [40]. The organic

resin catalysts such as sulfonic acid cation exchange resins are not stable for temperatures greater than ca. 140°C. This is a main drawback of this catalyst type to operate in the reactions required high reaction temperatures. For this kind of application, inorganic catalysts are more attractive.

An inorganic solid catalyst, zeolites are well-known catalysts for organic synthesis. General advantages of zeolites are that they can be synthesized in different crystal structures, framework Si/Al ratios, and proton exchange levels permitting different properties such as pore size and pore structure, strength of acid sites and their distribution, and surface hydrophobicity, which offers the additional advantages in achieving the effective segregation of water which is reported to poison the catalyst acid sites [42, 43]. For instance, catalyst activity of this material is found to be enhanced with increasing Si/Al ratio, indicating that the reaction is influenced by stronger acid site strength as well as surface hydrophobicity. Several zeolites such as modified H-Y, H-Beta, H-ZSM-5, aluminophosphate and silicoaluminophosphate molecular sieves have been employed as esterification catalysts [44-46].

However, the mass transfer limitations becomes critical with using microporous materials as a catalyst. Although zeolites are active catalysts for esterification, they catalyze the reaction rather slowly due to steric hindrance of the bulky fatty acids, or due to difficulty to adsorb inside the zeolite pores. According to a severe pore size limitation of microporous molecular sieves, the reaction with large molecules probably take place at the external surface of the crystals. Consequently, zeolites with larger pore size have been used with some success in fatty acid esterification [47]. Even though zeolite catalysts show high activity, the reaction always gives a variety of undesired by-products due to the higher reaction temperatures used.

Silica mesostructured materials have been studied extensively because of their combination of extremely high surface areas and flexible pore sizes. Silica mesoporous materials modified with sulfonic groups are utilized in the pretreatment esterification reaction of high free fatty acid oils [48]. Incorporated functionalized organic groups; organic hybrid mesoporous silicas functionalized with sulfonic acid

groups have shown successful results for acid catalyzed esterification. Moreover, the hydrophobic character of SO₃H-mesoporous materials has already been mentioned as being beneficial for the overall conversion and selectivity. The acid strength can be adjusted by choice of the organosulfonic precursor. Diffusion for the reactions of long chain hydrocarbon carboxylic acid has been demonstrated to be significant in the mesoporous catalysts. The pore diameter can be increased to decrease internal mass transfer resistance with using of the surfactant template.

MCM-41-supported heteropolyacids (HPAs) have been used as a catalyst in the gas phase esterification of acetic acid and 1-butanol [49]. This catalyst achieved 95% conversion of 1-butanol. MCM-41-supported HPAs were determined to be more active than pure HPA. The enhanced activity may be ascribed to a high dispersion of HPA on MCM-41, providing more surface proton sites than pure HPA. However this material is considerably more hydrophilic than original material; water formation from reaction can cause the HPA migration from MCM-41 pores to the outer surface. Moreover, the activities of spent catalysts decrease significantly due to sintering.

Recently, sulfated zirconia (SZ) catalysts have found application in several acid catalyzed reactions [50-52]. Although SZ is proposed as an active catalyst for esterification due to its high acid strength, it suffers from great deactivation due to coke formation and sulfate leaching [53, 54]. The latter may lead to homogeneous catalyzed reactions. For this catalyst, the presence of water not only inhibits the reaction, but also modifies the acid sites of SZ catalyst, leading to sulfate leaching [30, 54, 55]. SZ is easily hydrolyzed in free water to form other species such as SO₄²⁻, HSO₄⁻, and H₂SO₄ [56], resulting in sulfate group leaching. Sulfate leaching tests has been performed by several groups [51, 56, 57].

The diffusion of molecules to the active sites often becomes critical for porous solid acids such as zeolites. Pore size is a critical parameter much influencing catalyst selectivity and needs nevertheless to be tuned to meet the steric requirements of the different fatty monoesters. With larger pore diameter, allowing the processing of large molecule, the materials yield the high activity comparable to homogeneous catalyst, i.e., H₂SO₄. High acid density is required for acid catalyzed esterification. An acidic salt of HPA (C_{S_{2.5}H_{0.5}PW₁₂O₄₀}) and Nafion gave higher activities than

Amberlyst-15 and a metal oxide, SZ and, WZ. Nevertheless, preparation methods play an important role in affecting these catalyst characteristics, pore diameter, and acidity. To obtain the effective catalysts, the potential preparation method should to be determined.

Despite numerous advantages associated with the use of solid acid catalysts, research on the direct transesterification using heterogeneous acid catalyst for biodiesel synthesis has been scarcely explored due to their pessimistic activity. One of a few studies dealing with transesterification of TG feedstocks using inorganic resin acid catalysts, i.e., Amberlyst-15 and sugar-based catalysts [34, 35, 58], mild reaction conditions were employed to avoid catalyst degradation due to their polymeric matrix structure. As a result, for organic catalysts, swelling capacity is a critical issue since it controls substrate accessibility to the acid sites. Unfortunately, TG is not a good swelling agent due to lengthy alkyl tails of substantial hydrophobicity, disfavoring the promise of organic resins as biodiesel catalysts.

In this case, inorganic solid acid catalysts are more desirable where high reaction temperatures are required to enhance the catalyst performance [31, 59]. Among a variety of available inorganic acid catalysts, a number of solid acid catalysts, such as sulfonated aluminosilicates [60], aluminum phosphate [61], sulfated tin oxide [53], SZ [53, 54], tungstated zirconia alumina [53], and 12-tungstophosphoric acid impregnated on ZrO_2 , SiO_2 , Al_2O_3 , and activated carbon [62], have been explored for reaction using vegetable oils to estimate their potentials for biodiesel related application. Recently, increasing research has been devoted to the use of TG model compounds, i.e. triacetin [3, 28, 37], tricaprylin [38, 54, 62], for the biodiesel formation reactions in order to develop better fundamental understanding relevance to the catalyst activation and deactivation. By understanding the catalyst deactivation, one should be able to design catalysts and the catalytic systems more resistant to deactivation and, hence, more proficient and durable for applications concerning biodiesel synthesis.

Unfortunately, the reaction kinetics and mechanism of solid acid catalyzed hydrolysis of TGs have not been studied much. Only one paper by Yow and Liew [63] has reported an investigation of the kinetics of hydrolysis of palm oil catalyzed by a macroporous cation-exchanged resin. They suggested that this reaction follows a mechanism similar to that of homogeneous acid catalyzed hydrolysis reaction which has first-order kinetics at 155°C. The results for the solid acid catalyst also showed first-order kinetics for the triglyceride and a negligible effect of water concentration. There have been several studies, however, of the kinetics and mechanism of TG transesterification on solid catalysts [37, 64]. Lopez et al. [37] found that the mechanism of solid acid ion-exchange resin catalyzed transesterification of triacetin appears to be similar to that for the homogeneous acid catalyzed one at 60°C, where the rate determining step is the reaction of protonated triglycerides (on a single catalyst site) with bulk phase methanol, being both first-order in TG and in methanol. Božkel-Winkler and Gmehling [64] investigated the reaction kinetics of transesterification of methyl acetate and *n*-butanol catalyzed by Amberlyst 15 and also suggested a pseudo-homogeneous mechanism, but based on the assumption of the reaction taking place between two adsorbed molecules.

WZ is a strong inorganic solid acid catalyst, which has been used successfully for a wide range of acid catalyzed reactions, such as dehydration, esterification, hydrocarbon isomerization and cracking [27, 29, 65, 66]. Another study that investigated the esterification of palmitic acid with methanol on WZ found correlations among the conversion of palmitic acid, the acidity of WZ (as measured by NH₃-TPD), and the percentage of tetragonal phase of the ZrO₂ support [67]. Goodwin group also reported based on turnover frequency (TOF) results, that WZ has a site activity comparable to H₂SO₄ for catalyzing biodiesel-forming transesterification reactions [27]. Another advantage of WZ is that catalyst deactivation appears to be not rapid for transesterification of triglycerides with methanol [5, 27] due its thermal stability. The nature of the active sites is a key factor in order to achieve high catalytic performance. For instance, the calcination temperature and tungsten loading affects on the structure of WO_x presented in an isolated surface monotungstates, polymeric surface polytungstates and crystalline WO₃ particles on a zirconia support as reported in numerous studies [24, 25, 68-71]. Barton et al. [69] reported that the maximum activity for tungsten loading was slightly

greater than a monolayer coverage, forming the so called polytungstate species for hydrocarbon isomerization. Gregorio et al. [72] suggested that the 15% of tungsten loading is a critical value to achieve high activity, selectivity, and stability of the catalyst on stream and good activity for saturated hydrocarbon isomerization. Lopez et al. [29] reported that the calcination temperature of 800°C contributed with tungsten oxide polymeric structure can achieve the highest catalytic activity for both esterification and transesterification. In many cases, the preparation method of zirconia permits us to make different surface species [73-76]. The generation of new active sites on the surface can bring about various influences on activity and selectivity for certain types of reactions [77]. Lebarbier et al. [78] reported that no significant effect of the initial form of the support (Zr oxyhydroxide versus predominantly tetragonal zirconia) was observed for *n*-hexane isomerization. Wongmaneevil et al. [79] found that the calcination of ZrO₂ support in the reductive atmosphere (H₂) can achieve higher conversion for esterification of acetic acid than that of oxidative atmosphere (O₂).

CHAPTER III

EXPERIMENTAL

To achieve the research objectives and research scope, the research methodology will be provided in this chapter which consist of material and chemicals, catalyst preparation, catalyst characterization and reaction study in hydrolysis, transesterification, and esterification.

The first section depicted all materials and chemicals used for this research. The next section illustrated the pretreatment of the commercially available catalysts, and the catalyst preparation. The catalyst characterization techniques such as XRD, BET surface area, FT-IR and Raman spectroscopy, TGA and Ion exchange titration were presented in the next section. The last section was provided the reaction procedure for hydrolysis, transesterification, and esterification.

3.1 Material and chemicals

All chemicals used in this research were high purity chemicals and used as received as follows:

1. Acetic acid ($C_2H_4O_2$, 99.8%) purchased from Merck.
2. Anhydrous methanol (CH_4O , 99.8%) purchased from Sigma-Aldrich.
3. 1,4-Butanediol ($C_4H_{10}O_2$, 99%) purchased Sigma-Aldrich.
4. Caprylic acid ($C_8H_{16}O_2$, 99%) purchased from MP Biomedicals Inc.
5. Dicaprylin ($C_{19}H_{36}O_5$, 97%) purchased from Sigma-Aldrich.
6. Dodecanoic acid or lauric acid ($C_{12}H_{24}O_2$, 98%) purchased from Sigma-Aldrich.
7. Double distillation and deionization water provided from our laboratory.
8. Glycerol ($C_3H_5(OH)_3$, 99%) purchased from Acros.
9. 1-Heptanol ($C_7H_{16}O$, 99%) purchased from Merck.
10. Heptyl acetate ($C_9H_{18}O_2$, 98%) purchased from Wako Pure Chemical Industries.

11. Hexane (C₆H₁₄, 99.9%) purchased from Fisher Scientific Inc.
12. 2-Isopropanol (C₃H₇OH, HPLC grade 99%) purchased from Fisher Scientific Inc.
13. Methyl valerate (C₆H₁₂O₂, 99%) purchased from Sigma-Aldrich.
14. Methyl caprylate (C₉H₁₈O₂, 99%) purchased from Sigma-Aldrich.
15. Monocaprylin (C₁₁H₂₂O₄, 99%) purchased from Sigma-Aldrich.
16. Tricaprylin or glyceryl trioctanoate (C₂₇H₅₀O₆, 99%) purchased from Sigma-Aldrich.
17. Tungsten (VI) chloride (WCl₆, 99.9%) purchased from Aldrich.
18. Zirconium tetra-*n*-butoxide (C₁₆H₃₆O₄Zr) 80 wt% solution in 1-butanol purchased from Aldrich.

The commercially available catalysts used for this study are following:

1. Amorphous tungstated zirconium hydroxide precursor (XZ01251) containing 16 wt% WO₃ was kindly provided by Magnesium Electron, Inc. (MEI, Manchester, UK).
2. Nafion[®] SAC-13 purchased from Sigma-Aldrich.

3.2 Pretreatment for the commercially available catalysts and catalyst preparation

The detail of pretreatment of commercially available catalyst namely WZ and SAC-13 and catalyst preparation namely WZ-NT and WZ-H₂ were presented as follows:

3.2.1 Pretreatment for the commercially available catalyst

The commercially available catalysts namely WZ and SAC-13 were activated. They were placed inside sealed containers and stored in a desiccator until use. The WZ precursor was activated by calcination under static air (zero grade) at 800°C for 2 h. SAC-13 pellets were ground, sieved to get catalyst particles >200 mesh (<0.075 mm), and then dehydrated overnight at 80°C under vacuum.

3.2.2 Catalyst preparation

Zirconia as a support was prepared via a solvothermal method as well as reported by Kongwudthiti et al. [80]. Zirconium tetra-*n*-butoxide 80 wt% solution in 1-butanol (Aldrich) was suspended in 100 mL of 1,4-butanediol (99%, Sigma-Aldrich) in a test tube, which was then placed in a 300 mL autoclave. 30 mL of 1,4-butanediol was filled in the gap between the test tube and the autoclave wall. The autoclave was purged with nitrogen. The mixture was heated to 300°C at a rate of 2.5°C/min. The temperature was held constant at 300°C for 2 h. The system set-up for this preparation was shown in Appendix A. After reaction, this autoclave was cooled and the resulting powder yield was repeatedly washed with methanol by centrifugation. Subsequently, they were dried in air and designated as Z-NT (non-treated zirconia). Another ZrO₂ support was treated at 400°C with heating rate of 10°C/min under flowing H₂ atmosphere (UHP grade of gases from TIG) for 2 h, designated as Z-H₂ (H₂ treated zirconia).

Tungstated zirconia (WZ) catalysts were prepared by the incipient wetness impregnation of zirconia with an aqueous solution of WCl₆ to obtain the final catalyst having 15 wt% of tungsten loading as given more details in Appendix B. The hydrolysis of WCl₆ possibly resulted in the well dispersion of WCl₆ species in the aqueous solution which is corresponding to the report by Kob et al. [81]. This probably leads to obtained well dispersion on the zirconia support. The freshly impregnated catalyst was dried at 110°C for 12 h. Then, it was calcined at 500°C for 3 h [79]. The nomenclatures given as WZ-NT and WZ-H₂ were used for the tungstated on non-treated zirconia and H₂ treated zirconia surface, respectively.

3.3 Catalyst characterization technique

The various characterization techniques were used to gain more understanding about the catalyst structure and texture properties resulting in their catalytic properties.

3.3.1 X-ray Diffraction (XRD)

Monochromatic powder X-ray diffractograms were recorded in the 10-90° 2 θ range using a XDS 2001 (Scintag Inc.) instrument with Cu K α radiation ($\lambda = 1.54\text{\AA}$ wavelength) for commercially available catalyst namely WZ. The preparation catalysts namely WZ-NT and WZ-H₂ were collected with a SIEMENS XRD D5000 using CuK α radiation with a scan rate of 0.04°(2 θ) per second from 2 $\theta = 10^\circ$ to 80°.

3.3.2 N₂ physisorption (BET surface area)

BET surface area (S_{BET}) measurements were made for every solid catalyst after its respective calcination or dehydration. Prior to surface area measurement, WZ catalyst samples were degassed at 200°C under vacuum (2×10^{-2} mm Hg) for 3 h. SAC-13 samples were degassed overnight at 90°C. Adsorption measurements were carried out using UHP N₂ adsorption at -196°C in a Micromeritics ASAP 2010. Physical properties, such as BET surface area (S_{BET}), pore diameters and BJH cumulative pore volumes for both WZ-NT and WZ-H₂ were evaluated with N₂ adsorption–desorption at -196°C in a Micromeritics ASAP 2020 in a similar procedure with WZ catalyst.

3.3.3 Fourier Transform Infrared Spectroscopy (FT-IR)

FT-IR analysis of ZrO₂ support was carried out in a Nicolet model 6700 of the IR spectrometer using the wavenumber ranging from 400–4000 cm⁻¹ with a resolution of 4 cm⁻¹. A small amount of sample (0.2 g) was thoroughly mixed with ground KBr in an agate mortar and pressed as pellets.

3.3.4 Thermogravimetric analysis (TGA)

Thermal gravimetric analysis (TGA) was used to verify the deposition of carbonaceous residues on the WZ and SAC-13 catalyst surface at these mild reaction temperatures. This experiment was conducted under the condition of temperature from 30 to 1000°C with the ramp of 10°C/min in Air zero grade (100 cc/min).

3.3.5 Electron Spin Resonance Spectroscopy (ESR)

A JEOL, JESRE2X model electron spin resonance spectroscopy (ESR) was used to measure the surface F-center and Zr^{3+} on the surface of ZrO_2 support, WZ-NT, and WZ- H_2 catalysts. Before measurement, the sample was dried at $110^\circ C$ overnight. 0.1 g of sample was placed in a sample tube, which was sealed at atmospheric pressure and room temperature.

3.3.6 Raman Spectroscopy

The Raman spectra of the samples were collected by projecting a continuous wave YAG laser of Nd (810 nm) through samples at room temperature. A scanning range of $200-1400\text{ cm}^{-1}$ with a resolution of 2 cm^{-1} was applied.

3.3.7 Acid site density by Ion Exchange titration

Ion-exchange and titration were used to estimate the acid site concentrations of the catalyst. First, Na^+ ions were exchanged with the WZ H^+ ions, and then the solid catalyst was filtered from the solution. The aqueous solution was thereafter titrated with HCl (0.05N) [37].

3.3.8 Single or dual site mechanism by pre-adsorption of pyridine

For prepoisoning experiments, fresh WZ was added to a known concentration of pyridine in acetone with continuous stirring (1790 rpm) for 1 h at $30^\circ C$. After that, the prepoisoned WZ was decanted from the pyridine-acetone solution and dried at room temperature for 24 h. The amount of pyridine on a sample of the pyridine-poisoned WZ was measured by back titration.

3.4 Reaction procedure and sample analysis

There are three systems used in this research. Firstly, the semi-batch reactor was chosen in order to maintain the low ratio of water-to-oil because water has a deleterious poisoning effect on Brønsted acid catalysts. A high temperature and high pressure reactor (Parr 4590 batch reactor) was used to investigate the kinetics and mechanisms due to this reactor can maintain all components in the liquid phase under this operating condition. Lastly, the operating condition under atmospheric pressure in a batch reactor aims to simulate the 2-phase reaction system with the purpose of examination the catalytic performance of the synthesized WZ catalyst.

3.4.1 3-Phase reaction system in a semi-batch reactor

Reaction kinetics were investigated using a well-mixed isothermal semi-batch reactor (Figure 3.1) consisting of an oil-bath heated, three-neck 50 mL round bottom-flask wrapped with heating tape on the top. Vented gases passed through an ice bath connected to a tap water-cooled reflux condenser. A syringe pump (Genie programmable syringe pump, Kent Scientific Corp.) was used to feed water to the reactor. The temperature range studied was 110-150°C. No organic solvent was used. Eighteen mL of TCp was heated to the desired reaction temperature and then liquid water was injected into the oil at the desired flow rate using a syringe pump (Note: the inlet line leading to the reactor was filled up with water prior to reaction to prevent a “pseudo” induction period). When a constant concentration of water in the liquid mixture was reached (after about 10 min), the solid acid catalyst (typically 1.23 g for 18 mL of TCp, 7 wt%) was added to the reaction mixture over a one minute period while stirring at 900 rpm. Time zero for the reaction was at the end of the complete addition of the catalyst.

Water condensate was collected in the ice bath trap. Samples of 0.15 mL were taken periodically from the reactor and injected into 0.4 mL of 2-propanol solvent at room temperature for analysis. Any solid catalyst present was separated from the liquid sample by centrifugation to limit further reaction. Then a 0.05 mL sample of the resulting liquid solution sample was diluted a second time with 4.85 mL of 2-

propanol and 0.1 mL of methyl valerate was added (as an internal standard). A sample of this final solution (0.1 μL) was then injected into an HP 6890 GC equipped with an automatic injector, an EC-WAX column (30m x 0.25 mm x 0.25 μm), and an FID detector. The GC temperature program consisted of 3 min at 40°C, a ramp of 40°C/min to 180°C (hold for 5 min), and a ramp of 10°C/min to 270°C (hold for 3 min).

Autocatalysis was able to be ignored compared to WZ or SAC-13 catalysis under the experimental conditions used because of its negligible contribution to the overall reaction rate. Initial rate kinetics were measured for TCp (conversion < 10%). Initial reaction rates were determined by a slope of a plot of TCp concentration as a function of time [42].

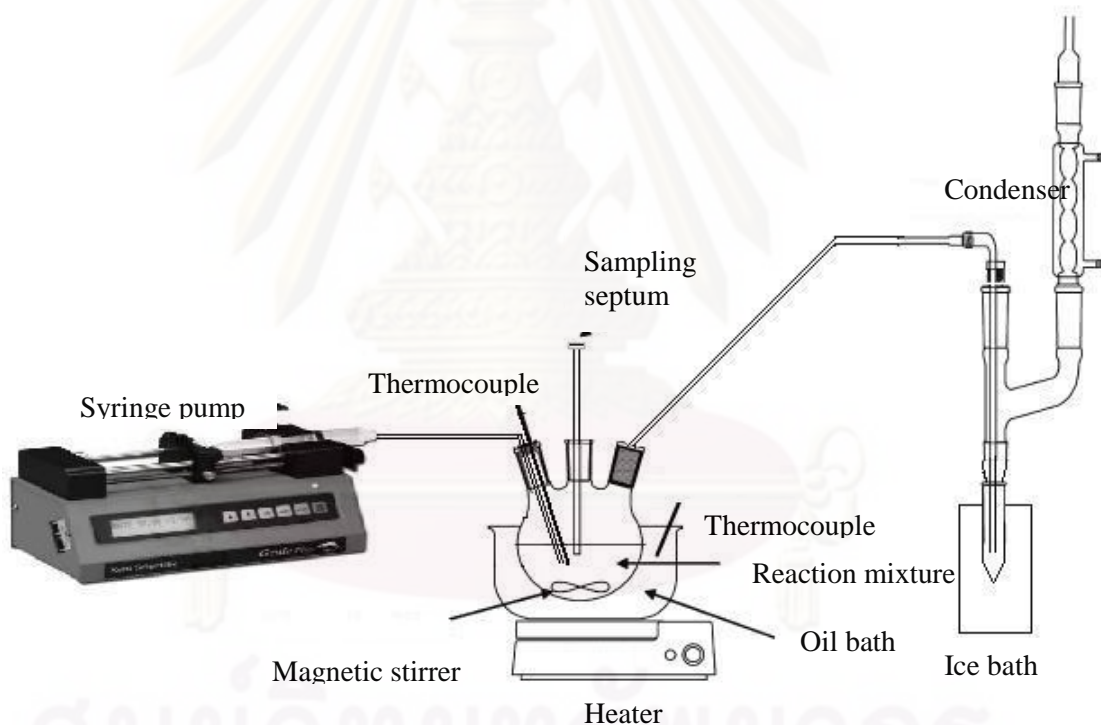


Figure 3.1 Schematic semi-batch reaction system used.

3.4.2 Batch reaction system in a Parr reactor

Reaction kinetics were carried out using an iso-thermal, well-mixed (2140 rpm) Parr 4590 batch reactor consisting of a four bladed pitched turbine stirrer driven

by a high-torque magnetic coupling, a K-type thermocouple and a stainless steel reactor vessel with glass liner. The temperature range studied was 100-130°C. To ensure that all components of reaction mixture were in the liquid phase, the reactor was initially pressurized at 130 psi (higher than the vapor pressure of methanol at 130°C). A constant concentration of WZ catalyst was used (6 wt%) based on the total weight of the reaction mixture. The reactant mixture with solvent (25 mL) and WZ catalyst in the 30 mL glass liner were stirred with a speed of 1280 rpm for 5 min at room temperature. Afterwards, the reaction mixture was heated to the desired reaction temperature during a period of 10 min. Finally, the stirrer speed was increased to 2140 rpm and the time zero for the reaction established at this point. To monitor reaction progress, sample aliquots (0.15 mL) of the reaction mixture were withdrawn at specified time intervals, rapidly allowed to cool and further diluted with 0.4 mL of 2-propanol at room temperature. This resulting solution was then centrifuged to separate out any catalyst particles to limit further reaction. Fifty microliters of the centrifuged liquid were taken and diluted a second time with 4.85 mL of 2-propanol and 0.1 mL of methyl valerate (as an internal standard for GC analysis). A sample of this final solution (0.1 μ L) was analyzed by a Hewlett-Packard 6890 GC with an on-column automatic injector, an EC-5 column (30m x 0.25 mm x 0.25 μ m), and an FID detector. To achieve complete separation, the column temperature program consisted of 3 min at 40°C, a ramp of 40°C/min to 180°C (hold for 5 min), and a ramp of 15°C/min to 270°C (hold for 3 min).

For hydrolysis, the stoichiometric ratio of water-to-TCp for complete conversion is 3:1. However, precise measurement of reaction kinetic data using the stoichiometric ratio was not possible since the high concentration of water led to an induction period due to the formation of a separate immiscible phase of water in TCp. Thus, the range of water and TCp concentrations used in this study was from 1.0 to 1.5 M. In addition, only hydrolysis can exhibit autocatalysis; but it was able to be ignored compared to WZ catalysis under the experimental conditions used because of its negligible contribution to the overall reaction rate. Thus, it did not have to be accounted for in the rate determinations. In order to compare the kinetics of transesterification to those of hydrolysis, a methanol-to-TCp ratio was used in a similar range to that for hydrolysis. However, an extended range of methanol-to-TCp

ratios was also included to address more conventional operating conditions for that reaction. Although the ratio of MeOH (water)/TCp was less than stoichiometric, there was no limitation on reaction due to reactant consumption since only conversions < ca. 15% were studied to determine the kinetics.

The kinetic measurements focused particularly on the initial period of reaction (TCp conversion < 10%) in order to be able to ignore the reverse reaction. The same methodology as described in the previous section [42] was used to determine initial reaction rates.

3.4.3 Batch reaction system in a three neck round bottom flask reactor

The catalytic activity via the esterification reaction between dilute acetic acid (6 wt%) and 1-heptanol was conducted in a stirred batch reflux system at temperature 90°C. A three-necked flask equipped with a condenser and stirrer was charged with certain amount of 6 wt% of dilute acetic acid (6.8 mL) and catalyst samples (0.3 g). Then, the system was heated up to the reaction temperature after which the pre-heated heptanol (3.2 mL) was added. Sufficient stirring of the mixture was used to avoid external mass or heat transport limitations. The reaction temperature was maintained by means of a thermostatic paraffin bath in which the reactor was immersed. For catalytic activity measurement, samples were diluted with 2-propanol (10 mL) to stop reaction and perform in a single phase, and then analyzed by GC (Shimadzu) equipped with a flame ionization detector and Chrompack SE52 column. A sample of this final solution (2 µL) was analyzed using the column temperature program of 3 min at 50°C, a ramp of 10°C/min to 210°C (hold for 10 min) and use He as a carrier gas.

The reaction was repeated at different reaction times in order to obtain the acetic conversion profiles. All catalysts were employed under similar reaction conditions. GC analysis confirmed that no by-products were formed. The acetic acid conversion (%) was calculated as follows:

$$\% \text{ acetic acid conversion} = \frac{\text{initial acetic acid conc.} - \text{acetic acid conc. at time (t)}}{\text{initial acetic acid conc.}} \times 100$$

CHAPTER IV

RESULTS AND DISCUSSION

The results and discussion in this chapter are divided into three sections. Section 4.1 is described the kinetic study using solid acid catalyzed hydrolysis of TCp in semi-batch reactor. Section 4.2 provided the kinetics and mechanisms study in WZ catalyzed hydrolysis and transesterification of TCp in batch reactor. The role of zirconia surface on catalytic activity of tungstated zirconia via 2-phase esterification of acetic acid was illustrated in Section 4.3

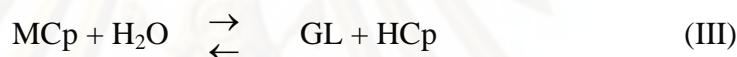
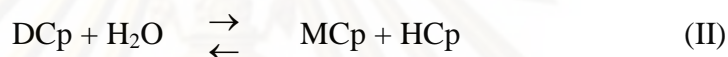
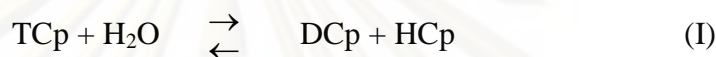
4.1 Solid acid catalyzed hydrolysis of TCp in a semi-batch reactor

The study reported here focused on the applicability of solid acid catalysts for the hydrolysis of oils and fats as a means to ultimately lower the capital and operating costs for TG hydrolysis by conducting the reaction under moderately low reaction conditions (110-150°C and atmospheric pressure). Such a process could be applied in a novel 2-step (hydrolysis-esterification) biodiesel synthesis process using low cost feedstocks containing > 5-15% FFAs. Since the esterification of FFAs is faster than transesterification of triglycerides on acid catalysts, there could be a possibility to construct a more efficient biodiesel synthesis process around the use of 2-step hydrolysis-esterification on solid acids rather than what is now done with 3-step pre-esterification (homogeneous acid catalyzed)–separation (removal of acid and water)–transesterification (homogeneous base catalyzed) [11]. The research involved an investigation of the kinetics of solid acid catalyzed hydrolysis of tricaprylin (TCp) at atmospheric pressure. TCp was used as a model compound for larger TGs and for mixtures (as are typical in fats and oils) in order to facilitate the kinetic study.

The catalysts chosen for this study were SAC-13 and WZ. SAC-13 is a Nafion[®]/silica nanocomposite catalyst, containing only Brønsted acid sites with an acid strength similar to concentrated H₂SO₄, as estimated by Hammett H₀ values (-

H₀~12) [82]. As a result, SAC-13 should catalyze TG hydrolysis—on a site basis—as effectively as H₂SO₄ [28, 83]. The other catalyst chosen for this study, WZ, is a strong inorganic solid acid catalyst, which has been used successfully for a wide range of acid catalyzed reactions, such as dehydration, esterification, hydrocarbon isomerization and cracking [27, 29, 65, 66].

At moderate temperatures, triglycerides (TGs) (main components of vegetable oils and fats) can be hydrolyzed with water/steam to produce three moles of FFAs and one mole of glycerol by the following consecutive reactions:



where TCp = tricaprylin, DCp = dicaprylin, MCp = monocaprylin, GL = glycerol and HCp = caprylic acid.

4.1.1 Catalyst characterization

XRD measurements of WZ calcined at 800°C mostly showed the tetragonal structure of zirconium dioxide, with only small amounts of the monoclinic structure of zirconia with crystallite sizes ≤ 5 nm and of bulk WO₃-like species being detectable [29]. Thermogravimetric analysis of SAC-13 was used to determine the fraction of Nafion in the Nafion[®]/silica composite [82], calculated to be 14 wt% Nafion on silica. This fraction of Nafion corresponds to an acid site density of 0.125 mmol/g, in agreement with the value of 0.131 mmol/g determined from elemental sulfur analysis. Table 4.1 provides a summary of catalyst textural properties determined by the BET method and acid site concentrations as determined by ion-exchange titration for the catalysts studied. The surface areas and acid site concentrations of WZ and SAC-13 were in good agreement with previous reports by Lopez et al. [29] and Mo et al. [31], respectively. The average pore size of WZ was smaller than that of SAC-13, but was

still large enough that pore diffusion limitations of the bulky triglyceride molecules should not have been a problem.

Table 4.1 Pretreatment conditions and characterization results for WZ and SAC-13.

Catalyst	Pretreatment conditions	Parameter			
		S_{BET}^a (m^2/g)	Pore volume ^a (cm^3/g)	Average Pore size ^a (\AA)	Acid Site concentration ^b ($\mu\text{mol}/\text{g}$)
WZ	calcined in static air at 800°C for 2 h	64	0.14	77	155
	methanol wash	61	0.12	74	NA
	re-calcined	65	0.14	77	NA
SAC-13	dehydrated at 80°C under vacuum overnight	208	0.58	80 ^c , 250 ^c	137
	methanol wash	105	0.37	80 ^c , 250 ^c	NA

^a Experimental error = $\pm 5\%$

^b Based on the titration method [37], experimental error = $\pm 7\%$.

^c Bimodal distribution of pores with average pore diameters.

4.1.2 The exclusion of mass transfer limitations

The mixing speed used (900 rpm) was determined to be sufficient to eliminate any mass transfer limitations, as there was no change in reaction rate when the stirred speed was varied from 400-1000 rpm. In addition, by varying particle size for the catalysts, it was found that there were no internal mass transfer effects on the reaction rate, as shown in Figure 4.1 for WZ.

ศูนย์วิทยทรัพยากร

จุฬาลงกรณ์มหาวิทยาลัย

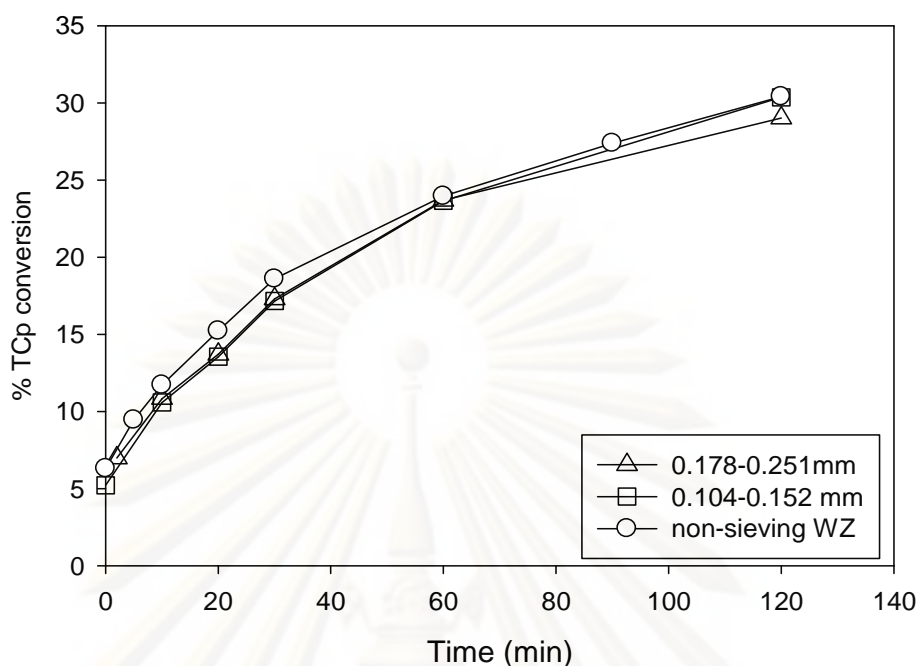


Figure 4.1 The exclusion of internal mass transport effects during WZ catalyzed hydrolysis of TCp at 140°C with water flow rate of 5 $\mu\text{L}/\text{min}$.

4.1.3 Effect of water flow rate on TCp hydrolysis

Water concentration can be a crucial parameter as it may control the reaction rate. Therefore, the influence of flow rate on the concentration of water in the reaction mixture and on the catalyst activity was investigated. Hydrolysis of TCp was measured at 130°C with water flow rates of 5, 10, and 20 $\mu\text{L}/\text{min}$, corresponding with space time 60, 30, and 15 s respectively. For the three-phase reaction system used, water was continuously fed to the reaction mixture in the reactor where it either dissolved or vaporized. The vapor phase leaving the reactor contained only non-reacted water as GC analysis showed no measurable concentrations of organic compounds in the condensate obtained from the cold trap (Figure 3.1).

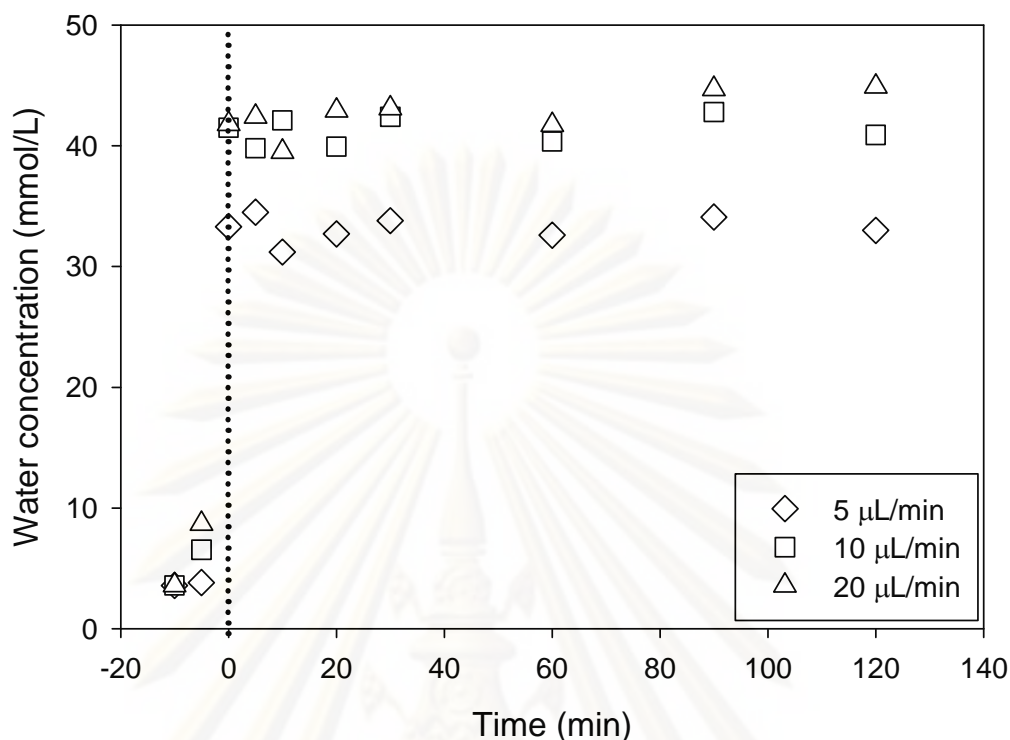


Figure 4.2 Water concentration in the reaction liquid with time-on-stream at different water flow rates (5, 10 and 20 $\mu\text{L}/\text{min}$) in the absence of a catalyst at 130°C.

As shown in Figure 4.2 (with no catalyst addition), a constant concentration of water in the lipid mixture was reached within 10 min (water flow started at -10 min) regardless of the water flow rate used. The offset axis in Figure 4.2 is used to indicate that only after the water concentration in the lipid mixture was constant, the catalyst was added and time zero for the reaction assumed. The amount of water in the lipid mixture increased significantly when the water flow rate was changed from 5 to 10 $\mu\text{L}/\text{min}$. The water concentration in the reaction mixtures also increased somewhat upon increasing the flow rate from 10 to 20 $\mu\text{L}/\text{min}$. The water concentration depends not only on the solubility but also the flow rate of water in, the rate of vaporization of water from the solution and from non-dissolved water, as well as the rate of hydrolysis when a catalyst is present. Thus, there were only slightly higher water concentrations in the reaction mixture for the higher flow rates of water due to the fact that the concentrations of water in solution were nearer to the equilibrium concentration at 130°C. The relative differences seen in the concentration of water on

the catalyst versus those in the liquid phase were within the 10% experimental error. Obviously, the concentration of water on the catalyst is related directly to that in the liquid phase.

How the concentration of water changed when reaction occurred from time $t = 30$ min to 2 h for a water flow rate of $5 \mu\text{L}/\text{min}$ was also investigated. It was found that the water concentration slightly increased from 34.6 to 38.1 mmol/L for WZ catalyzed hydrolysis. The concentration of water for the SAC-13 catalyzed hydrolysis also showed a similar tendency with a slight increase from 36.4 to 39.7 mmol/L. This phenomenon was due to the production of FFA which served as an emulsifying agent thereby affecting the solubility of water in oil [11, 84-86].

As shown in Figure 4.3 (a), similar reaction profiles were observed for WZ when water flow rates of 5 and $10 \mu\text{L}/\text{min}$ were employed, with small variations during the initial stage of the reaction. When a water flow rate of $20 \mu\text{L}/\text{min}$ was used, however, some catalyst deactivation was obvious as the reaction proceeded. There were similar initial reaction curves at short time on stream (TOS) but the significantly lower activity at 2 h TOS (18% lower activity) for the system using a water flow rate of $20 \mu\text{L}/\text{min}$ was confirmed by multiple runs.

As previously reported by us [28, 30, 42], water can cause catalyst deactivation by the hydration of strong Brønsted acid sites. This occurred faster with time for the higher water flow rate even though the concentration of water in the liquid phase remained the same as for $10 \mu\text{L}/\text{min}$ due to the higher water flow rate allowing faster replenishing of the water in solution as adsorption on the catalyst occurred. The conversion curve for a water flow rate of $10 \mu\text{L}/\text{min}$, thus, have been higher than that for $5 \mu\text{L}/\text{min}$ given the higher water (reactant) concentration but for the increase in deactivation of the Brønsted acid sites with increase in water concentration.

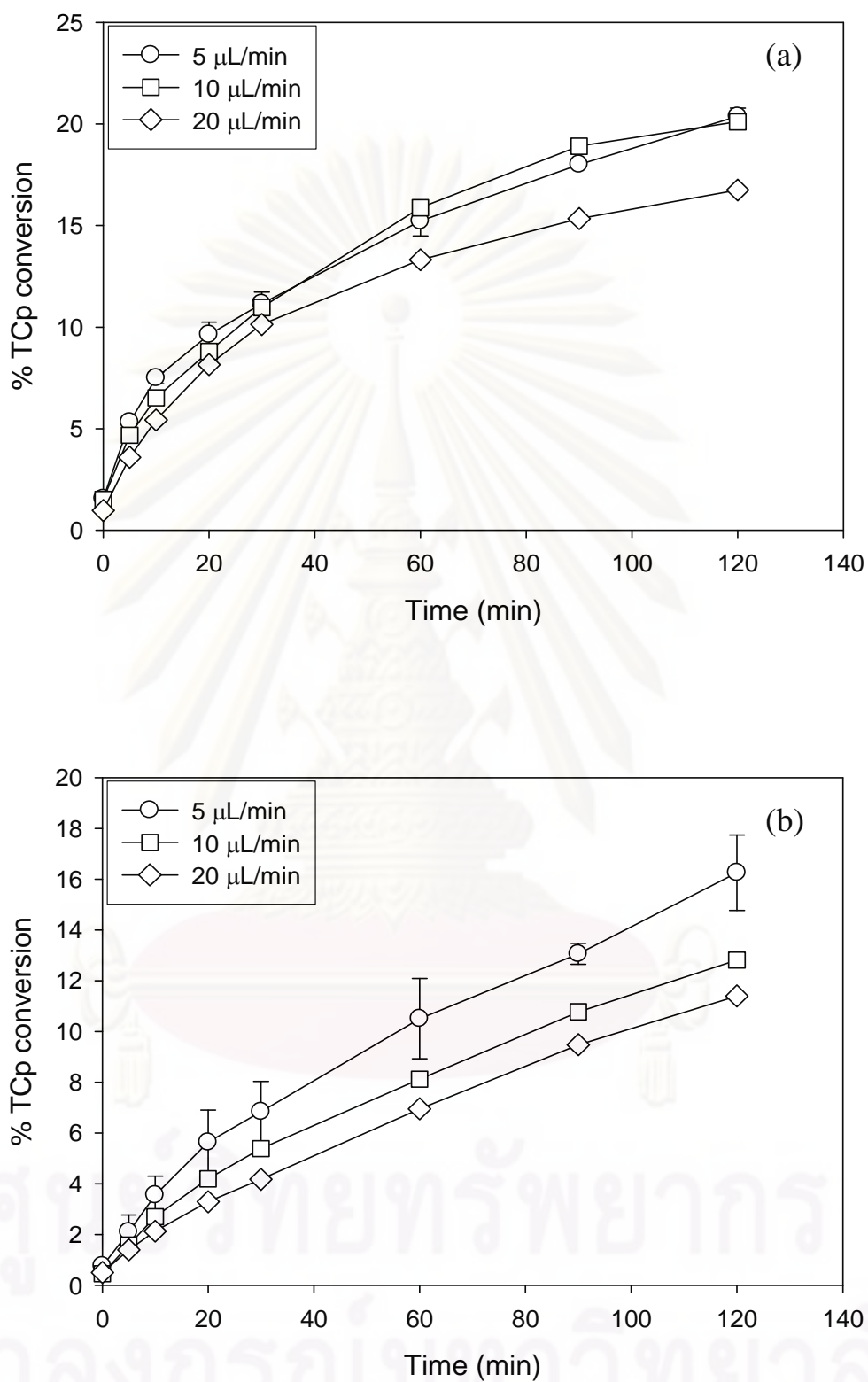


Figure 4.3 Effect of water flow rate on the catalytic activity for TCp hydrolysis of: (a) WZ and (b) SAC-13 [T = 130°C, P = 1 atm, water flow rate (5, 10 and 20 $\mu\text{L}/\text{min}$)].

Table 4.2 The catalytic activity, selectivity, and absolute amount of water on the catalyst after 2 h TOS at different water flow rates for both WZ and SAC-13 at 130°C.

Water feed flowrate (μmol/min)	Initial rate of TCp conv. (mmol / g cat-min) ^a	% TCp conv. ^a @ 2h	% HCp yield ^a @ 2h	% Selectivity ^a @ 2h				Amount of water adsorbed on catalyst ^b after 2h of reaction	
				DCp	MCp	GL	HCp	mmol/g. cat	% (v/v) of pore vol filled with adsorbed water
<u>WZ catalyst</u>									
5	0.14	20.4	9.5	72	14	14	100 ^c	0.07	0.88
10	0.12	20.1	10.1	68	20	12	100 ^c	0.12	1.52
20	0.12	16.7	8.1	70	20	10	100 ^c	0.15	1.91
<u>SAC-13 catalyst</u>									
5	0.06	16.3	8.7	67	12	21	100 ^c	0.08	0.25
10	0.02	12.8	7.2	62	15	23	100 ^c	0.12	0.38
20	0.02	11.4	6.4	65	13	22	100 ^c	0.19	0.58

^a Experimental error = ± 5 %.

^b Experimental error = ± 10 %.

^c Selectivity of the products of the carboxylic acid side chains on the glycerides

The amount of adsorbed water on the catalyst was determined after 2 h of reaction with different water flow rates. To measure the amount of water adsorbed on the used catalyst samples, the used catalyst (after a 2 h reaction run) was washed with methanol at room temperature for 30 min (the amount of water removed was not different even using 2 h of washing). Then, the water in the alcohol wash was determined using Karl Fisher titration (Cou-Lo Aquamax KF Moisture Meter, GR Scientific Co.). As presented in Table 4.2, the absolute amount of adsorbed water on WZ after 2 h of reaction increased as water flow rate increased, indicating that indeed higher flow rates of water translated into higher water concentrations adsorbed on the surface of WZ and in the catalyst pores.

A similar deactivation phenomenon with increased water flow rate was observed also for the SAC-13 catalyst (Figure 4.3 (b), Table 4.2). However, for SAC-13, the deactivating effect of water could be seen from the beginning. The somewhat difference in response to increase water flow rate for SAC-13 vs. WZ may have been caused by the presence of Lewis acid sites on WZ. As has been shown in a previous

report [25, 33, 87], in the presence of water, Lewis acid sites can be converted into Brønsted acid sites. If so, for the WZ-catalyzed reaction using a 10 $\mu\text{L}/\text{min}$ water flow rate, there would have been two possible counterbalancing effects: 1) initially, excess water promoted the formation of new Brønsted acid sites that contributed to increased catalyst activity and; 2) excess water deactivated strong Brønsted acid sites by hydration. Thus, it is likely that the combination of these two counteracting effects resulted in the similar reaction profiles observed when using water flow rates of 5 and 10 $\mu\text{L}/\text{min}$ with WZ. SAC-13, on the other hand, has only one type of acid sites: strong Brønsted acid sites on the Nafion, which undergo deactivation in the presence of water. Even though water is required for reaction, deactivation of some sites probably occurs even at low water concentrations. Although adsorption of water molecules can decrease Brønsted acid site strength and may block accessibility by virtue of the formation of water clusters, it is not surprising that SAC-13, and even more so WZ, still has activity when the amount of adsorbed water molecules exceeds the number of sites since the poisoning effect is not 1:1 [33, 87].

As shown in Table 4.2, the water flow rate had only a minimal effect on the selectivity to GL for both the WZ and SAC-13 catalyzed hydrolysis of TCp.

Based on these results, a water flow rate of 5 $\mu\text{L}/\text{min}$ was chosen for the rest of the studies to minimize water deactivation of the catalysts.

4.1.4 Temperature effect on TCp hydrolysis

Temperature plays an important role in the hydrolysis of fats and oils [88-94]. Increasing reaction temperature can lead to better reaction kinetics and improved phase miscibility, important in a potentially diffusion-limited process. The influence of reaction temperature on the hydrolysis of TCp was studied in the presence of WZ and of SAC-13 at 110-150°C, 1 atm, and using a water flow rate of 5 $\mu\text{L}/\text{min}$. The water concentration in the reaction mixture for the reaction temperature range of 110-150°C with no catalyst addition was determined by Karl Fisher titration. It did not appear to vary with temperature and was 1.9 ± 0.05 wt%, corresponding to a water concentration of 32.6 mmol/L. This suggests that the amount of water in the reaction

mixture was not significantly influenced by the reaction temperature in the range 110-150°C for these reaction conditions. The effect of temperature on TCp conversion is illustrated in Figures 4.4 (a) and (b) for WZ and SAC-13, respectively. As expected, reaction temperature impacted positively the rate of TCp hydrolysis. The initial rate of reaction (r_0) for both catalysts increased about 6-fold over the temperature range of 110-150°C. r_0 increased from 0.032 to 0.207 mmol/g. cat.-min for WZ and from 0.025 to 0.143 mmol/g cat.-min for SAC-13. For both catalysts, at 110°C, 10% TCp conversion was achieved within 90 min, whereas the same TCp conversion was obtained in about 10 min at 150°C.

As shown in Figures 4.5 (a) and (b), at a given conversion level of TCp, HCp yield did not depend on reaction temperature, meaning that the three consecutive reactions that constitute the complete hydrolysis of TCp to HCp and glycerol have a parallel thermal dependency for both WZ and SAC-13. This result is similar to that reported for the glycerolysis of rapeseed oil catalyzed by MgO for the synthesis of monoglycerides [95] and the transesterification of poultry fat with methanol using Mg-Al hydrotalcite derived catalysts [96].

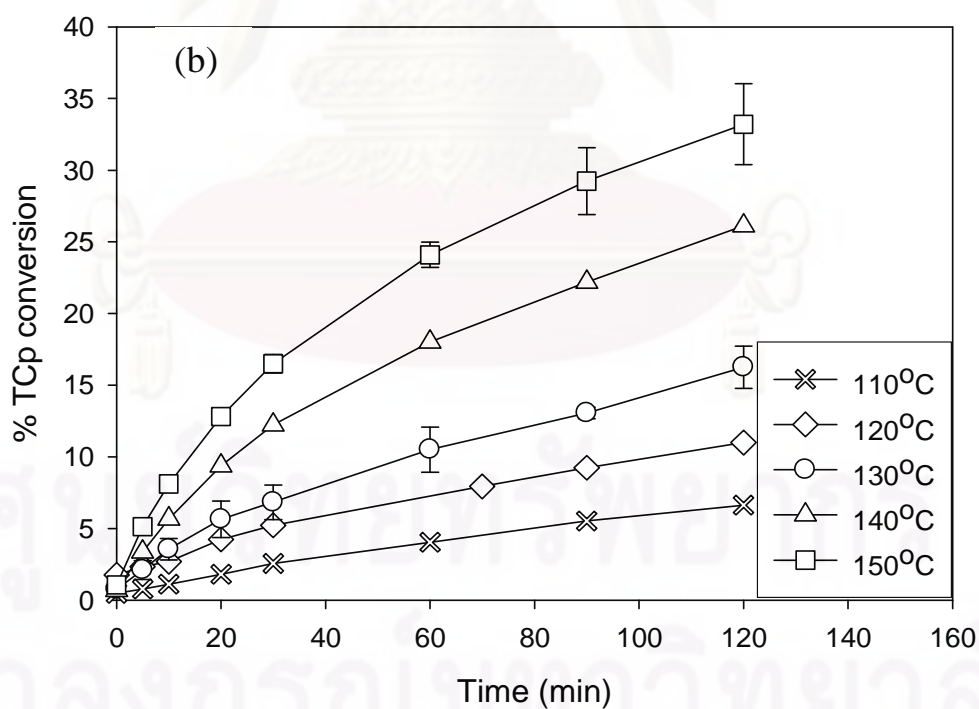
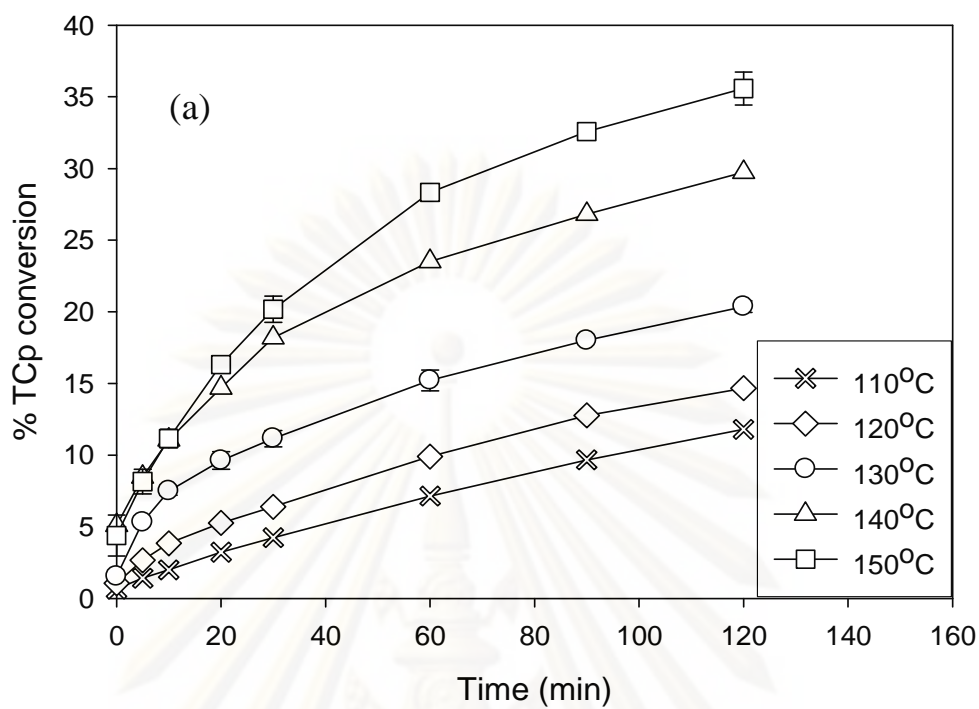


Figure 4.4 Effect of temperature on the catalytic activity in the hydrolysis of TCp at a water flow rate of 5 $\mu\text{L}/\text{min}$ using: (a) WZ and (b) SAC-13.

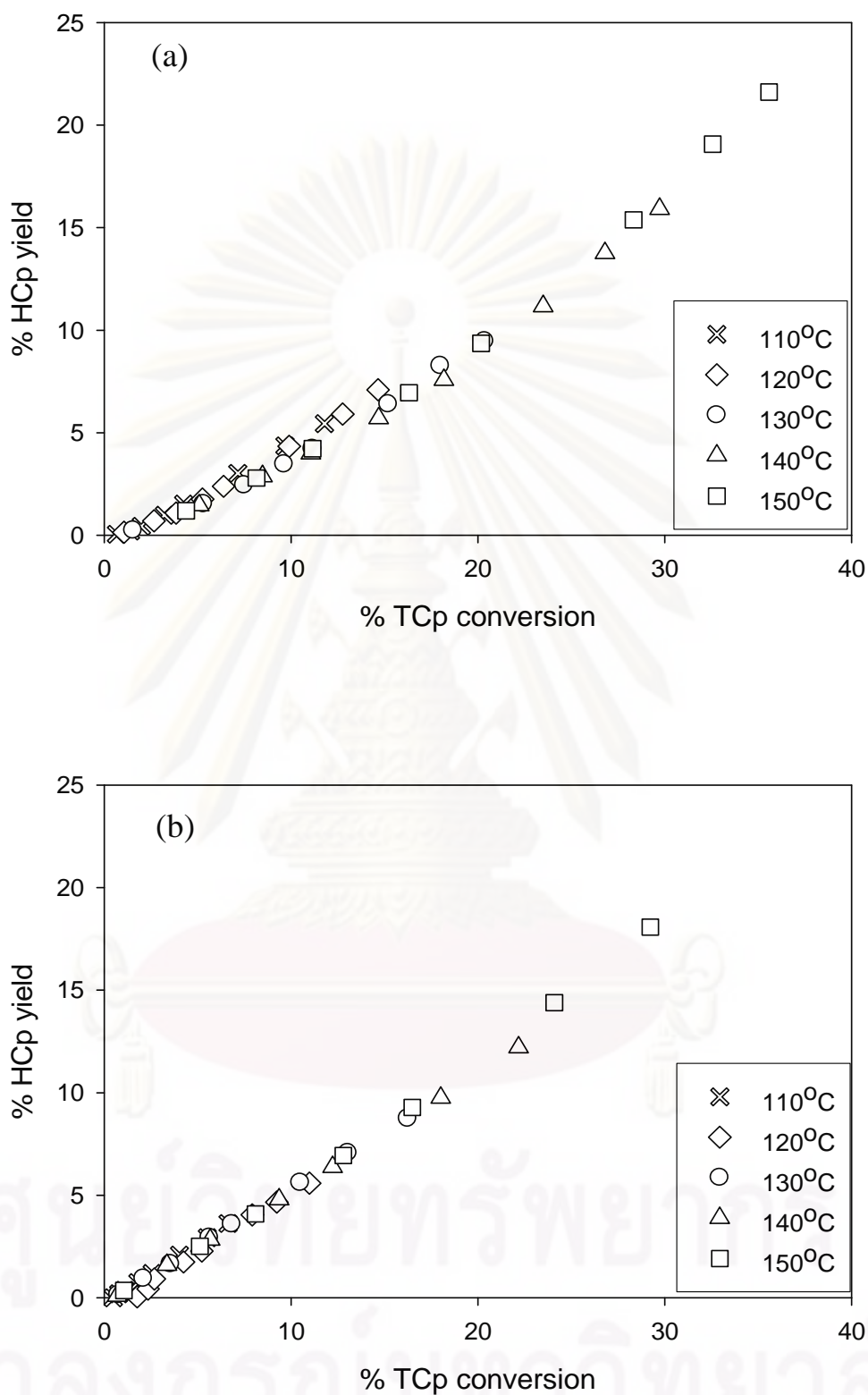


Figure 4.5 Influence of reaction temperature on the extent of TCp hydrolysis to HCp at a water flow rate 5 µL/min: (a) WZ and (b) SAC-13.

4.1.5 Activation energy of TCp hydrolysis

The apparent activation energy (E_{app}) for the solid acid catalyzed hydrolysis of TCp was determined based on the reaction rates measured in the temperature range of 110-150°C as given above. As previously mentioned, the concentration of water in the reaction mixture was unchanged in this temperature range used to determine E_{app} . The Arrhenius plot for WZ shows a deviation for the data point at 150°C from the straight line through the other data points. The observed deviation was not a result of diffusion limitations as the internal and external mass transport limitations for WZ catalyzed in hydrolysis of TCp were examined by varying the average WZ particle size in the range 105-to-250 μm and by using different stirrer speeds from 400-to-900 rpm at 150°C, respectively. The deviation in the Arrhenius plot for WZ at 150°C was found to be due to a more pronounced catalyst deactivation during initial reaction at this higher temperature (not shown). For this reason, the data point at 150°C was excluded from the E_{app} calculation for WZ. The calculated E_{app} values were 70.6 kJ/mol for the WZ catalyzed reaction (110-140°C) and 62.3 kJ/mol for the SAC-13 catalyzed one (110-150°C) (Figure 4.6). The high values of E_{app} confirm the results found by varying catalyst particle size and stirring speed that the overall reaction is kinetically controlled under these reaction conditions. These E_{app} results are in agreement with literature reports of apparent activation energies of 45-68 kJ/mol for the self-catalyzed (by FFAs) hydrolysis of oils (coconut, peanut, and beef tallow) in the temperature range of 225-280°C [84]. In addition, the linearity of the Arrhenius plots in Figure 4.6 for WZ and SAC-13 also provides evidence of a lack of change in the reaction mechanism throughout the range of temperature studied.

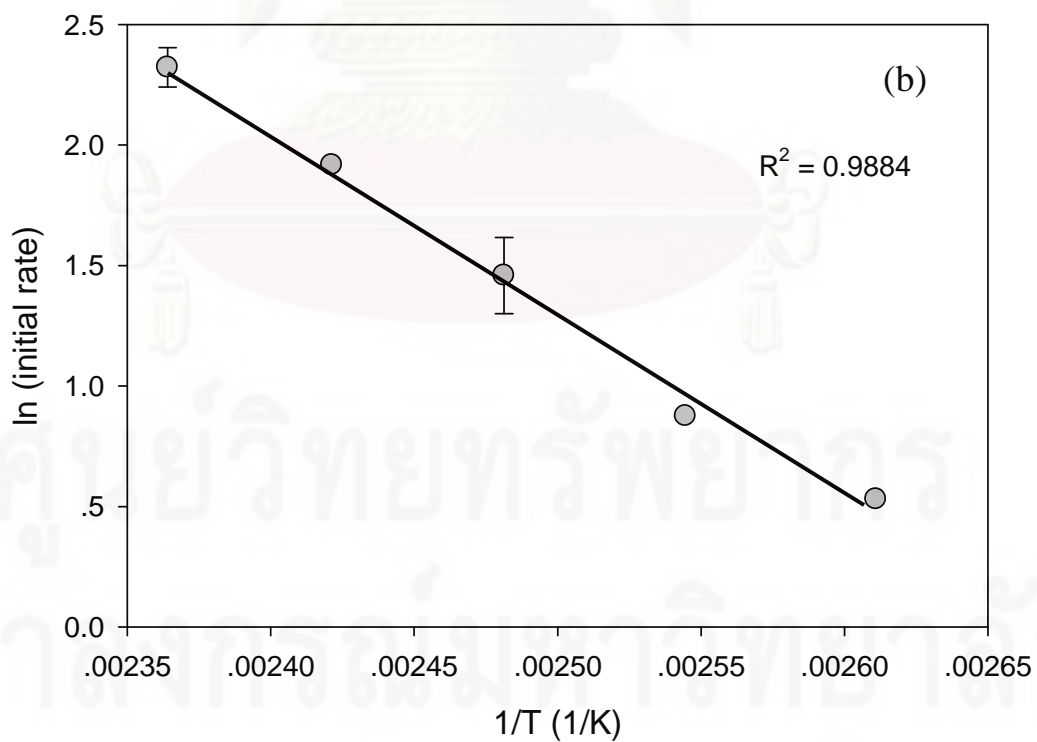
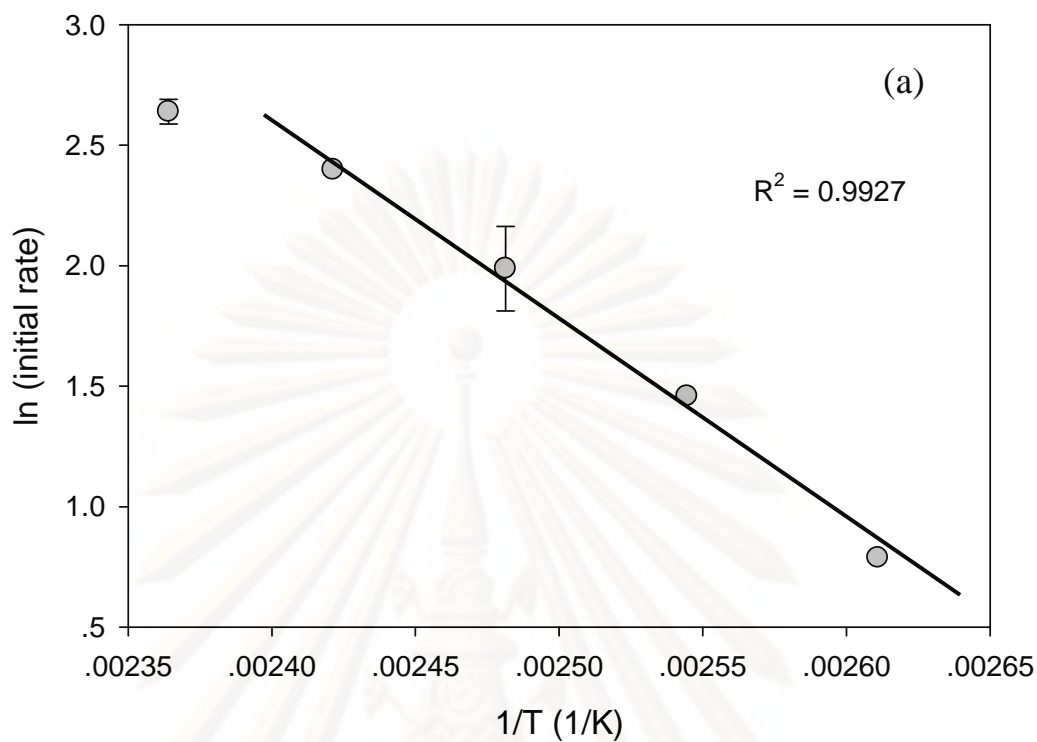


Figure 4.6 Arrhenius plot of the hydrolysis of TCp to DCp in the temperature range of 110-to-150°C: (a) WZ and (b) SAC-13.

4.1.6 Kinetic study of TCp hydrolysis

For a more detailed comparison of the kinetics of the catalysts studied, three-phase hydrolysis of TCp at 130°C, atmospheric pressure, a 60 s space time of liquid water (5 $\mu\text{L}/\text{min}$) or 49 s space time of water vapor, and a catalyst loading of 7 wt% (1.23 g/18 mL of TCp) were used. For these conditions, based on the evidence presented above, there were no mass and heat transfer effects or excessive poisoning of the catalyst by water. Table 4.3 shows the catalytic activity for WZ and SAC-13. A blank test (no catalyst used) was also carried out as water may self-catalyze the reaction since the water self-dissociation constant increases with temperature, promoting the formation of hydronium and hydroxide ions that can give rise to acid/base catalyzed reactions [97]. No significant activity was observed due to catalysis by water, in agreement with Pinto et al. [86], who reported that no oil conversion was found at 150°C and 200°C in the hydrolysis of corn oil using an oil-to-water mass ratio of 85:15. Also, as the amount of FFAs in the reaction mixture increases, the solubility of water in the oil also increases. However, under the reaction conditions used (reaction temperature higher than 100°C, atmospheric pressure), there was no liquid phase separation for the water fed to the reactor since any water not in solution with the TG had to be in the vapor phase.

Turnover frequency (TOF) is an excellent way to compare catalysts on a rational basis. Thus, TOFs, calculated based on TCp conversion less than 10%, are presented in Table 4.3. Both WZ and SAC-13 exhibited 100% HCp selectivity of the carboxylic acid side chains on the glycerides at the less severe reaction conditions employed in this study. This is to be compared to the products from the conventional process operated at high temperature and high pressure, which are of a much lower quality due to the presence of TG cracking products.

Table 4.3 Comparison of catalyst activities in the three-phase reaction system for WZ and SAC-13 (TCp hydrolysis at 130°C with TCp = 2.03 mol/L, H₂O flow rate = 5 μL/min, and 7 wt% catalyst loading based on TCp).

Catalyst	Reactivity						
	% TCp conv. ^a		% HCp yield ^a		Initial rate ^b (mmol/L-min)	Initial rate ^{b,c} (mmol/g.cat-min)	Initial TOF ^{b,d} (min ⁻¹)
	@10 min	@2h	@10 min	@2h			
Blank (no catalyst)	0.0	0.9	0.0	0.0	0.1	NA	NA
WZ	7.5	20.4	2.4	9.5	9.3	0.14	0.88
SAC-13	3.6	16.3	1.6	8.7	4.3	0.06	0.46

^a Experimental error = ±5%.

^b Initial rates were calculated using data below 10% TCp conversion and represent rate of TCp conversion, experimental error = ±5 – 15%.

^c Initial rate (mmol/g.cat-min) was calculated by dividing the initial rate by the weight of catalyst given in Table 1 as follows: initial rate (mmol/g.cat-min) = $\frac{\text{initial rate} \times \text{vol. of reaction mixture}}{\text{wt. of cat}}$

^d Initial TOF was calculated by dividing the initial rate by the acid site concentration given in Table 1 as follows: initial TOF = $\frac{\text{initial rate} \times \text{vol. of reaction mixture}}{\text{acid site concentration} \times \text{wt. of cat}}$

WZ and SAC-13 showed initial TOFs of 0.88 and 0.46, respectively. It is known that the Nafion resin domains on SAC-13, containing sulfonic groups, have an acid strength comparable to that of concentrated sulfuric acid [82], while the acid sites on WZ are rather a distribution of weak-to-strong acid sites [98]. Thus, one would expect that the TOF for SAC-13 should be greater than that for WZ, rather than smaller. In addition, it can be seen that TCp conversion and HCp yields are not much different for both catalysts after 2 h (Table 4.3). It is in agreement with the titration method used primarily measures the strong acid sites on WZ, resulting in similar TOFs for the two catalysts. As reaction progressed, the rate of conversion decreased due in part to the consumption of the triglyceride in the semi-batch reactor but also due to a partial deactivation of the catalysts with TOS.

After 2 h of reaction, product selectivities were similar, but with SAC-13 slightly better at taking the reaction to completion ($\text{TG} + 3 \text{H}_2\text{O} \rightarrow \text{GL} + 3 \text{HCp}$) than WZ, producing more GL (Table 4.2). However, by looking at the correlation between

the yield of GL and of DCp with TCp conversion (Figure 4.7), GL was observed as early as at 2% TCp conversion for the reaction catalyzed by SAC-13. In contrast, for the reaction using WZ, GL formation was observed only after 7% TCp conversion. Thus, in the initial stages of the reaction, DCp yield was higher for WZ than for SAC-13. Note, however, that after 7% TCp conversion was reached, an identical dependence of DCp yield with TCp conversion was obtained for both cases.

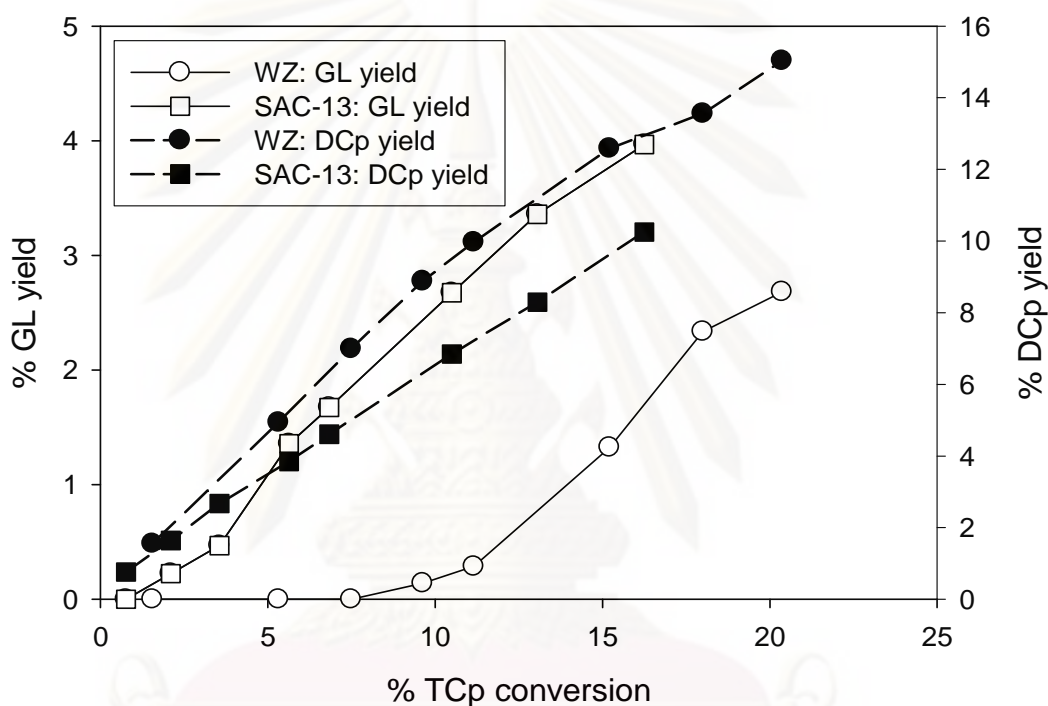


Figure 4.7 GL and DCp yields in WZ and SAC-13 catalyzed TCp hydrolysis as a function of TCp conversion.

ศูนย์วิทยุทรัพยากร

จุฬาลงกรณ์มหาวิทยาลัย

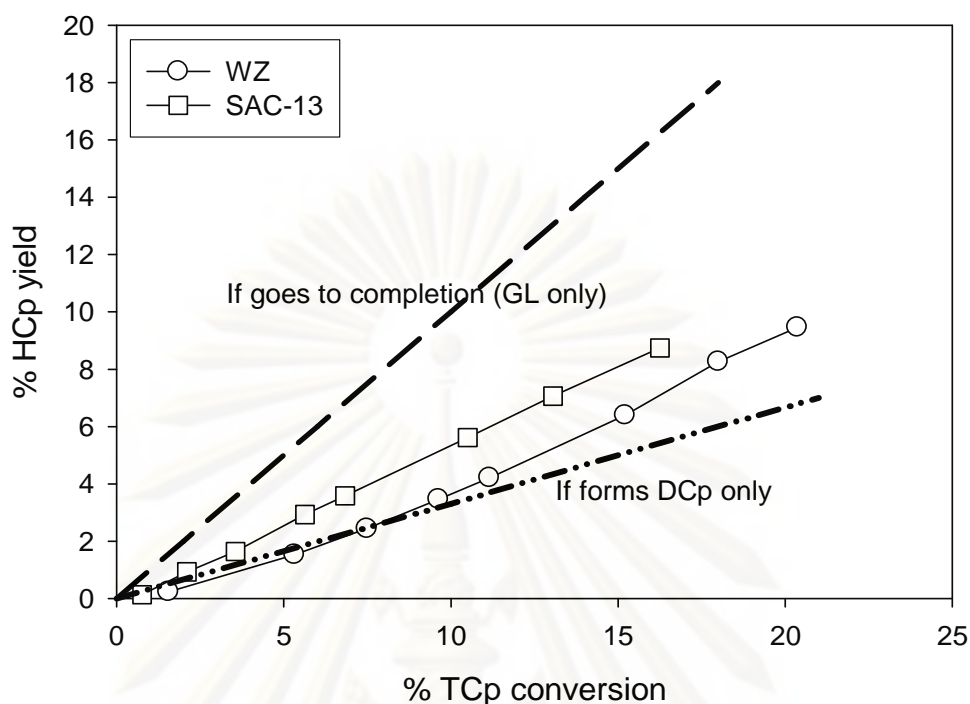


Figure 4.8 HCp yield in WZ and SAC-13 catalyzed TCp hydrolysis as a function of TCp conversion.

Figure 4.8 presents the evolution of the HCp yield with TCp conversion for both WZ and SAC-13. The dashed lines represent theoretical curves. The lower dot-dashed line represents a scenario where only the TG hydrolysis (reaction I in the scheme above) takes place (meaning that DCp and HCp would be the only possible products). The upper dashed line represents a case where every TG molecule reacting would be converted all the way to GL with no significant presence of the intermediates, DCp or MCp. Any plot for HCp yield vs. %TG conversion should fall between these two extreme cases. The plots for the two catalysts shown in Figure 4.8 supports the previous observation that, during the initial period of the reaction, reaction (I) (TG hydrolysis) is preferentially carried out over WZ, while with SAC-13 such preference does not take place. Note, for instance, how for conversions up to 7% the WZ reaction shows an almost identical slope to the theoretical plot for TG hydrolysis only (the lower dot-dashed line), suggesting that this reaction dominates over the other two at this stage of the reaction for WZ. The plot profile for SAC-13, on the other hand, falls in between the theoretical extreme reaction profiles (the

dashed lines), as would be expected for a system where the three series reactions (reactions (I, II, and III)) are all occurring. As can be seen from Figure 4.8, above 7% TCp conversion the HCp yield vs. TCp conversion plots for both WZ and SAC-13 show the similar slopes, indicating that only after this point do reactions II and III (DCp and MCp hydrolysis, respectively) start to take place on WZ to the same extent as they do on SAC-13. An explanation for this behavior has been related to the surface characteristics of the resin vs. the WZ catalyst. For instance, the more polar WZ surfaces should prefer interaction with intermediates such as DCp and MCp through their hydroxyl groups, hindering the activation of the carbonyl functions, and hampering further reaction [7]. Nafion domains, on the other hand, made of perfluorinated carbon polymeric chains (highly hydrophobic [82]), should prefer interaction with the remaining carbonyl groups of DCp and MCp, thereby promoting reaction to glycerol. Thus, initially there was significant conversion of the TG to the DG on both catalysts, but subsequent conversion of intermediates to GL is severely restricted on WZ as can be seen in Figure 4.7.

As reaction progressed above 7% conversion of TCp on WZ, there was a significant change in selectivity as glycerol began to be produced in significant quantities on WZ. This would appear to have been caused by, as also suggested by Liu et al. [36], a transformation of the catalyst surface to a less polar one as the catalyst partially deactivated as a result of carbonaceous species being deposited on the surface. Thus, we speculate that the resulting hydrophobic microenvironments that develop on the WZ surface must be sufficient to promote reaction to completion after an induction period during which only the first step in the hydrolysis primarily occurred.

Apparent activation energy reflects the activation energy of the rate limiting step, but it includes some heats of adsorption that may also reflect in a weaker way the effect of a polar versus non-polar surface. However, issues such as steric hindrance contribute more to the frequency factor of the rate constant, helping to determine the rate of reaction but having a lesser effect, if any, on the apparent activation energy. Thus, based on the evidence given in Figure 4.5, the sequential reactions for TCp hydrolysis to GL on WZ would appear to have similar apparent

activation energies while exhibiting selectivity differences with TOS due to initial steric considerations and surface modification during partial deactivation.

While an effect of adsorbed water on the modification of the catalyst surface is possible, due to the low concentration of water in the reaction mixture and the large amount of hydrocarbon species on the catalyst surface, it is more likely that adsorbed hydrocarbon species had more of an effect on selectivity by modification of the surface characteristics. If pore size of the catalyst played a role in the selectivity, one would expect the catalyst with the smaller pores to be more likely to carry out the reaction to completion than the catalyst with much larger pores due to greater likelihood of further reaction before leaving the catalyst pore. Since this did not happen for WZ, the catalyst with the smaller average pore size, the surface characteristics of the catalysts are likely to have been the main reason for the differences in selectivity of these two catalysts, as also surmised by Liu et al. [36].

4.1.7 Catalyst deactivation and regeneration

Solid acid catalysts have the potential to be recovered, regenerated, and reused, which give them a significant advantage over homogeneous catalysts. The reusability of WZ and SAC-13 was investigated by carrying out subsequent reaction cycles. After each cycle, reaction mixtures were carefully withdrawn, the catalyst recovered, and a new reaction cycle started with fresh reactants. Reusability of WZ and SAC-13 during four consecutive 2 h-reaction cycles of TCp hydrolysis at 130°C with a water flow rate 5 $\mu\text{L}/\text{min}$ are shown in Figure 4.9 (a) and (b), respectively.

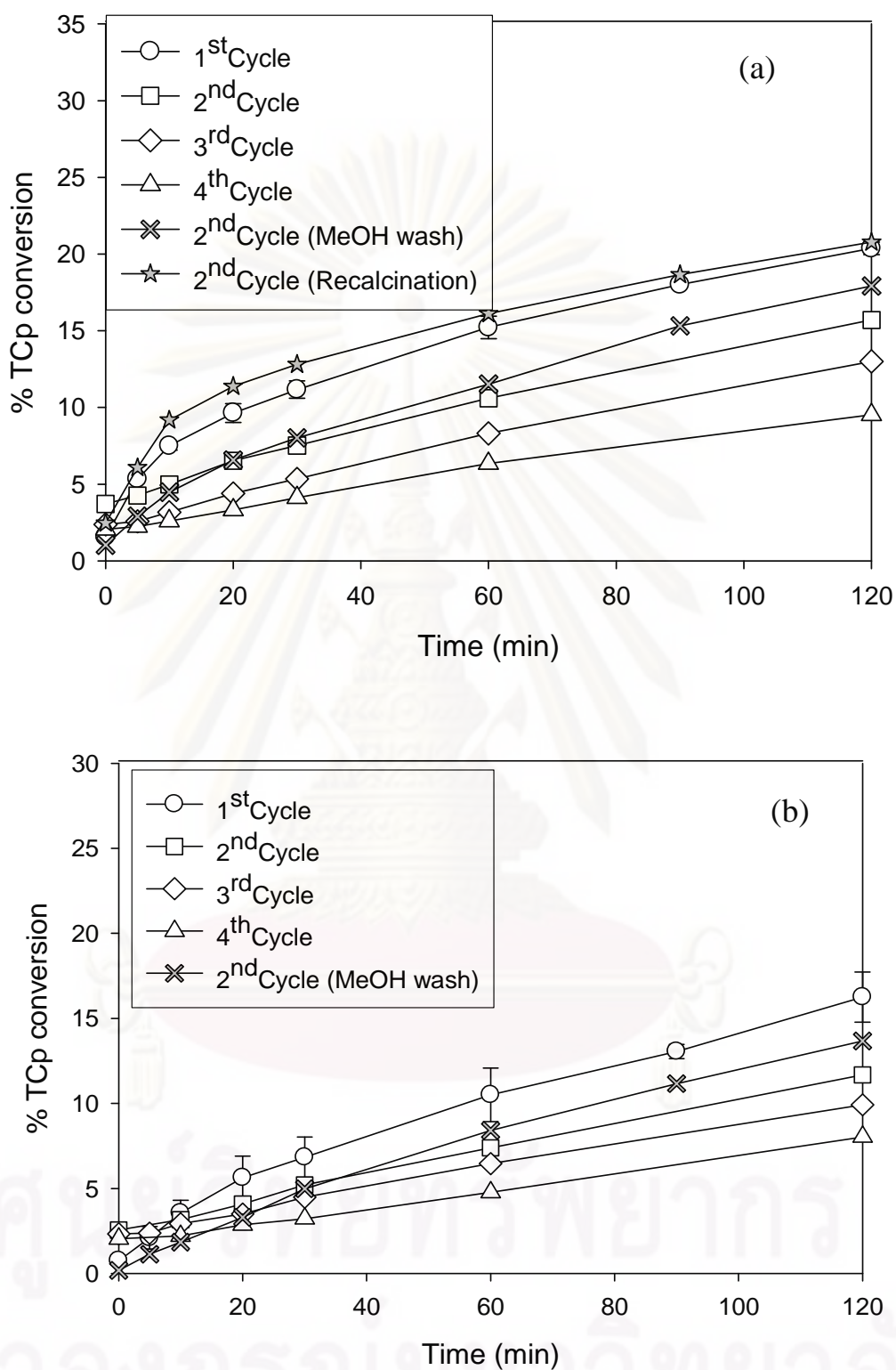


Figure 4.9 Catalytic activity during multiple hydrolysis of TCp cycles with catalyst reuse and regeneration: (a) WZ and (b) SAC-13.

Continuous activity loss with each reaction cycle was observed for both the WZ and SAC-13 catalysts. The reusability of the two catalysts were similar. As has been reported, water can inhibit the catalytic activity of Brønsted acid-based catalysts like WZ and SAC-13 [28, 33, 41]. Thus, water retained from the previous reaction cycle may have been an important factor in catalyst deactivation. However, in accordance with this hypothesis, water deactivation of SAC-13 should have been greater as its stronger acid sites are able to retain more effectively water molecules (see Table 4.2). Therefore, the activity pattern show in Figure 4.9 cannot be explained by catalyst deactivation due to water alone.

Another probable source for catalyst deactivation could have been the accumulation of reactants, intermediates, and/or products on the catalyst surface blocking further access of reactants to acid sites, thereby decreasing reaction. Indeed, the deposition of hydrocarbon residues on the catalyst surface at these mild reaction temperatures (60-130°C) has been observed by FT-IR, thermogravimetric analysis (TGA) and elemental analysis [27, 41, 65]. Figure 4.10 (a) and (b) shows IR spectra in the range 1200-3200 cm^{-1} for the fresh, regenerated and used catalysts for both WZ and SAC-13, respectively. For both used WZ and SAC-13 catalysts, three strong signals were easily distinguished. The stretching frequency of C=O at 1700 cm^{-1} indicates the presence of species with carbonyl moieties. IR peaks at 1460 and 2900 cm^{-1} are ascribed to the bending and/or scissoring vibration of C-H and stretching frequencies of the same in $-\text{CH}_2-$ and $-\text{CH}_3$ groups, respectively [41]. TGA in air supports the further assessment of hydrocarbon accumulation on the used catalysts. As can be seen in Figure 4.11 (a) and (b), for both of WZ and SAC-13, the spent catalysts recovered from TCp hydrolysis have a significant extra loss in mass with temperature compared to the fresh catalyst samples. In these materials, the weight loss before 250°C results from a loss of physisorbed and chemisorbed water or reversibly adsorbed hydrocarbon compounds [29, 41]. The extra loss in mass after 250°C (compared to the fresh catalyst samples) is the result of strongly adsorbed organic species on the WZ catalyst surface except for SAC-13 where it is also due to decomposition of Nafion [41].

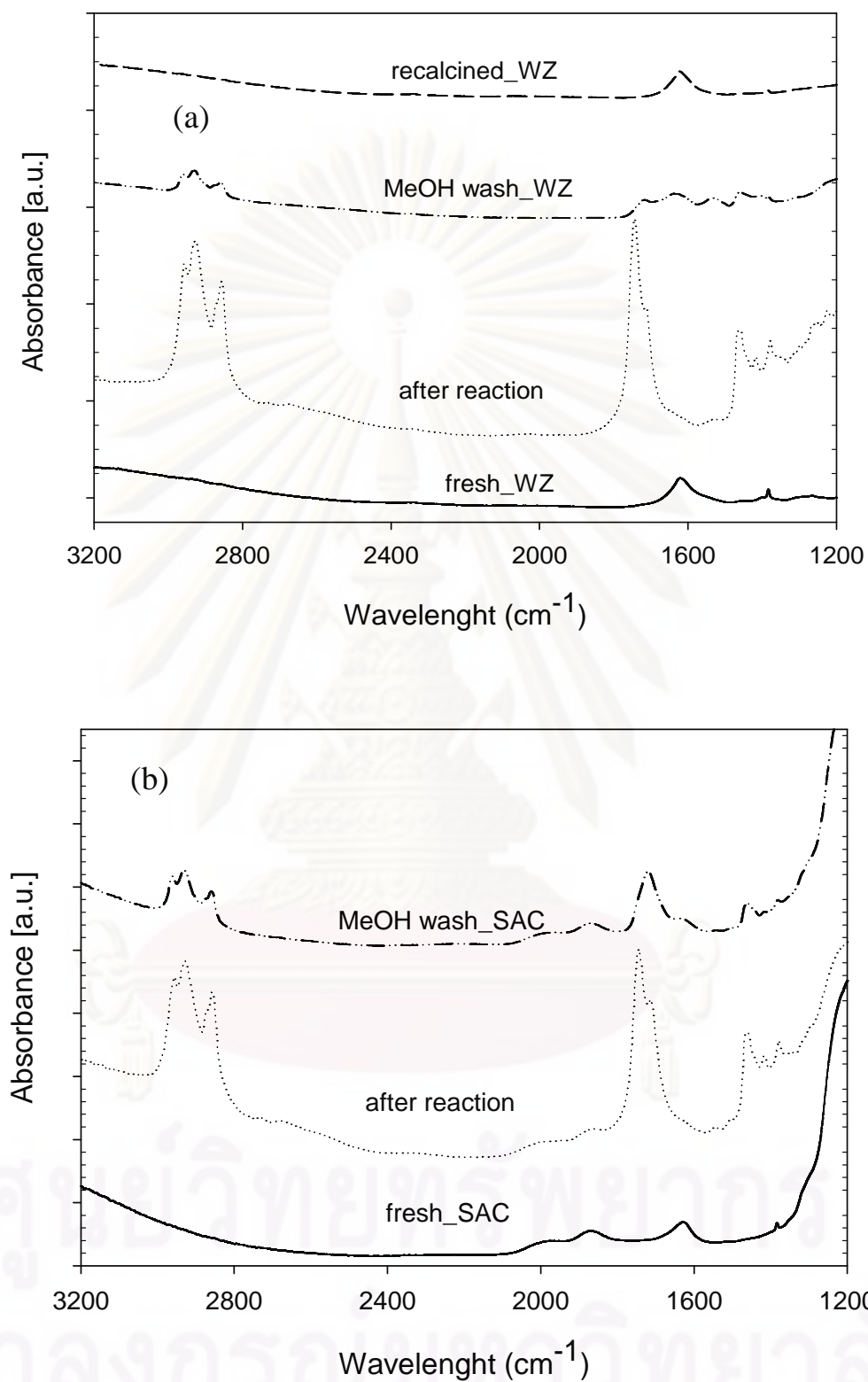


Figure 4.10 IR spectra of the fresh, regenerated and used (after TCp hydrolysis for 2 h at 130°C) catalyst samples: (a) WZ and (b) SAC-13.

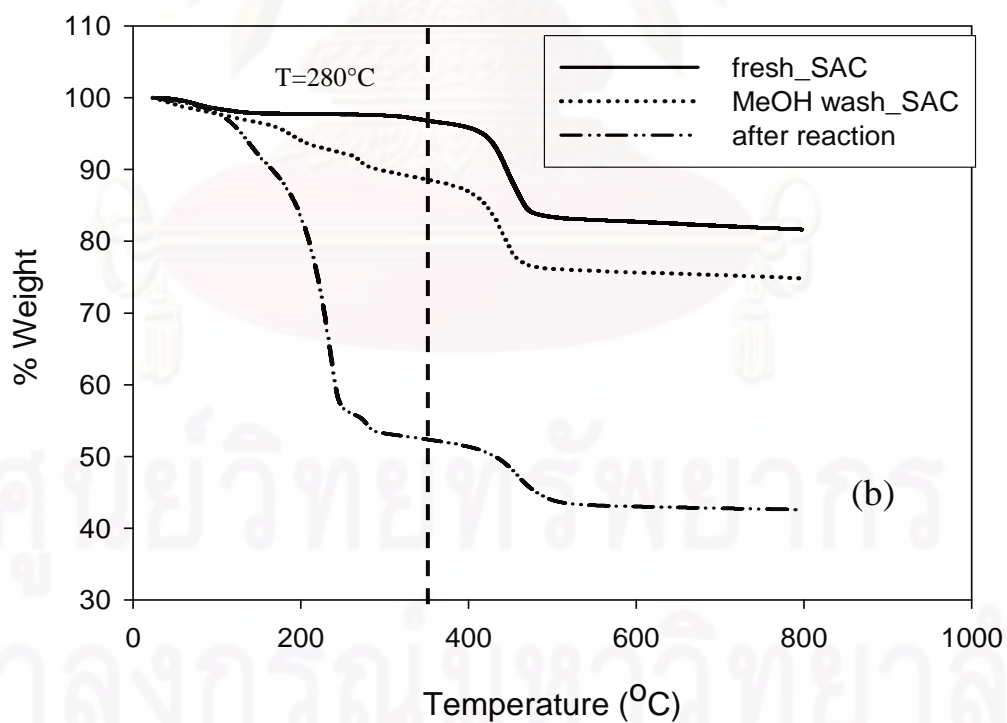
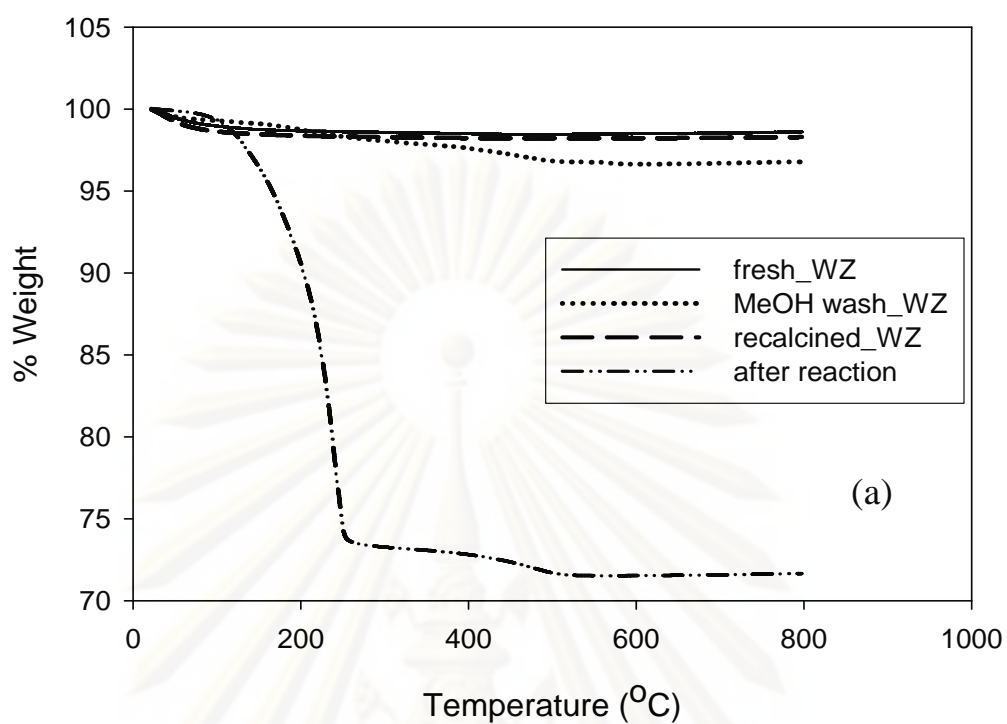


Figure 4.11 Thermogravimetric analysis (TGA) of the fresh, regenerated and used catalyst samples after TCp hydrolysis for consecutive 2 h reaction cycles: (a) WZ and (b) SAC-13.

Elemental analysis results were in good agreement with the results obtained by TGA analysis as shown in Table 4.4. In this study, hydrocarbons deposited on SAC-13 could not be measured directly by carbon elemental analysis (ICP technique) since Nafion contains carbon. Hence, we assumed that the $-\text{SOH}_3$ ligands in SAC-13 were unchanged by reaction due to no leaching of the active catalyst species into solution. This was proved by subjecting fresh SAC-13 to TCp at 130°C under atmospheric pressure with constant stirring. After 2 h, the resulting solution was centrifuged and filtrated to remove the solid catalyst. Then, the solution was used for reaction without any catalyst. It was found that there was no activity from the resulting solution, indicating no leaching of $-\text{SOH}_3$ by the reaction mixture solution as has been shown to occur in transesterification using methanol [54]. Elemental analysis of fresh and used SAC-13 catalyst indicated 4.2 and 2.7% of S-content. Hydrocarbons deposited on SAC-13 affected the S-content in by decreasing the relative amount of S-content in the used catalyst, since the used catalyst contained original catalyst and hydrocarbon. Therefore, the catalyst weight in the sample could be assumed to have 4.2 % of S-content, the amount of hydrocarbon could be easily estimated. As shown in Table 4.4, the average amount of hydrocarbon deposited on the catalyst surface for the used catalysts was 24% and 39% for WZ and SAC-13, respectively. This characterization data further supports the hypothesis of acid site blockage by deposition of organic matter on the catalyst surface, hindering access to active sites for further reaction, as a cause for catalyst deactivation. Moreover, it also supports the hypothesis of a change in surface properties of WZ due to accumulation of hydrocarbon species.

ศูนย์วิจัยทรัพยากร

จุฬาลงกรณ์มหาวิทยาลัย

Table 4.4 Thermogravimetric and elemental analysis for fresh, spent, and regenerated catalysts (WZ and SAC-13).

	WZ				SAC-13		
	Fresh	Spent	Methanol washed	Recalcined	Fresh	Spent	Methanol washed
TGA (wt.% lost)	1.5 ^a	27 ^a	3.3 ^a	1.8 ^a	2.3 ^b	42.7 ^b	14.6 ^b
Elemental analysis (C wt%)	0.18 ^c	19.9 ^c	0.75 ^c	< 0.5 ^c			
Calculation of hydrocarbon deposited (S-analysis) (wt%)					0.0 ^d	35.7 ^d	7.1 ^d
Average amount of Hydrocarbon deposited ^e (wt%)	0.8	24	2.0	1.2	1.1	39	11

^a From room temperature to 800°C.

^b From room temperature to 280°C.

^c Elemental analysis based on carbon deposited

^d Calculation of weight gain from deposited hydrocarbons based on elemental analysis assuming S-content constant

^e Average amount of hydrocarbons deposited based on both TGA and elemental analyses

Attempts to regenerate the used catalyst samples were carried out for both catalysts. Due to thermal stability limitations, attempts to remove deposited organic matter from SAC-13 could only be carried out through methanol washing. For regeneration by methanol washing, after the catalyst (WZ or SAC-13) was recovered from the 1st reaction cycle, it was extensively washed with methanol and dried under vacuum at 30°C for 6 h before a new reaction cycle was started with fresh reactants. WZ was also regenerated by re-calcination in flowing air. The used WZ catalyst sample was washed with methanol one time and then calcined under flowing air (zero grade) at 500°C for 4 h.

As can be seen in Figure 4.9 (a) and (b), methanol washing was not able to completely regenerate catalyst activity to the original activity (1st reaction cycle activity) for either WZ or SAC-13. IR spectra of the methanol-washed regenerated

catalyst samples period are shown in Figure 4.10. This procedure was not able to completely remove strongly adsorbed organic species on the catalyst surface, as shown by the weak IR signals that still can be distinguished in the respective spectra. Catalyst regenerated by methanol washing showed about 2 and 11 wt% more of removable material than a fresh sample of WZ and SAC-13, respectively (Table 4.4). Methanol washing resulted in an activity recovery of 88% for WZ and 84% for SAC-13 with respect to their original activities (Figure 4.9).

In contrast, thermal treatment (recalcination in air) of used WZ samples after the first reaction cycle resulted in 100% recovery of catalyst activity, offering an efficient route for catalyst regeneration. The IR spectrum of the WZ sample regenerated by re-calcination under flowing air in Figure 4.10 (a) shows features identical to that of a fresh WZ sample. TGA profiles for the fresh and the re-calcined WZ samples were also identical (Figure 4.11). Thus, as expected, the air re-calcination method was able to remove all organic species from the catalyst surface.

4.2 Reaction kinetics and mechanisms for hydrolysis and transesterification of TCp on a WZ catalyst

The reaction pathway of transesterification [12], namely alcoholysis is similar to that of hydrolysis [99]. Hydrolysis and transesterification of TGs each consist of three consecutive reversible reactions. In the reaction sequence, TGs are converted stepwise to diglycerides (DG), monoglycerides (MG) and finally glycerol (GL) accompanied by the formation of a FFA in hydrolysis or a methyl ester in transesterification with each step. For each TG molecule, the net reaction produces 3 molecules of FFA (hydrolysis) or 3 molecules of methyl esters (transesterification) and 1 molecule of GL.

In this study, the hydrolysis and the transesterification of TGs with methanol were investigated in order to gain more insight into the kinetics and mechanisms of these reactions at a relatively high temperature (100–130°C) on tungstated zirconia (WZ). Tricaprylin (TCp) was used as a pure model compound for the mixture of large TGs typically found in fats and oils in order to simplify analysis and increase the accuracy of the kinetic measurements. This research provides a comprehensive kinetic study of both liquid phase hydrolysis and transesterification of TCp with the same ratio of reactants at 100–130°C and moderate pressures (120–180 psi). In addition, this work also presents the kinetics of transesterification for a wide range of methanol-to-TG ratios.

4.2.1 Catalyst characterization

The elemental analysis using ICP indicated 13.6 wt% of tungsten in the calcined WZ catalyst, in agreement with the tungsten content reported by the manufacturer (15 wt%). The acid site concentration of calcined WZ determined by ion exchange–titration was 155 μ mol eq H^+ /g.cat. The WZ catalyst had a BET surface area of 64 m^2/g , an average pore size of 8 nm and a pore volume of 0.14 cm^3/g , suggesting that diffusion of the bulky triglycerides molecules into the pores should not be an obstacle for reaction. Powder X-ray diffraction (XRD) of WZ calcined at 800°C exhibited primarily the tetragonal phase of zirconium oxide (2 θ

diffraction peaks at 30.17° , 35.31° and 49.79°) and the formation of detectable WO_3 -like species. The catalyst textural properties of WZ and the XRD results are in good agreement with those found by Lopez et al. [29].

4.2.2 Influence of solvents on the kinetics of hydrolysis and of transesterification for TCp

To study the kinetics and mechanisms of both hydrolysis and transesterification of TCp, the use of a solvent is necessary for liquid phase reaction in order to vary the concentration of one reactant while keeping that of the other constant. In addition, solvents have been employed in biodiesel production processes at low temperature ($30\text{--}60^\circ\text{C}$) to eliminate reaction induction periods due to poor mixing of alcohols and TGs [100, 101]. Since the transesterification of TCp was carried out here at a relatively high temperature ($100\text{--}130^\circ\text{C}$), phase separation was not a major problem and hexane was used as a solvent to maintain the constant volume of the reaction mixture. For the hydrolysis of TCp, it was found in our previous study of this reaction that, due to the significantly different polarities of water and TCp, a reaction induction period is observed even at a temperature of 130°C if no solvent is used. A detailed investigation of the effects of different solvents on the hydrolysis of TCp also indicated that a mixture of hexane and lauric acid (HLA) with 2 wt% of HLA in hexane solution leads to a minimum initial reaction induction period and minimal phase separation compared to other solvents at reaction conditions; thus, this solvent mixture was used for the hydrolysis study. With regards to the influence of solvent on transesterification, one has to note that methanol is less polar than water. This means that methanol and TCp are more miscible, especially at higher temperatures, than a water-TCp mixture, resulting in a more homogeneous distribution of species within the liquid and on the catalyst surface. Because of the esterification reaction of HLA with methanol, the use of a mixture of hexane and HLA was excluded for transesterification, and only hexane was used as a solvents.

4.2.3 Exclusion of mass transport effects for both hydrolysis and transesterification

To obtain precise reaction kinetic data, heat and mass transport effects had to be excluded. Negligible heat transport effects are usually observed in liquid phase reactions [27]. Mass transport depends on the stirring speed of reaction mixtures for diffusion to the external surfaces of catalyst particles and pore size for internal mass transport [30]. The highest reaction temperature was chosen to determine the presence of any mass transport limitations since, if they do not occur at the highest temperature where the reaction rate is the highest, they will not occur for that temperature range. The reaction profiles for TCp conversion in both hydrolysis and transesterification at 130°C were observed to be independent of external diffusion limitations for stirrer speeds more than 2140 rpm as shown in Figure 4.12 (a) and Figure 4.13 (a). Furthermore, internal diffusion did not appear to affect either hydrolysis or transesterification at 130°C for catalyst particles ≤ 0.251 mm since the rate of reaction did not vary with particle size, as shown in Figure 4.12 (b) and Figure 4.13 (b).

In addition, since the triglycerides molecules were much smaller than the pore size of WZ, they would also not be screened from the active sites. These results clearly show the lack of an effect of pore diffusion on reaction kinetics for either reaction, in agreement with previous studies [7, 102]. Thus, for the reaction kinetic studies carried out in this work, an agitation rate of 2140 rpm and catalyst particles ≤ 0.251 mm were employed.

ศูนย์วิทยทรัพยากร

จุฬาลงกรณ์มหาวิทยาลัย

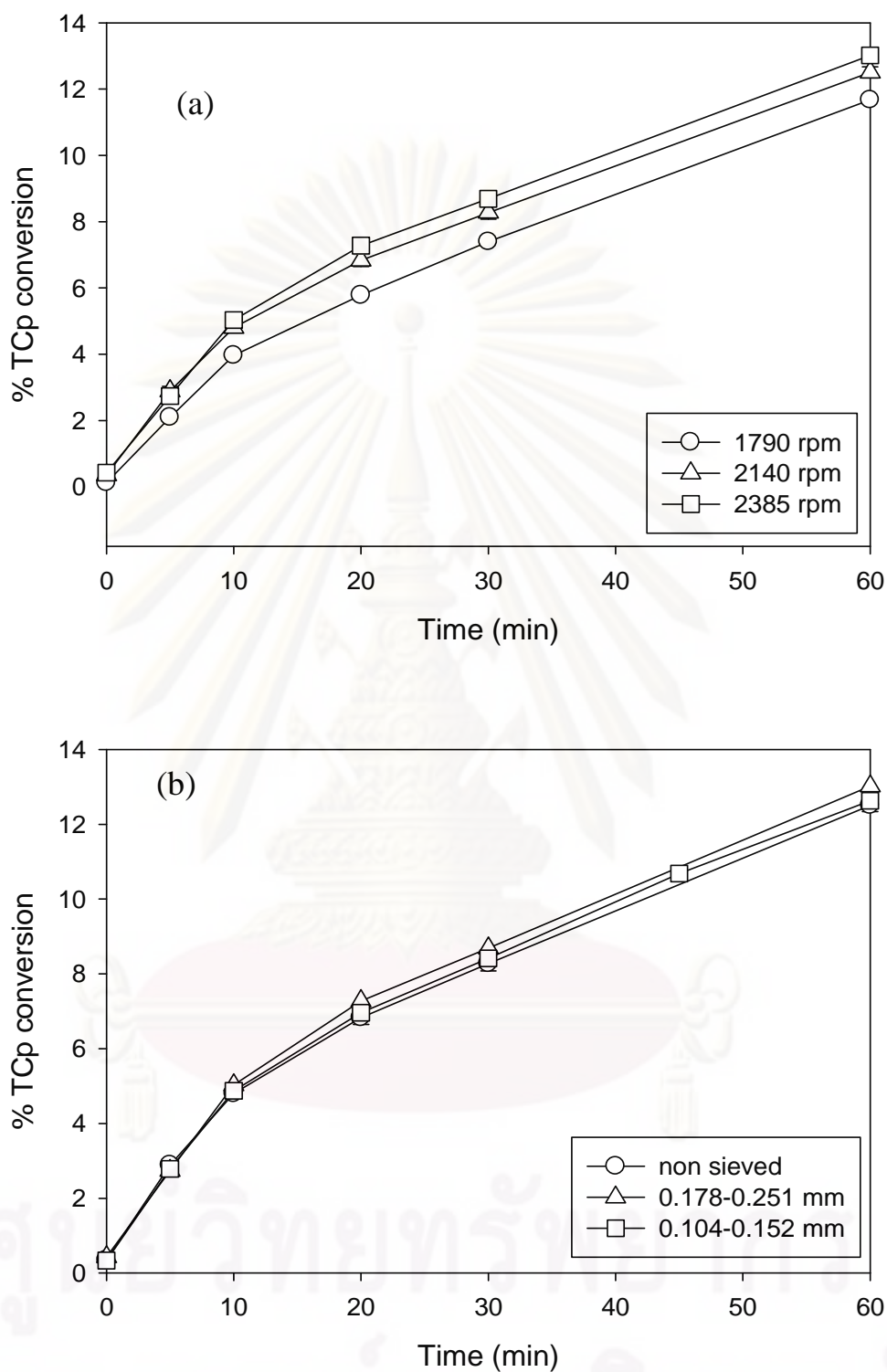


Figure 4.12 Reaction profiles for experiments to exclude mass transport effects on hydrolysis (130°C, 32% v/v of solvent/total reaction volume, H₂O:TCp = 1:1 and WZ loading of 0.06g/mL): (a) various stirring speeds (1790-2385 rpm) and (b) various WZ particle sizes (0.104-0.251 mm and non-sieved WZ).

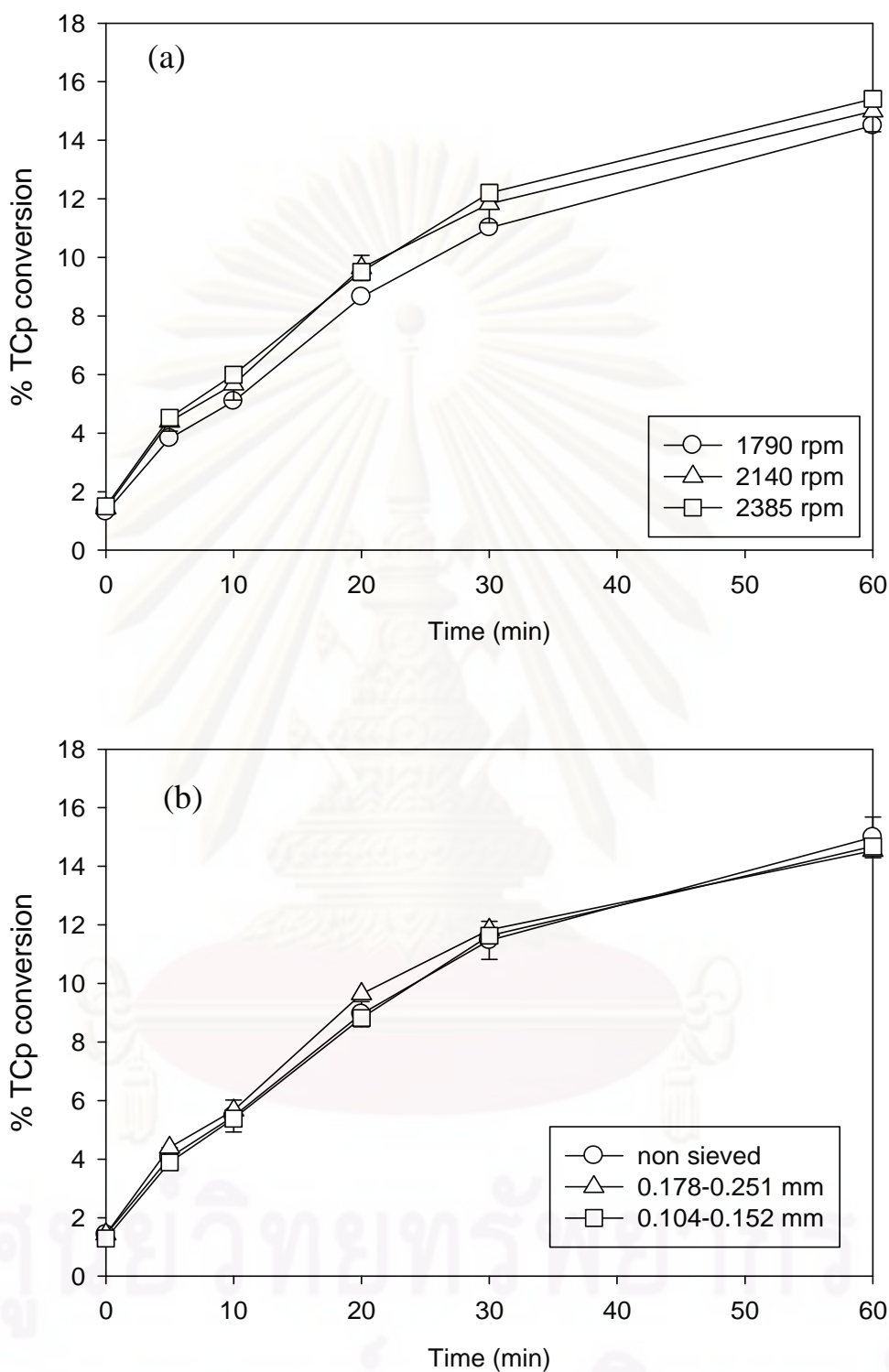


Figure 4.13 Reaction profiles for experiments to exclude mass transport effects on transesterification (130°C , 32% v/v of solvent/total reaction volume, MeOH:TCp = 1:1 and WZ loading of 0.06g/mL): (a) various stirring speeds (1790-2385 rpm) and (b) various WZ particle sizes (0.104-0.251 mm and non-sieved WZ).

4.2.4 Catalytic activity of WZ for hydrolysis and transesterification

Blank tests for both hydrolysis and transesterification of TCp were carried out at 130°C and 130 psi in the absence of the WZ catalyst. Negligible activity (<0.5% TCp conversion after 1 h) was observed in all cases. The maximum % TCp conversions obtained with WZ in place at time zero (at the end of the start-up period) were 0.5% and 2% for hydrolysis and for transesterification, respectively.

Table 4.5 compares the reactivities of WZ catalyzed hydrolysis and transesterification under similar conditions after 10 min and 1 h of reaction. Each reaction demonstrated 100% selectivity to the carboxylic acid or the methyl ester side chains on the triglyceride (HCp and MeCp, respectively). The reactivity based on % TCp conversion for hydrolysis after 1 h reaction period was lower than that of transesterification. However, if one looks at the initial TOF based on TCp conversion (first 10 min of reaction period), the rate of hydrolysis was comparable to that of transesterification. The initial TOF for WZ catalyzed transesterification, here, is greater than that reported by Lopez et al. [27] on a site basis ($\text{TOF}_{\text{WZ}} = 0.355 \text{ min}^{-1}$). This, however, was most probably just due to the higher reaction temperature used here than for the Lopez study. Even though transesterification was run with a MeOH/TCp ratio of 1.0, way below the stoichiometric ratio of 3, while hydrolysis was carried out at the stoichiometric ratio of H₂O/TCp of 1.0, even after an hour the rates of transesterification and of hydrolysis were still similar (not shown in Table 4.5).

The different reaction characteristics of hydrolysis and transesterification can be ascribed to the different impacts of water and methanol, which can be further interpreted mainly by polarity and steric effects. Water has a higher polarity than methanol and is more likely to interact with the acid sites of the catalyst, resulting in faster deactivation of the catalyst. Liu et al. [42] proposed a deactivation effect of water on sulfuric acid catalyzed esterification and suggested that the inhibition effect of water is not significant during the initial reaction period. However, with time-on-stream, water causes the deactivation of the catalyst through a continuous decline in the acid strength due to strong solvation of protons by water molecules. Our earlier study also found that the catalytic activity of WZ for the hydrolysis of TCp in a semi-

batch system decreases with increasing water feed flowrate [102]. On the other hand, methanol has less tendency to interact with the acid sites of WZ, but it is also harder for methanol to form a tetrahedral intermediate by nucleophilic attacking a protonated TCp compared to water due to a steric effect. Thus, it is not surprising that although the initial TOF of hydrolysis of TCp was comparable to that of transesterification for TCp, the 1 h conversion for TCp by hydrolysis was lower than that by transesterification.

Table 4.5 Comparison of WZ catalyzed hydrolysis of TCp ($\text{H}_2\text{O}:\text{TCp} = 1:1$)^a and transesterification of TCp with methanol ($\text{MeOH}:\text{TCp} = 1:1$)^a

Reaction	Reactivity						
	% TCp conv. ^b		% HCp or MeCp yield ^b		Initial rate ^c (mmol/L -min)	Initial rate ^{c,d} (mmol/g.cat- min)	Initial TOF ^{c,e} (min ⁻¹)
	@ 10 min	@ 1h	@ 10 min	@ 1h			
Hydrolysis	4.9	12.6	2.6	7.7	5.7	0.10	0.61
Trans-esterification	5.9	15.5	3.6	10.5	5.25	0.09	0.56

^a At a reaction temperature of 130°C with WZ loading of 0.06 g/mL of reaction mixture.

^b Experimental error = ± 0.5 .

^c Initial rates were calculated using data below 10% TCp conversion and represent the rate of TCp conversion, experimental error = ± 0.1 .

^d Initial rate per gram of catalyst (mmol/g.cat-min) was calculated by dividing the initial rate by catalyst loading (mg/mL).

^e Initial TOF was calculated by dividing the initial rate per gram of catalyst by the acid site concentration of the catalyst per gram.

Water and methanol also led to different final product distributions as shown in Figure 4.14. It is obvious that transesterification drove the reaction more completely towards the final product GL than hydrolysis did since DCp was the primary short term product in TCp hydrolysis, whereas GL, the final product, dominated in TCp transesterification. A higher MeCP yield was also produced from transesterification than HCp yield from hydrolysis, as shown in Table 4.5. This phenomenon suggests a modification of surface characteristics during reaction on the catalyst. Adsorbed water molecules (hydrophilic) probably made the WZ surface more polar [29], while the $-\text{CH}_3$ groups of adsorbed methanol molecules generated a more hydrophobic WZ surface [41]. Liu et al. [36] proposed that intermediate

compounds and solvents can affect the selectivity to GL in the transesterification of triacetin by changing surface chemistry. Thus, the interaction of hydroxyl groups on the glyceride intermediates (DG and MG) with a surface having adsorbed water on it (polar) should be thermodynamically more favorable decreasing further reaction to GL. On the contrary, the WZ surface with adsorbed methanol is less polar, enhancing the adsorption of the FFA side chains of tri/di/monoglycerides and the subsequent surface reaction to the final product GL [37].

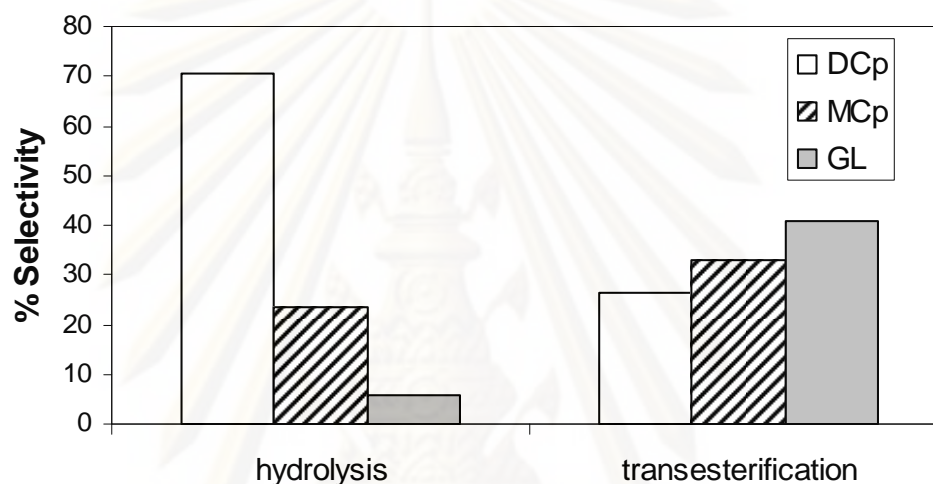


Figure 4.14 Selectivity for DCp, MCp and glycerol on WZ after 1 h of reaction for hydrolysis ($\text{H}_2\text{O}:\text{TCp} = 1:1$) and transesterification ($\text{MeOH}:\text{TCp} = 1:1$) at 130°C with a loading of WZ of 0.06 g/mL .

4.2.5 Influence of reaction temperature on WZ catalyzed hydrolysis and transesterification

Both hydrolysis and transesterification of TCp were conducted at various reaction temperatures, ranging from $100\text{--}130^\circ\text{C}$ with a water-to-TCp ratio of 1:1 (hydrolysis) and a methanol-to-TCp ratio of 1:1 (transesterification). Not surprisingly, as the reaction temperature increased, the initial rates of both hydrolysis and transesterification also increased as shown in Figure 4.15. The estimated value of $E_{app,H}$ for the TCp hydrolysis reaction catalyzed by WZ was 83 kJ/mol as derived from the plot presented in Figure 4.15 (a). This value is higher than the values of 45--

68 kJ/mol, reported by Patil et al. [84] for the autocatalyzed hydrolysis by FFAs in oils (coconut, peanut, and beef tallow) in the temperature range of 225–280°C. The difference in E_{app} is probably due to the use of a solid catalyst and to changes in the mechanism and rate determining step (RDS) [30]. The high value of $E_{app,H}$ found here confirms the results found by varying catalyst particle size and stirring speed that the overall reaction is kinetically controlled by reaction under these conditions.

The apparent activation energy for WZ catalyzed transesterification of TCp ($E_{app,T}$) for the same temperature range was 45 kJ/mol as demonstrated in Figure 4.15(b). This result is consistent with previous reports by Lopez et al. [37] and Bozek-Winkler and Gmehling [64] while it is somewhat lower than that reported by Freedman et al. [21], perhaps due to an effect of reactant chain length [41].



ศูนย์วิจัยทรัพยากร
จุฬาลงกรณ์มหาวิทยาลัย

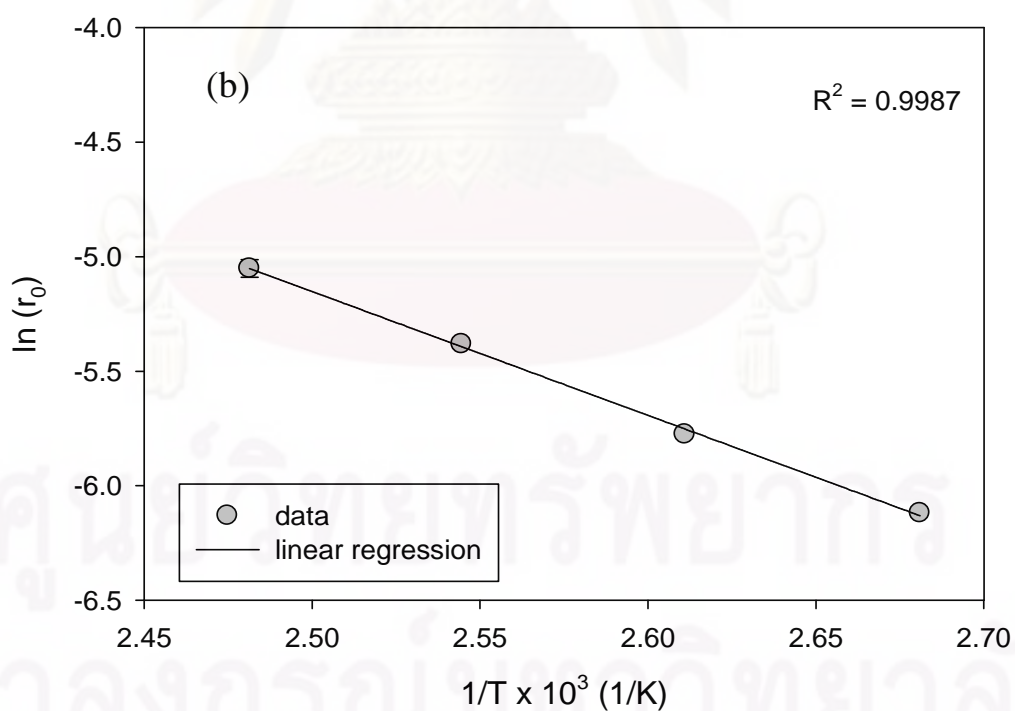
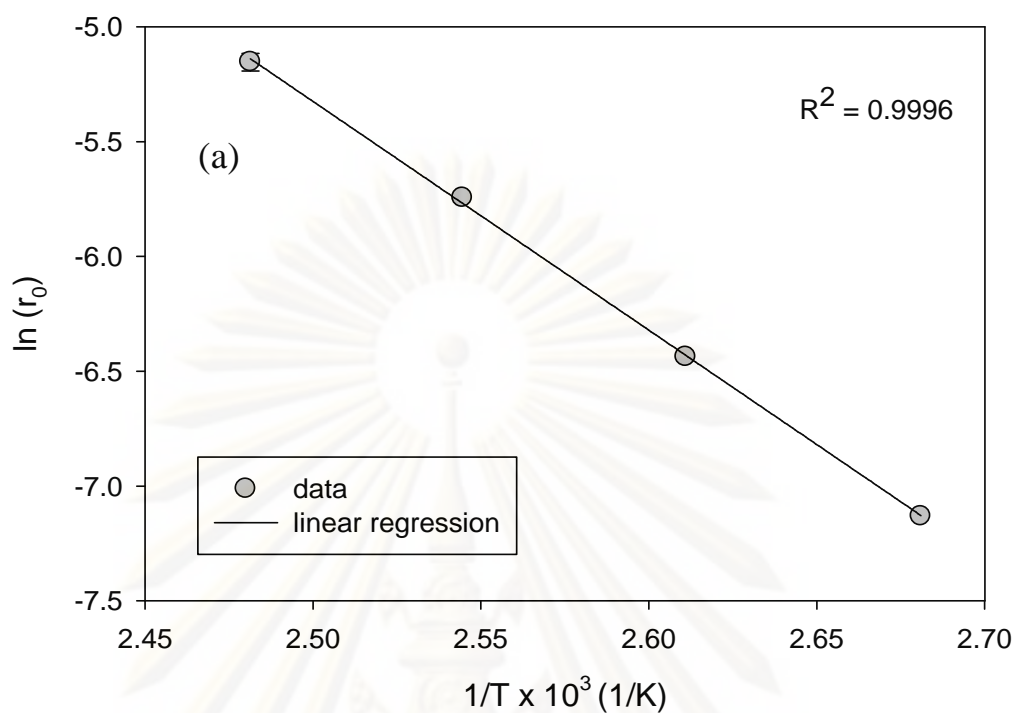


Figure 4.15 Arrhenius plots in the temperature range of 100-130°C with 32% v/v of solvent/total reaction volume using a WZ loading of 0.06g/mL: (a) hydrolysis ($\text{H}_2\text{O}:\text{TCp} = 1:1$) and (b) transesterification ($\text{MeOH}:\text{TCp} = 1:1$).

4.2.6 Concentration effects on the initial rate of reaction for WZ catalyzed hydrolysis and transesterification at 130°C

The concentration effects on the initial rate of reaction were determined by varying the concentration of one reactant while fixing that of the other at 1.25 M as shown in Table 4.6 and measuring the initial reaction rate at 130°C. For hydrolysis, the concentrations of both TCp and water were varied in the narrow range from 0.75 to 1.5 M. These relatively low concentrations of water were used for hydrolysis because water can poison the acid sites of the catalyst [42] and 2-phase behavior (reaction induction period) can occur if the water-to-TCp molar ratio is equal to or more than 2.

Table 4.6 Orders of reaction for WZ catalyzed hydrolysis of TCp and transesterification of TCp with methanol at 130°C for various reactant molar ratios.

Apparent order	α^c			β^g		
Water or MeOH:TCp ratio	0.3– 0.8 ^d	0.8– 1.2 ^e	1.2– 1.7 ^f	0.6– 0.8 ^h	0.8– 1.2 ⁱ	1.2– 7.0 ^j
Hydrolysis ^a $r_{initial} = C_{TCp}^\alpha C_W^\beta$	–	1.34	–	–	–1.15	–
Transesterification ^b $r_{initial} = C_{TCp}^\alpha C_M^\beta$	1.13	0.98	0.85	0.66	0.17	–0.72

^a Maximum error = ± 0.10

^b Maximum error = ± 0.09

^c initial concentration of water (for hydrolysis) or methanol (for transesterification) = 1.25 M

^d initial concentration of TCp = 1.5–4.2 M

^e initial concentration of TCp = 1.0–1.5 M

^f initial concentration of TCp = 0.75–1.0 M

^g initial concentration of TCp = 1.25 M for both hydrolysis and transesterification

^h initial concentration of methanol = 0.75–1.0 M

ⁱ initial concentration of water/methanol = 1.0–1.5 M

^j initial concentration of methanol = 1.5–8.7 M

In order to make the kinetic study of transesterification comparable to that for hydrolysis, the ratio range of methanol-to-TCp used should be the same as that of the water-to-TCp ratio for hydrolysis. This was done as presented in Table 4.6. However, since the operating molar ratio of methanol-to-TCp for studies in the literature has usually been 6:1 in order to achieve higher conversions [4, 8, 12], it was

decided to also explore the effect of methanol-to-TCp ratio up to 7:1. Because of the high molecular weight of TCp, limitation of reaction mixture volume, and amount of solvent used, the concentration of TCp was able to be varied only in the range of 0.75–4.2 M (methanol-to-TCp = 1.7–0.3).

The rates of WZ catalyzed hydrolysis of TCp with water and transesterification of TCp with methanol at 130°C using different initial concentrations are shown in Figures 4.16 and 4.17, respectively. For WZ catalyzed hydrolysis, the initial reaction rate (<10% TCp conversion) was observed to increase as the concentration of TCp increased. Increasing the concentration of water, on the other hand, resulted in a decrease in the initial reaction rate at this temperature (130°C).

For WZ catalyzed transesterification using methanol at 130°C, when the concentration of TCp increased, the initial rate also increased. The concentration of methanol, on the other hand, had a significantly different effect on the initial rate of reaction (Figure 4.17(b)). At low methanol concentrations, the initial rate of reaction increased with increasing methanol concentration from 0.75 to 1.0 M. The concentration of methanol then had an insignificant effect on the initial rate of reaction when it was increased from 1.0 to 1.5 M. At high methanol concentrations (1.5–8.7 M), however, the initial rate of reaction continuously decreased with increasing methanol concentration at this reaction temperature of 130°C.

ศูนย์วิทยทรัพยากร

จุฬาลงกรณ์มหาวิทยาลัย

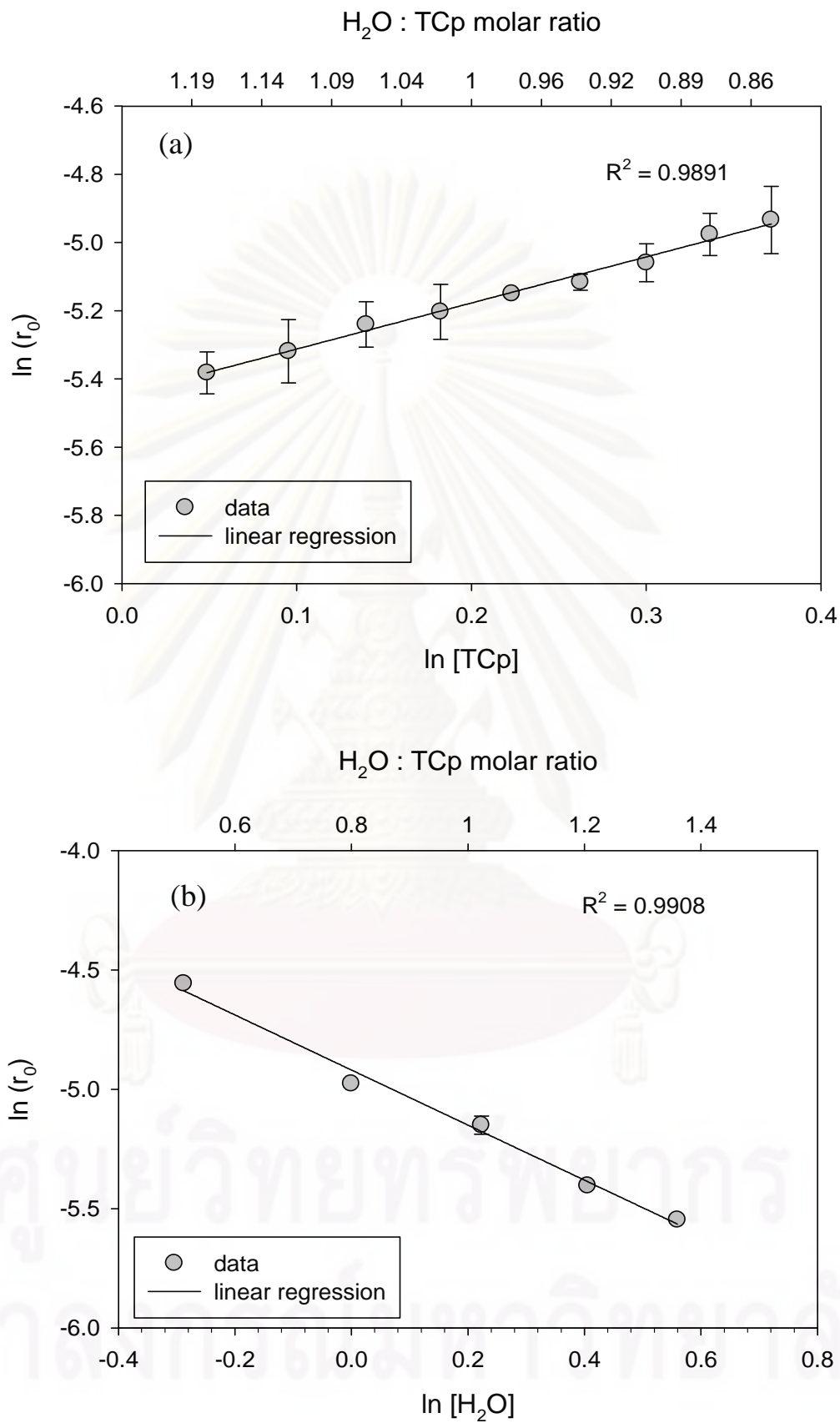


Figure 4.16 Effect of reactant concentration on the initial reaction rate for TCp hydrolysis at 130°C: (a) $C_{TCp,0} = 1.25$ mol/L and (b) $C_{w,0} = 1.25$ mol/L.

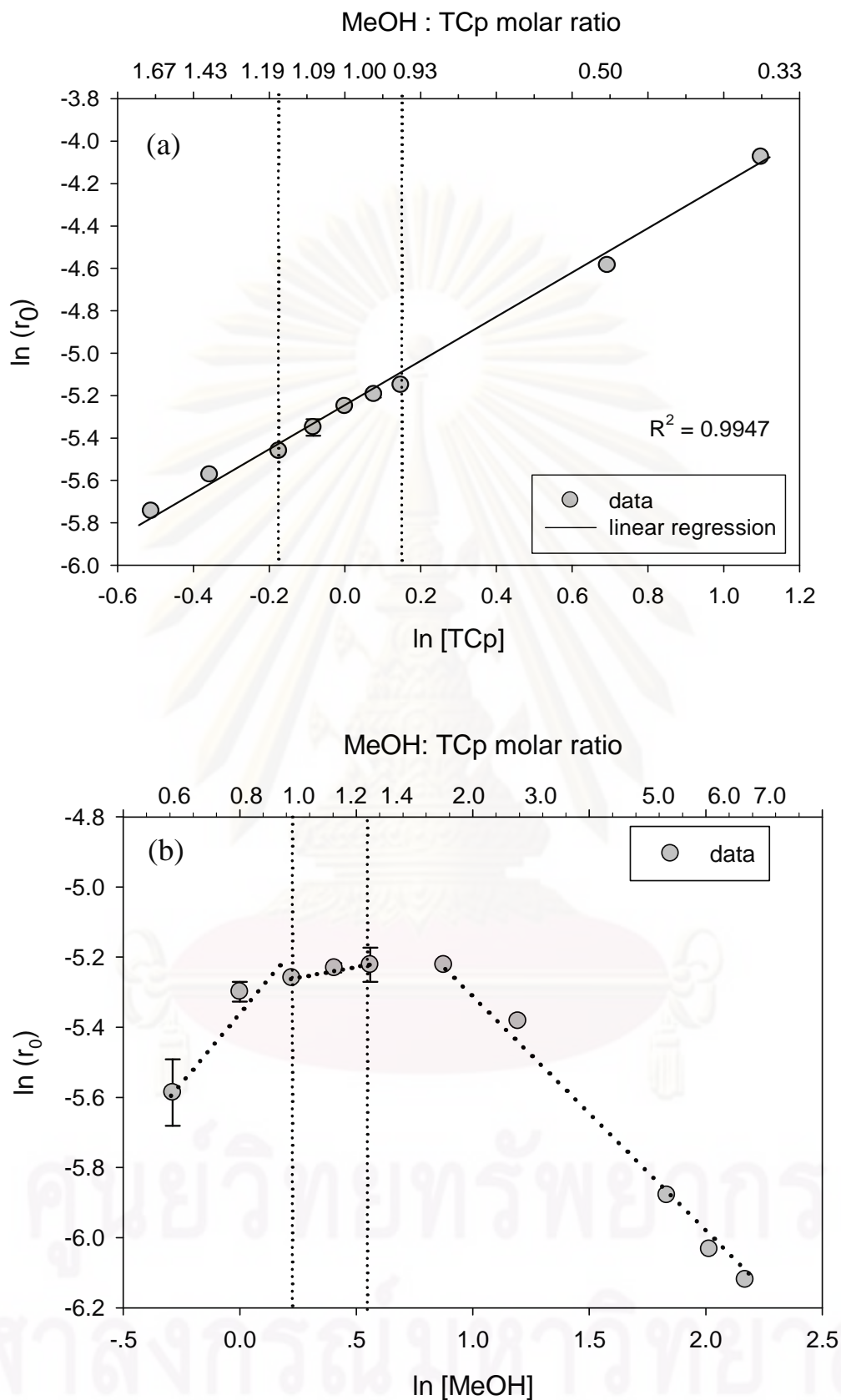


Figure 4.17. Effect of reactant concentration on the initial reaction rate for TCp transesterification with methanol 130°C: (a) $C_{TCp,0} = 1.25$ mol/L and (b) $C_{M,0} = 1.25$ mol/L.

4.2.7 Apparent reaction orders for WZ catalyzed hydrolysis and transesterification at 130°C

Although acid catalyzed hydrolysis of TGs has been known for a long time, the mechanistic pathway is still unclear. Many studies have reported the kinetic parameters for the non-catalytic hydrolysis of refinery rapeseed oil in sub-critical water [11], of canola oil in supercritical carbon dioxide media [99, 103] and of various oils (coconut, peanut, and beef tallow) in a batch reactor [84]. However, the solid acid catalyzed hydrolysis of TGs has only been investigated by Yow and Liew using palm oil [63]. The complexity of water-oil mixtures makes it difficult to obtain good initial kinetic data due to 2-liquid phase behavior [104]. It was found that for the 2-phase situation, the rate of dissolving of water in oils is the RDS of hydrolysis with the solubility of water in oil increasing with FFA formation [63, 99, 103]. Use of a model triglyceride (TCp) and low concentrations of water in this kinetic study permitted us to determine the solid–acid catalyzed hydrolysis mechanism without 2–phase problems. Even though TCp is a smaller TG compared to most in actual fats and oils, it has a reactivity for these types of reaction similar to that of the larger TGs [7, 54].

Using the power rate law approximation,

$$r_0 = kC_A^\alpha C_B^\beta \quad (4.1)$$

the apparent reaction orders for hydrolysis for TCp (A) and water (B) based on slopes of the plots in Figure 4.16 (a) and (b) were $\alpha = 1.34$ and $\beta = -1.15$ for water-to-TCp molar ratios of 0.8–1.2.

The reaction orders for non-catalytic reaction in the temperature range of 100–250°C [84, 99, 103] and for catalyzed hydrolysis on a macroporous cation-exchange resin at 155°C [63] have been reported to be 1 for both TG and water. Under non-catalytic conditions, acid sites are not required to carry out this reaction, thus when the amount of water as a reactant increases, the reaction rate should increase [105]. For acid catalyzed hydrolysis, on the other hand, water has a counterbalancing effect

on the catalytic activity (being not only a reactant for this reaction but also a poison for the active sites), in agreement with the results from the literature [25, 28, 33, 42, 87] for the effects of water on reaction.

For transesterification within a similar reactant ratio range as hydrolysis, the apparent reaction order of transesterification with respect to TCp was $\alpha = 0.98$ (methanol-to-TCp ratio of 0.8–1.2) from Figure 4.17(a). This apparent reaction order of TCp is similar to that for SAC-13 catalyzed transesterification of triacetic at 60°C, as reported by Lopez et al. [37]. The methanol concentration exhibited a strong effect on the apparent reaction order for the transesterification of TCp at 130°C. It was found that there was curvature from the effect of methanol concentration on rate in the methanol-to-TCp ratio range of 0.8–1.2. Therefore, in order to determine if this curvature was due to a transition in order as opposed to just data scatter, the investigation of the apparent order of reaction for methanol was further extended to the methanol-to-TCp ratio of 0.6–7.0. The apparent methanol order went from positive to negative order over the total range. For the ratio of methanol-to-TCp from 0.6–0.8, the apparent methanol order (β) was 0.66. From 0.8–1.2, it was ca. 0.17, and from 1.2–7.0, it was ca. -0.72, as seen in Figure 4.17(b). On the other hand, no significant change in apparent order of TCp was observed in a wider methanol-to-TCp range of 0.3 to 1.7.

It has been reported that the apparent reaction order of methanol for transesterification is zero when larger amounts of methanol (methanol-to-TG ratios $\gg 6:1$) are used [8, 87, 106]. Lopez et al. [37] reported a first-order dependence of methanol for the transesterification of triacetin at low temperature (60°C) using methanol concentrations from 0.67–5.2 M (methanol-to-triacetin = 0.3–2.3). However, an order of -0.7 was obtained for a similar ratio in this study at 130°C. This change in order is likely due to the higher operating temperature especially, or to a lesser degree the different catalyst used. Further discussion of this is given in section 4.2.9.

4.2.8 Selective poisoning of WZ acid sites for hydrolysis and transesterification

To obtain more insight into the number of sites involved in the RDS of WZ catalyzed hydrolysis and transesterification, selective poisoning of the acid sites on WZ was carried out using pyridine (an organic base) [25, 37]. For pre-poisoning experiments, fresh WZ was added to a known concentration of pyridine in acetone with continuous stirring (1790 rpm) for 1 h at 30°C. After that, the pre-poisoned WZ was decanted from the pyridine-acetone solution and dried at room temperature for 24 h. The amount of pyridine on a sample of the pyridine-poisoned WZ was measured by back titration. Figure 4.18 shows that the initial reaction rates at 130°C for hydrolysis (water-to-TCp = 1:1) and for transesterification (methanol-to-TCp = 1:1) catalyzed by pyridine-poisoned WZ decreased linearly with increasing amounts of adsorbed pyridine. These results suggest that the reaction mechanisms for both hydrolysis and transesterification involve a single site for the RDS because of the linearity of the rate with poisoning [32, 37, 107]. An exponential type decay in the activities should have been observed if the RDS of the reactions had involved two sites. Note that both initial reaction rates of hydrolysis and of transesterification were not zero (Figure 4.18) even with what should have been a fully pyridine-poisoned WZ surface ($155 \mu\text{mol eq H}^+/\text{g.cat}$ or $9300 \mu\text{eq H}^+/\text{L}$), perhaps due to some small amount of desorption of pyridine from the WZ surface at the reaction temperature of 130°C.

ศูนย์วิทยุทรัพยากร

จุฬาลงกรณ์มหาวิทยาลัย

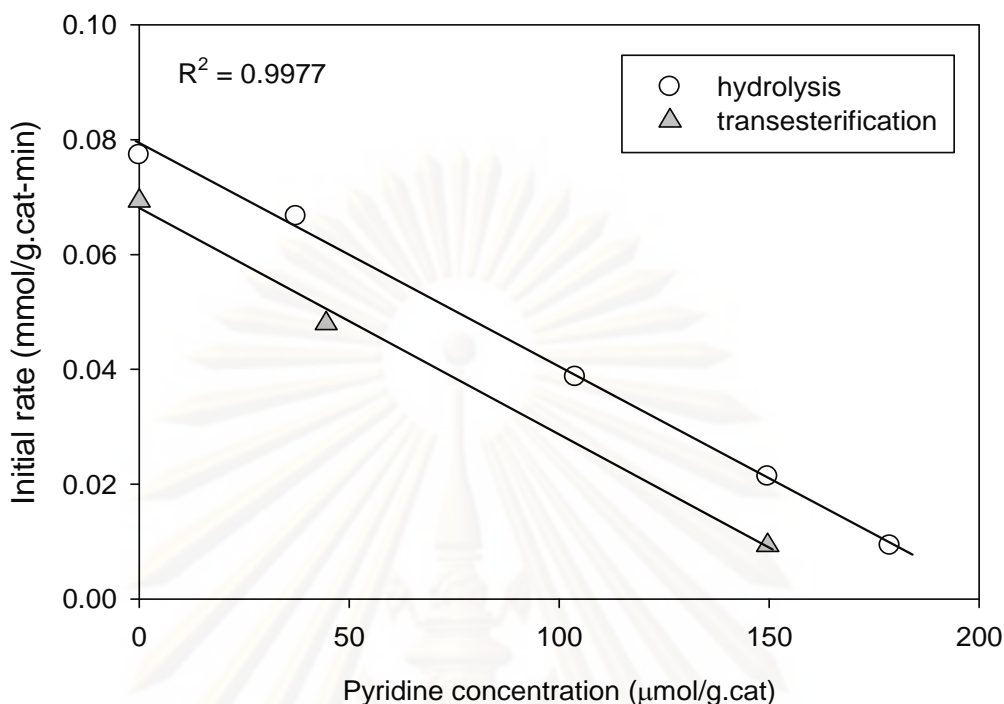


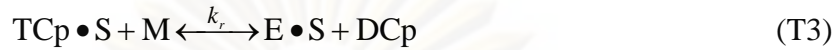
Figure 4.18 Selective poisoning of the acid sites on WZ catalyst using pyridine adsorption (Reaction conditions: $C_{TCp,0} = 1.25$, $C_{W,0}$ and $C_{M,0} = 1.25$ mol/L at 130°C with 0.06g/mL of WZ).

4.2.9 Proposed mechanisms for WZ catalyzed hydrolysis and transesterification at 130°C

The mechanistic pathway for homogeneous acid catalyzed transesterification is well-established to occur via protonation of the triglyceride carbonyl moiety, followed by the attack of the alcohol nucleophile to form a tetrahedral intermediate, which, after proton transfer and disproportion, yields diglyceride and ester products in the temperature range of 60–120°C [8, 21, 106]. For solid acid catalyzed transesterification, Lopez et al. [37] proposed a similar mechanistic pathway as homogenous catalysis involving in a single reaction site based on results for SAC-13 (having only Brønsted acid sites like H₂SO₄ acid) catalyzed transesterification at low temperature (60°C).

Based on the evidence from pyridine poisoning of a single-site mechanism on the WZ surface and apparent orders of reaction of TCp and methanol, a mechanism

similar to that suggested for reaction on SAC-13 at 60°C can also be proposed for WZ catalyzed transesterification of TCp at 130°C. It is as follows:



where M represents methanol, S is a vacant acid site on the catalyst surface, and E is MeCp. TCp • S, M • S and E • S are molecules adsorbed on the catalytic acid sites. This mechanism can also apply to the reaction of DCp or MCp to form GL and MeCp.

This represents an Eley-Rideal type mechanism since non-adsorbed methanol reacts with adsorbed TCp. As Lopez et al. [30, 37] earlier discussed, although it is well known and has been shown that methanol adsorbs on acid catalysts like SAC-13 and WZ, it would appear that for transesterification and esterification its adsorption does not lead to reaction—only partial deactivation of the catalyst.

Using Langmuir-Hinshelwood (L-H) kinetic analysis based on this mechanism, different rate expressions were derived assuming different RDS. The only rate expression obtained this way showing possible first order for TCp and positive order for methanol is the one with surface reaction (T3) as the RDS:

$$r_0 = \frac{k_R K_{TCp} C_{TCp} C_M}{(1 + K_M C_M + K_{TCp} C_{TCp})} \quad (4.2)$$

where r_0 is the initial rate reaction per gram catalyst, K_{TCp} and K_M are adsorption equilibrium constants for adsorption of TCp and methanol respectively, and C_{TCp} and C_M are concentrations of TCp and methanol, respectively.

It would appear that the adsorption term for TCp ($K_{TCp} C_{TCp}$) is small relative to the other adsorption terms. Thus, the order of reaction for TCp is always positive.

Given the strength of methanol adsorption on acid sites, its contribution in the adsorption term is significant. However, a positive order of methanol can be obtained when the concentration of methanol is very low. As the methanol concentration increases, an approximately zero order in methanol can be obtained. But, it is not possible to develop a negative 1st order in methanol based on Equation (4.2). However, since methanol becomes even more competitive for adsorption on the active sites as the concentration of methanol increases, it can be greatly hinder the adsorption of TCp and thus, changing the RDS from surface reaction to the adsorption of TCp. The L-H rate expression would therefore become:

$$r_0 = \frac{k_{TCp} C_{TCp}}{(1 + K_M C_M)} \quad (4.3)$$

This rate expression perfectly fits the experimental results for methanol-to-TCp ratios greater than 1.2, where the apparent orders of reaction are 0.85 for TCp and -0.72 for methanol.

Thus, the above proposed mechanism fits all the experimental evidence for WZ catalyzed transesterification of TCp at 130°C for methanol-to-TCp ratios from 0.3 to 7.0, assuming the RDS changes from surface reaction controlling at low methanol concentrations to adsorption of TCp controlling at high relative methanol concentrations. Such a change in RDS may be due to the polar characteristics of the WZ surface which makes it more likely to adsorb methanol (a strong nucleophile) than TCp (a non-polar compound). The apparent order of methanol for WZ catalyzed esterification of acetic acid has been shown to follow a similar mechanism as the one given above for transesterification. For that reaction, the apparent order of methanol has been found to change from 0.98 (positive order) with surface reaction being RDS to -0.58 (negative order) with adsorption of acetic acid being RDS as the temperature increases from 40°C (liquid phase reaction) to 130°C (gas phase reaction) [30]. SAC-13 (Nafion/SiO₂) catalyzed esterification of hexanoic acid at 150°C also was found to exhibit a decrease in the reaction rate (apparent negative first-order reaction in alcohol) with increasing alcohol concentration [108]. Therefore, it is likely that both temperature and methanol concentration can affect the RDS for transesterification.

Certainly the use of higher methanol-to-TCp ratios, as is commonly done for transesterification at lower temperature in order to increase reaction rate and conversion, actually causes a decrease in rate at higher temperature.

While the mechanism of solid acid catalyzed hydrolysis has not been studied before, the mechanism for homogeneous acid catalyzed hydrolysis of esters is well known in organic chemistry [109]. It is not surprising that its mechanistic pathway is similar to that for homogeneous acid catalyzed transesterification [8, 21, 106] due to the similar nature of the reactants and the overall reaction. Water and methanol share a lot of similarities. The initial step in the hydrolysis of TGs is the protonation of the ester carbonyl, making it more electrophilic, followed by nucleophilic attack by water to create a tetrahedral intermediate. The last step is the deprotonation of the oxonium ion to form the carboxylic acid product and regeneration of the acid site. This reaction sequence is repeated twice to ultimately yield FFAs and glycerol as final products [11, 109].

In this study, the negative reaction order found for water in the hydrolysis of TCp catalyzed by WZ indicates that water does indeed have an inhibitory effect on hydrolysis on a solid acid surface by competing for active sites on the catalyst surface. Water molecules are well known to adsorb on solid acid sites. Based on the experimentally determined apparent reaction orders for TCp ($\alpha = 1.34$) and water ($\beta = -1.15$) for water-to-TCp ratios of 0.8–1.2, a single site being involved in the RDS as indicated by the pyridine poisoning experiments, the well known adsorption of water on acid sites, and the known homogeneously catalyzed mechanism for hydrolysis, a similar mechanism as that for transesterification can be proposed for the hydrolysis of TCp using on WZ for a water-to-TCp ratio of 0.8–1.2,



where W represents water, S is a vacant acid site on the catalyst surface, FFA is HCp.

TCp•S, W•S and FFA•S are molecules adsorbed on the catalytic acid sites. This reaction sequence can be repeated twice to yield FFAs and glycerol as final products.

Based on the experimental evidence, for this mechanism the RDS being the adsorption of TCp provides a L-H mechanistic rate expression that best fits the reaction results:

$$r_0 = \frac{k_{TCp} C_{TCp}}{(1 + K_w C_w)} \quad (4.4)$$

where k_{TCp} is rate constant for TCp adsorption, K_w is the adsorption equilibrium constant for water, and C_{TCp} and C_w are concentrations of TCp and water, respectively. This represents a rate of reaction that is positive order in TCp and negative order in water.

Note that no single-site L-H model will produce an apparent reaction order of TCp greater than 1, assuming that the RDS does not involve 2 molecules of TCp adsorbing on a single site. There is no evidence that this latter situation can happen or would ever give rise to the products of hydrolysis. Thus, the deviation of the experimental apparent TCp order of reaction ($\alpha = 1.34$) from a L-H order of 1 is likely due to assumptions made in L-H kinetic analysis.

This mechanism is also fundamentally an Eley-Rideal type. Although, water can certainly adsorb on the active sites of the catalyst, the actual hydrolysis apparently occurs by reaction of water from the liquid phase with an adsorbed TCp molecule. No term for TCp appears in the denominator in Equation (4.4) due to its adsorption being the RDS.

The mechanisms suggested by the data in which adsorbed TG on the acid site is first protonated and then reacted with water or methanol from the liquid phase successfully describe both catalyzed hydrolysis and transesterification of TCp at 130°C on WZ and are in agreement with the literature [8, 11, 21, 37, 106, 109].

4.2.10 Comparison of hydrolysis and transesterification

As it can be seen in the previous section, an Eley-Rideal single site mechanism with adsorbed TCp reacting with bulk phase water or methanol can successfully describe the kinetic data for both hydrolysis and transesterification on WZ at 130°C. However, it was also found that at same low water (methanol)-to-TCp ratio, the RDS for hydrolysis is the adsorption of TCp while the RDS for transesterification is surface reaction. This may be due to the fact that water is more competitive for adsorption on the active sites than methanol at the same concentration. Thus, water had a more negative impact on reaction at a much lower concentration (even for a water-to-TCp ratio of 0.8); whereas, only after the methanol-to-TCp ratio was greater than 1.2 did transesterification become negative order in methanol and the RDS shift to being the adsorption of TCp.

4.3 The role of zirconia surface on catalytic activity of tungstated zirconia via two-phase esterification of acetic acid and 1-heptanol

This work has been focused on the behaviors of surface nature for the ZrO_2 support prepared by the solvothermal method before and after loading of 15 wt% of tungsten. Based on the similar texture properties, non-treated ZrO_2 support (crystalline zirconia bonding with hydroxide, Zr-OH) was compared to the thermal treated ZrO_2 under H_2 as a reduction atmosphere (crystalline zirconia, ZrO_2). All catalyst characteristics have been investigated by means of XRD, N_2 physisorption, FT-IR spectroscopy, Raman spectroscopy, and electron spin resonance (ESR). The two-phase esterification of dilute acetic acid and 1-heptanol was performed to measure the catalytic activity of WZ catalysts in a batch reactor. This is due to the outstanding properties of WZ (distribution of acid site between Brønsted and Lewis acid sites) that would gain more beneficial for the two-phase esterification, which requires the heterogeneous catalyzed reaction [25, 33, 87, 102].

4.3.1 Catalyst characterization

Upon different treatments of zirconia, it was observed that the color of Z-NT was white, whereas the color of the Z- H_2 changed from white to dark yellow with the treatment of H_2 . This suggested that the thermal treatment under reductive atmosphere generated the F-center (color center) [110] due to the strong Zr-O bond energy that is less likely reduced by H_2 [79]. However, the color of catalyst (WZ and WZ- H_2) has returned to white again after calcination because re-oxidation was obtained [111]. This phenomenon supports the hypothesis in the color change with the presence of F-center which is only observed on the Z- H_2 support.

Figure 4.19 shows the XRD patterns of ZrO_2 support as synthesized (Z-NT) and treated in H_2 atmosphere (Z- H_2). Tetragonal phase (t-ZrO_2) is the primary crystalline structure for Z-NT and Z- H_2 with the diffraction peaks at 30.2° , 35.3° and 49.8° [29]. A crystallite size was calculated from Scherrer's equation of the tetragonal (101) peak [112] as shown in Table 4.7. After the thermal treatment under reduction atmosphere (H_2) was applied on the ZrO_2 , it was found that the crystallite size and the fraction of tetragonal phase structure of Z- H_2 were still similar to those of

Z-NT sample. The crystallite sizes of WZ-NT (4.5 nm) and WZ-H₂ (4.7 nm) were slightly larger than those zirconia supports before the tungsten loading when increasing of the calcination temperature to 500°C. The increase calcination temperature was also allowing to present a fraction of monoclinic phase (m-ZrO₂) with the diffraction peak at 24.3° (Figure 4.19), which is in agreement with the work reported by Wongmaneevil et al. [79].

For this study, the deposit of tungsten did not exhibit to stabilize t-ZrO₂ phase because the impregnation method appeared to permit tungsten being present on the ZrO₂ crystallite surface. It is known that the co-precipitation and sol-gel synthesis are the methods for incorporating tungsten atom into ZrO₂ lattice, which stabilizes the tetragonal structure [73, 74, 113]. WO₃, on the other hand, has not been detected for both WZ-NT and WZ-H₂. This may be due to either relatively low calcination temperature or tungsten loading [24, 25, 68, 69, 71, 114].

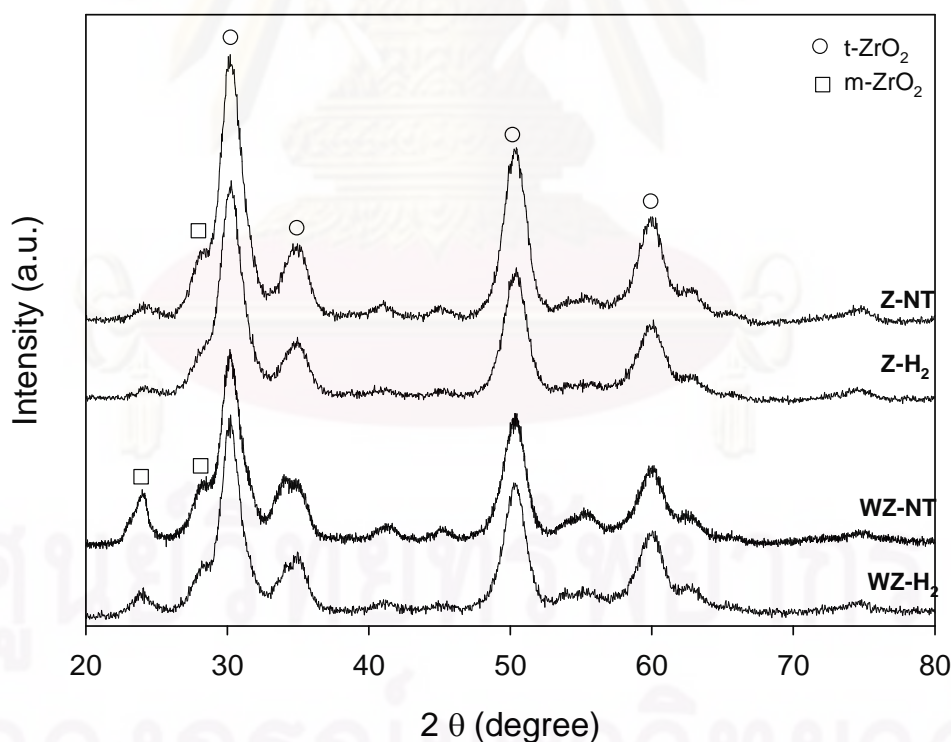


Figure 4.19 XRD patterns for ZrO₂ supports and WZ catalysts.

Table 4.7 Surface area, theoretical W surface density, surface acidity, crystallite size and XRD phases for ZrO₂ support and WZ samples.

Sample	BET surface area (m ² /g) ^a	W surface density (W-atom/nm ²)	Surface acidity by exchange/titration (μmol/g) ^b	Crystallite size (nm)	XRD phases
Z-NT	161	-	-	4.1	t-ZrO ₂ , m-ZrO ₂
Z-H ₂	155	-	-	4.3	t-ZrO ₂
WZ-NT	125	3.93	233.0	4.5	t-ZrO ₂ , m-ZrO ₂
WZ-H ₂	125	3.93	133.0	4.7	t-ZrO ₂ , m-ZrO ₂

^a Experimental error ± 7%

^b Experimental error ± 10%

The catalyst textural properties determined by the BET method and acid site concentrations as measured by ion-exchange titration are listed in Table 4.7. The surface areas of Z-H₂ and Z-NT were comparable within the experimental error. This result suggested that the reductive calcination treatment did not affect on the surface area as corresponding to our previous study [79]. In general, the penetration of tungsten species into the pore of ZrO₂ support could reduce the surface area of WZ-NT and WZ-H₂ [115]. In order to estimate the theoretical nominal W surface densities, WZ surface area and amount of tungsten loading were used [116]. It was found that the W surface coverage of both WZ-NT and WZ-H₂ were presented as the growing surface polytungstated domain and crystalline of WO₃ (~ 4 W atom/nm²) [70, 117, 118].

The other physical properties, such as crystallite size, tetragonal structure, and BET surface area for both Z-H₂ and Z-NT were almost similar, except for the surface defect. The electron spin resonance (ESR) spectroscopy is one of the most powerful techniques used to detect the structural defect, as shown in Figure 4.20. The ESR signal of ZrO₂ can be found with g values, $g_{\perp} = 1.97$ assigned to Zr³⁺ [119] and $g = 2.00$ assigned to F-center [120]. As seen, no ESR signal for the Z-NT sample was observed in the magnetic field ranging between 310 and 370 indicating that no defect occurred on the surface of Z-NT sample. When the ZrO₂ was treated in a reductive atmosphere (H₂), the F-center was present. The dominated intensity of F-center on Z-

H₂ may be produced by the reduction of hydroxyl group on ZrO₂ surface, which is corresponding to the previous reports [79, 110, 121, 122]. Due to the strong Zr-O bond energy, H₂ may not reduce the ZrO₂ surface allowing to insignificant intensity of Zr³⁺ obtained [119].

The ESR spectra of WZ catalysts were also illustrated in Figure 4.20. WZ catalysts were in the oxidation atmosphere during the deposition of tungsten onto ZrO₂ support. Thus, the ESR signals of Zr³⁺ were detected on the ZrO₂ support for both WZ-NT and WZ-H₂ because the oxygen coordinatively unsaturated Zr sites under oxidation atmosphere [122]. In addition, the shift of F-center (V_0^-) to Zr³⁺ ($g_{\perp} = 1.97$) for WZ-H₂ was also observed within a good agreement to the previous reports [79, 110].

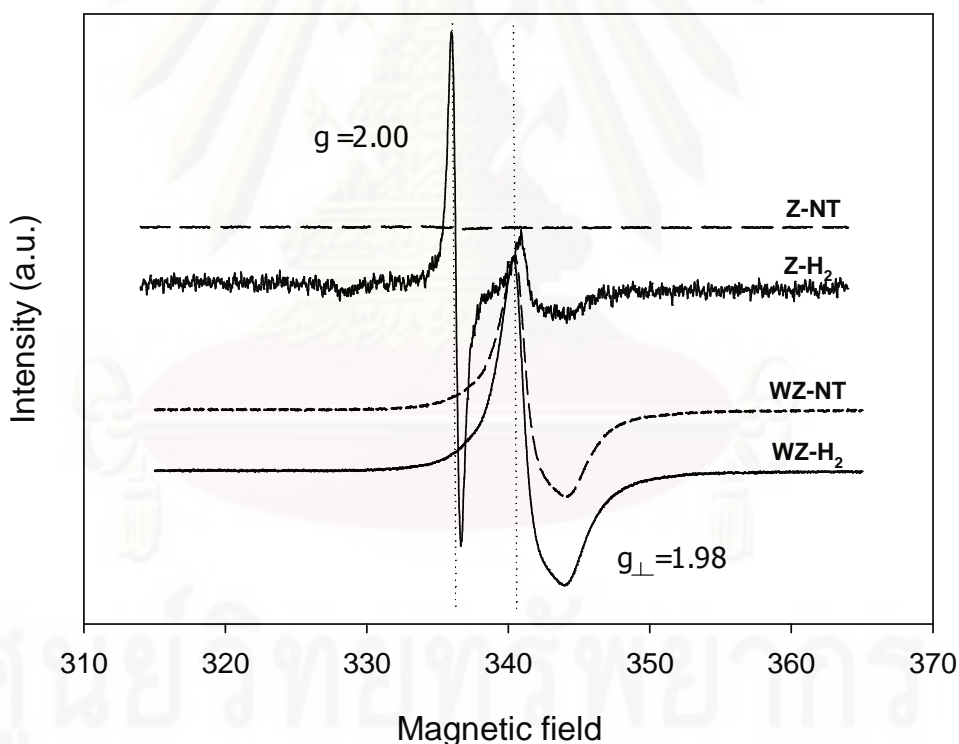


Figure 4.20 ESR spectra of ZrO₂ supports and WZ catalysts.

FT-IR spectroscopy was used to clarify the chemical bonding of ZrO₂ support obtained by different thermal treatments in the range of 400–4000 cm⁻¹ as presented in Figure 4.21. It was found that five transmittance peaks were observed over this range. A very broad band with the highest frequency at 3421 cm⁻¹

contributed to the physically adsorbed water molecular as reported in those literatures [123-125]. In addition, the band at 1631 cm^{-1} should be attributed to the OH group of free water related to alcohol. The IR band within the range of $617\text{--}632\text{ cm}^{-1}$ was corresponding to the bond of metal and oxygen (Zr-O) as presented for both ZrO_2 supports [125]. There were other two peaks observed at 1547 and 1402 cm^{-1} , which are corresponding to the metal and hydroxide (Zr-OH) bond [124, 125]. It can be concluded that ZrO_2 supported prepared from solvothermal method [80] exhibited the Zr-OH group. However, this metal hydroxide bond can be eliminated by the thermal treatment in the reduction atmosphere (H_2) indicated by the decrement of these characteristic peaks. The FT-IR spectrum of ZrO_2 support is corresponding to the ESR signal with the presence of F-center on the Z-H₂ surface. Therefore, the F-center is probably produced by the reduction of hydroxyl group on ZrO_2 surface through the following reaction [121, 122]:

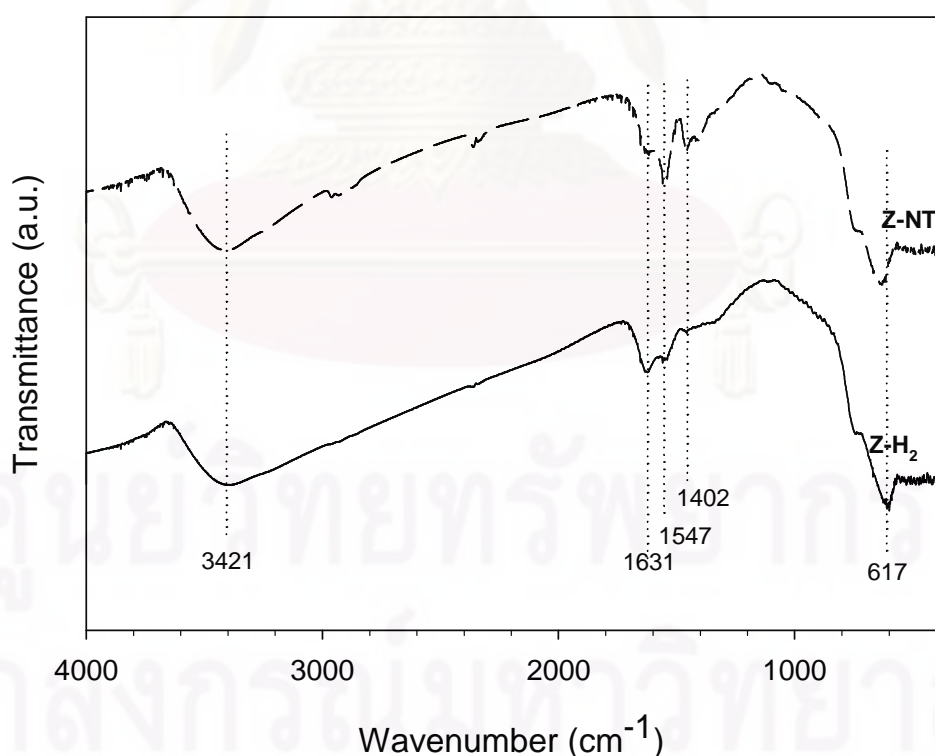
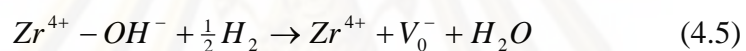


Figure 4.21 FT-IR spectra of ZrO_2 supports.

In order to obtain a better insight for the changes upon molecular level structure of the tungsten oxide overlayer for WZ catalysts, the Raman spectroscopy was performed as seen in Figure 4.22. The Raman bands at 310, 402, and 473 cm^{-1} were assigned to the tetragonal phase of ZrO_2 [29, 117, 126] as presented in both catalysts. Both WZ-NT and WZ- H_2 showed the characteristic peak of the terminal W=O band of the dehydrated surface WO_x species at 910 to 1030 cm^{-1} [29, 118]. The WZ- H_2 exhibited slightly higher intensity of crystalline WO_3 nano-particle (799 cm^{-1}) than that of WZ-NT. The crystalline WO_3 nano-particle was observed upon the W surface density at $\sim 4 \text{ W/nm}^2$ as reported by Wachs et al. [118]. The stretching and bending modes of the bridging for W-O-W were assigned at $\sim 500\text{--}800$ and $\sim 200\text{--}300$ cm^{-1} [117, 127]. As illustrated in Figure 4.22, WZ-NT had higher intensity of bending mode of the bridging W-O-W than that for the WZ- H_2 , whereas the stretching modes of bridging W-O-W were comparable. In summary, three different tungsten species (W=O, WO_3 , and W-O-W) were observed for both catalysts, which were probably due to the similar W surface density at $\sim 4 \text{ W/nm}^2$.

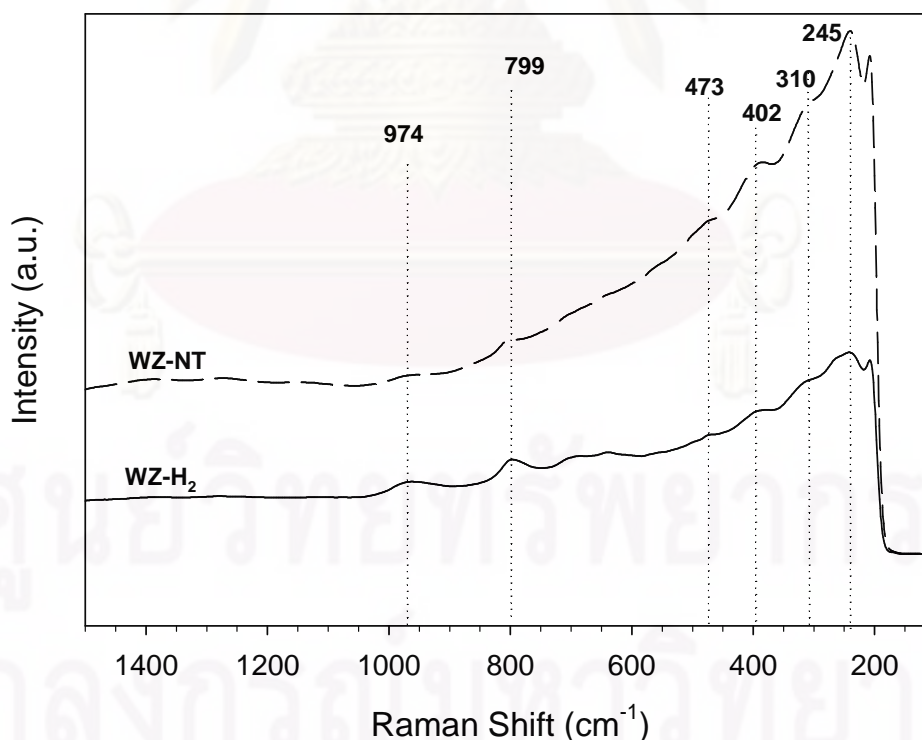


Figure 4.22 Raman spectra of WZ-NT and WZ- H_2 catalysts.

4.3.2 Proposed active species of tungstated zirconia

As known, acidity of WZ catalyst is a key factor to enhance the catalytic activity for several reactions by generation of active sites [5, 24, 25, 27, 29, 30, 68, 69, 102, 111, 128, 129]. The catalytic active sites were plausible for high surface acidity form with a monolayer of polytungstated species (WO_x) [29, 68, 69]. The surface acidity was obtained from a larger population of Brønsted acid sites and the presence of stronger Brønsted acid sites [74]. WZ-NT and WZ- H_2 catalysts exhibited the growing surface polytungstated domain and crystalline of WO_3 nano-particle. It is more likely to obtain the similar Brønsted acid site density based on the similar polytungstated domain. However, the WZ-NT has higher acidity compared to WZ- H_2 as presented in Table 4.7. The higher surface acidity of WZ-NT should be derived from the different forms of polytungstated domain.

The FT-IR spectra of zirconia support suggested that the Zr-OH bonding presented in Z-NT appeared to result in a super acid center (heteropolyacid of W, $[\text{XW}_{12}\text{O}_{40}]^{3-}$), which was proposed by Afanasiev et al. [130] and Scheithauer et al. [73, 126, 131]. In addition, the Raman spectrum of WZ-NT was resemble the finger print of Raman spectrum of tungstophosphoric heteropolyacid ($\text{H}_6\text{P}_2\text{W}_{18}\text{O}_{62}$) as a super acid [127]. The only substantial difference between the WZ-NT and WZ- H_2 catalysts in the monolayer region is the presence of the Zr-heteropolyacid species for the WZ-NT catalysts as illustrated in Figure 4.23. The catalytic activity sites seem to be fully oxidized from noncrystalline surface polytungstate networks incorporating trace levels of surface-exposed Zr capable of stabilizing delocalized protons for Brønsted acid sites as well as heteropolyacids did [73, 126, 131].

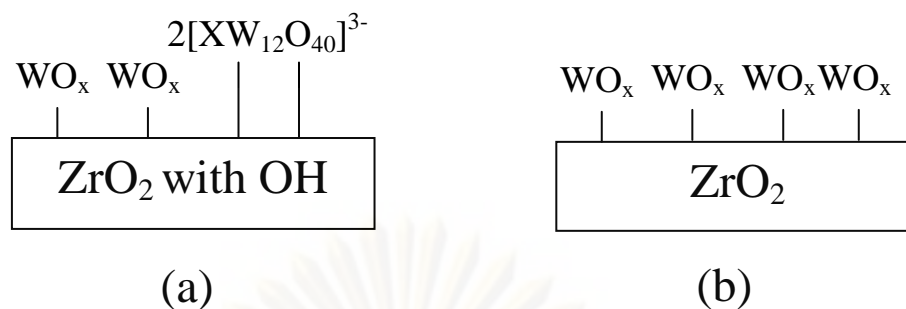


Figure 4.23 Schematic for proposed catalytic active species presented in (a) WZ-NT and (b) WZ-H₂ catalyst.

4.3.3 Catalytic activity for 2-phase esterification of dilute acetic acid and 1-heptanol

As expected, after 9 h reaction period, WZ-NT exhibited 17 % higher for an acetic acid conversion than that for WZ-H₂, as shown in Figure 4.24. Heteropolyacid as the strong Brønsted acid sites related to acid site density and catalytic activity of esterification as corresponding to the work reported by Park et al. [132]. This could be obtained from the crystalline zirconia with Zr-OH bonding. Our result is in good agreement to the work claimed by Scheithauer group [73, 126, 131] indicating that the Zr-OH group is required to create the strong Brønsted acid sites. This reveals that the crystalline zirconia support prepared from the solvothermal method also created Zr-OH bonding as well as amorphous zirconium oxide precursor. Based on the turnover number of catalyst (TON), the appreciable catalytic activity of both WZ-NT and WZ-H₂ were 100 times greater than that of the Amberlyst 15 as presented by Preserthdam and Jongsomjit [133]. As known, the somewhat difference in response of water flow rate for the Amberlyst 15 versus WZ may have been caused by the presence of Lewis acid sites on WZ resulting in enhanced activity [25, 33, 87].

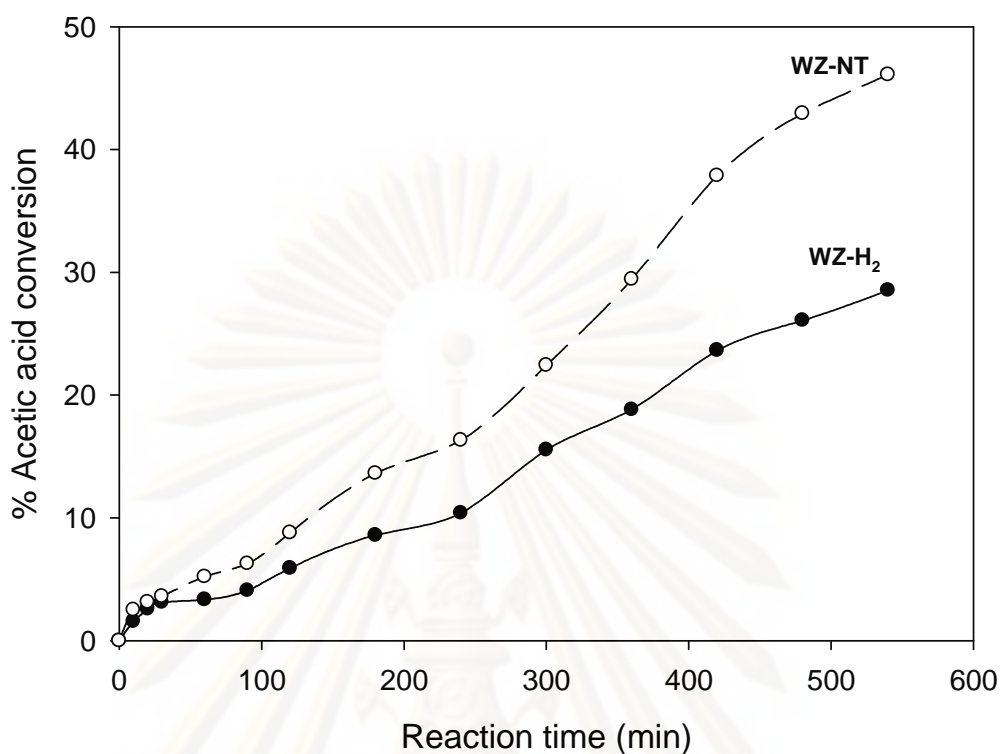


Figure 4.24 Reaction profiles of acetic acid conversion using the different WZ catalysts.

In addition, the WZ catalyst does not deactivate by leaching of active species in the liquid phase transesterification [27, 54], which is different from the SZ (sulfated zirconia) under similar condition. In order to prove that, the leaching experiment was also performed based on the procedure of Suwannakarn et al. [54]. It was found that the acetic acid conversion was less than 3%. This suggested that the leaching of active species in WZ catalyst did not occur for the WZ catalyst upon the preparation used in this work [7, 27, 102].

CHAPTER V

CONCLUSIONS AND RECOMMENDATIONS

This research has investigated the potential of heterogeneous catalysis in biodiesel synthesis while emphasizing the related fundamental aspects including the part of solid acid (WZ and SAC-13) catalyzed hydrolysis of TCp in a semi-batch reactor, the reaction kinetics and mechanisms of hydrolysis and transesterification of TCp on WZ catalyst, and the role of zirconia surface on catalytic activity of tungstated zirconia via two-phase esterification of acetic acid and 1-heptanol were described in section 5.1 as conclusions. The recommendation for further study is also given in section 5.2.

5.1 Conclusions

This section provided the summary following to the results and discussion part.

5.1.1 Solid acid catalyzed hydrolysis of TCp in a semi-batch reactor

This pioneering work, conducted using strong solid acid catalysts (WZ and SAC-13) for the continuous three-phase hydrolysis of oil to produce FFAs, has been carried out using TCp as a model compound for TGs and a well-stirred semi-batch reactor at atmospheric pressure. The temperature range studied was 110–150°C. Water was continuously fed into the reactor at a low flow rate. TCp conversion and TOF values calculated for WZ and SAC-13 indicate that both catalysts have the capacity to successfully catalyze the TCp hydrolysis with 100% selectivity of the carboxylic acid side chains on the triglyceride to HCp. The WZ catalyst exhibited a 2-fold higher initial rate of TCp conversion than SAC-13 but with similar HCp yields at higher conversions.

The surface characteristics of the catalysts played an important role in catalyst selectivity and deactivation behavior. Cycling experiments for both catalysts showed

continuous activity loss. Methanol washing was able to only partially recover catalytic activity to its original value for either WZ or SAC-13. Recalcination was the most efficient method for catalyst regeneration but was only applicable to WZ due to the thermal instability of SAC-13. Catalyst deactivation was likely mainly due to the adsorption and accumulation of organic species on the catalyst surface leading to catalytic site blockage. To obtain higher TCp conversions, this process could be improved by increasing the amount of catalyst, the reaction temperature, and the reaction time.

5.1.2 Reaction kinetics and mechanisms of hydrolysis and transesterification of TCp on WZ catalyst

The fundamental aspects of both liquid-phase hydrolysis and transesterification with low molar ratios of water (or methanol)-to-TCp catalyzed by WZ have been investigated at 100–130°C and 120–180 psi. The kinetic measurements were obtained under conditions where external and internal mass transport limitations were able to be ruled out. The catalytic activities of both hydrolysis and transesterification were comparable based on the initial TOFs with 100% selectivity to predicted products. Transesterification tended to produce more final products (GL and methyl esters) than hydrolysis did in the same time period.

The apparent activation energy of hydrolysis was 2-fold higher than that of transesterification in the temperature range of 100–130°C. For hydrolysis at low water-to-TCp ratios (0.8–1.2) necessary to maintain single phase behavior, the reaction was positive order in TCp and negative order in water. For transesterification, at similar methanol-to-TCp ratios, the apparent order of reaction for TCp was also positive, as was that for methanol as well (slightly positive). The apparent order of reaction of methanol transitioned to negative order only for methanol-to-TCp ratios greater than 1.2.

The mechanism for both reactions seem to be similar and best described as Eley-Rideal single site mechanisms. Reaction seems to occur between the adsorbed protonated TCp and methanol (water) from the liquid phase. Water, being more

strongly adsorbed than methanol, impacts the reaction negatively at a lower concentration (methanol or water-to-TCp ratio). Methanol, on the contrary, seems to inhibit by blocking of active sites only at a higher concentration. As the results for transesterification suggest, as the concentration of the polar reactant increases, the RDS shifts from surface reaction limited to being TCp adsorption limited. The same probably happens for hydrolysis as well although at much lower reactant ratios.

5.1.3 The role of zirconia surface on catalytic activity of tungstated zirconia via two-phase esterification of acetic acid and 1-heptanol

In summary, the surface nature of zirconia was found to be crucial for determining the catalytic properties of WZ catalysts. The formation of Zr-heteropolyacid can be obtained from crystalline zirconia with Zr-OH bonding as presented in WZ-NT. This active species provided the strong Brønsted acid sites, which are essential for the esterification of dilute acetic acid and 1-heptanol. The Zr-OH bonding for WZ-H₂ was eliminated by the thermal treatment in the reduction atmosphere of the crystalline zirconia support allowing to the presence of only polytungstated domain.

5.2 Recommendations

In order to further build up the scientific infrastructure for the application of heterogeneous catalysis to reaction related to biodiesel synthesis, a few aspects missed in and some ideas derived from this research are suggested here for future research:

1. TCp conversion for hydrolysis was comparable to transesterification and similar mechanistic pathway. Therefore, It should be carried out 2-step hydrolysis of TGs and further reacted via esterification in a semi-batch reactor.
2. The appropriate catalyst for the reaction system in the presence of water and triglyceride. The surface hydrophobicity control in solid acid catalysts used for TG hydrolysis. High surface hydrophobicity of solid

acid has been found to favorably drive TG conversion to completion as illustrated in SAC-13. On the other hand, such an effect may be complicated by the necessity of water adsorption in WZ catalyzed hydrolysis, since the adsorption of water on Lewis acid sites resulted to the formation of Brønsted acid sites likely leading to a higher reaction rate. This hypothesis suggested the best catalyst.

3. The correlation among acid site strength, catalyst activity and deactivation, and reaction conditions. Generally, higher acid site strength is assumed to correspond to higher catalytic activity. Nevertheless, as shown in this work, active sites of higher acid strength are more susceptible to deactivation caused by the strong/irreversible adsorption of bulky FFA/TG molecules or poison by water.
4. The sensitivity of hydrolysis, transesterification, and esterification to the characteristics of the catalyst sites, i.e., Brønsted and Lewis acid sites, respectively.



ศูนย์วิจัยทรัพยากร
จุฬาลงกรณ์มหาวิทยาลัย

REFERENCES

- [1] Canakci, M. and H. Sanli, *Biodiesel production from various feedstocks and their effects on the fuel properties*. Journal of Industrial Microbiology & Biotechnology, 2008. **35**(5): p. 431-441.
- [2] Canakci, M. and J. Van Gerpen, *Biodiesel production from oils and fats with high free fatty acids*. Transactions of the Asae, 2001. **44**(6): p. 1429-1436.
- [3] Canakci, M. and J. Van Gerpen, *A pilot plant to produce biodiesel from high free fatty acid feedstocks*. Transactions of the Asae, 2003. **46**(4): p. 945-954.
- [4] Canakci, M. and J. Van Gerpen, *Biodiesel production via acid catalysis*. Transactions of the Asae, 1999. **42**(5): p. 1203-1210.
- [5] Furuta, S., H. Matsubishi, and K. Arata, *Biodiesel fuel production with solid superacid catalysis in fixed bed reactor under atmospheric pressure*. Catalysis Communications, 2004. **5**: p. 721-723.
- [6] Garcia, C.M., S. Teixeira, L.L. Marciniuk, and U. Schuchardt, *Transesterification of soybean oil catalyzed by sulfated zirconia*. Bioresource Technology, 2008. **99**(14): p. 6608-6613.
- [7] Suwannakarn, K., E. Lotero, K. Ngaosuwan, and J.G. Goodwin, Jr., *Simultaneous free fatty acid esterification and triglyceride transesterification using a solid acid catalyst with in situ removal of water and unreacted methanol*. Industrial & Engineering Chemistry Research, 2009. **48**(6): p. 2810-2818.
- [8] Lotero, E., Y.J. Liu, D.E. Lopez, K. Suwannakarn, D.A. Bruce, and J.G. Goodwin, Jr., *Synthesis of biodiesel via acid catalysis*. Industrial & Engineering Chemistry Research, 2005. **44**(14): p. 5353-5363.
- [9] Kusdiana, D. and S. Saka, *Effects of water on biodiesel fuel production by supercritical methanol treatment*. Bioresource Technology, 2004. **91**(3): p. 289-295.
- [10] Kusdiana, D. and S. Saka, *Two-step preparation for catalyst-free biodiesel fuel production: hydrolysis and methyl esterification*. Applied Biochemistry and Biotechnology, 2004. **113-116**: p. 781-791.
- [11] Minami, E. and S. Saka, *Kinetics of hydrolysis and methyl esterification for biodiesel production in two-step supercritical methanol process*. Fuel, 2006. **85**(17-18): p. 2479-2483.
- [12] Lotero, E., J.G. Goodwin, Jr., D. Bruce, K. Suwannakarn, Y. Liu, and D.E. Lopez, *The catalysis of biodiesel synthesis*. Royal Chemistry Society Publishing, 2006. **19**: p. 41-81.

- [13] Zhang, Y., M.A. Dube, D.D. McLean, and M. Kates, *Biodiesel production from waste cooking oil: 2. Economic assessment and sensitivity analysis*. Bioresource Technology, 2003. **90**(3): p. 229-240.
- [14] Ma, F.R. and M.A. Hanna, *Biodiesel production: a review*. Bioresource Technology, 1999. **70**(1): p. 1-15.
- [15] Kiss, A.A., A.C. Dimian, and G. Rothenberg, *Biodiesel by catalytic reactive distillation powered by metal oxides*. Energy & Fuels, 2008. **22**(1): p. 598-604.
- [16] Gervajio, C.G., *Fatty Acids and Derivatives from Coconut Oil*, in *Bailey's Industrial Oil and Fat Products*, F. Shahidi, Editor. 2005, Wiley-Interscience: New York. p. 1-56.
- [17] Zhang, Y., M.A. Dube, D.D. McLean, and M. Kates, *Biodiesel production from waste cooking oil: 1. Process design and technological assessment*. Bioresource Technology, 2003. **89**(1): p. 1-16.
- [18] Warabi, Y., D. Kusdiana, and S. Saka, *Reactivity of triglycerides and fatty acids of rapeseed oil in supercritical alcohols*. Bioresource Technology, 2004. **91**(3): p. 283-287.
- [19] Bunyakiat, K., S. Makmee, R. Sawangkeaw, and S. Ngamprasertsith, *Continuous production of biodiesel via transesterification from vegetable oils in supercritical methanol*. Energy and Fuels, 2006. **20**(2): p. 812-817.
- [20] Saka, S. and D. Kusdiana, *Biodiesel fuel from rapeseed oil as prepared in supercritical methanol*. Fuel, 2001. **80**(2): p. 225-231.
- [21] Freedman, B., R.O. Butterfield, and E.H. Pryde, *Transesterification kinetics of soybean oil*. Journal of the American Oil Chemists Society, 1986. **63**(10): p. 1375-1380.
- [22] Kocsisova, T., J. Cvengros, and J. Lutisan, *High-temperature esterification of fatty acids with methanol at ambient pressure*. European Journal of Lipid Science and Technology, 2005. **107**(2): p. 87-92.
- [23] Hoydonckx, H.E., D.E. De Vos, S.A. Chavan, and P.A. Jacobs, *Esterification and transesterification of renewable chemicals*. Topics in Catalysis, 2004. **27**(1-4): p. 83-96.
- [24] Baertsch, C.D., K.T. Komala, Y.H. Chua, and E. Iglesia, *Genesis of Bronsted acid sites during dehydration of 2-butanol on tungsten oxide catalysts*. Journal of Catalysis, 2002. **205**(1): p. 44-57.
- [25] Macht, J., C.D. Baertsch, M. May-Lozano, S.L. Soled, Y. Wang, and E. Iglesia, *Support effects on Bronsted acid site densities and alcohol dehydration turnover rates on tungsten oxide domains*. Journal of Catalysis, 2004. **227**(2): p. 479-491.

- [26] Di Serio, M., R. Tesser, M. Dimiccoli, F. Cammarota, M. Nastasi, and E. Santacesaria, *Synthesis of biodiesel via homogeneous Lewis acid catalyst*. Journal of Molecular Catalysis A-Chemical, 2005. **239**(1-2): p. 111-115.
- [27] Lopez, D.E., J.G. Goodwin, Jr., D.A. Bruce, and E. Lotero, *Transesterification of triacetin with methanol on solid acid and base catalysts*. Applied Catalysis A-General, 2005. **295**(2): p. 97-105.
- [28] Liu, Y.J., E. Lotero, and J.G. Goodwin, Jr., *A comparison of the esterification of acetic acid with methanol using heterogeneous versus homogeneous acid catalysis*. Journal of Catalysis, 2006. **242**(2): p. 278-286.
- [29] Lopez, D.E., K. Suwannakarn, D.A. Bruce, and J.G. Goodwin, Jr., *Esterification and transesterification on tungstated zirconia: Effect of calcination temperature*. Journal of Catalysis, 2007. **247**(1): p. 43-50.
- [30] Lopez, D.E., K. Suwannakarn, J.G. Goodwin, Jr., and D.A. Bruce, *Reaction kinetics and mechanism for the gas- and liquid-phase esterification of acetic acid with methanol on tungstated zirconia*. Industrial & Engineering Chemistry Research, 2008. **47**(0): p. 2221-2230.
- [31] Mo, X., D.E. Lopez, K. Suwannakarn, Y. Liu, E. Lotero, J.G. Goodwin, Jr., and C.Q. Lu, *Activation and deactivation characteristics of sulfonated carbon catalysts*. Journal of Catalysis, 2008. **254**(2): p. 332-338.
- [32] Suwannakarn, K., E. Lotero, and J.G. Goodwin, Jr., *Solid Bronsted acid catalysis in the gas-phase esterification of acetic acid*. Industrial & Engineering Chemistry Research, 2007. **46**(22): p. 7050-7056.
- [33] Suwannakarn, K., E. Lotero, and J.G. Goodwin, Jr., *A comparative study of gas phase esterification on solid acid catalysts*. Catalysis Letters, 2007. **114**(3-4): p. 122-128.
- [34] Dos Reis, S.C.M., E.R. Lachter, R.S.V. Nascimento, J.A. Rodrigues Jr, and M.G. Reid, *Transesterification of Brazilian vegetable oils with methanol over ion-exchange resins*. JAOCS, Journal of the American Oil Chemists' Society, 2005. **82**(9): p. 661-665.
- [35] Vicente, G., A. Coteron, M. Martinez, and J. Aracil, *Application of the factorial design of experiments and response surface methodology to optimize biodiesel production*. Industrial Crops and Products, 1998. **8**(1): p. 29-35.
- [36] Liu, Y.J., E. Lotero, J.G. Goodwin, Jr., and C.Q. Lu, *Transesterification of triacetin using solid Bronsted bases*. Journal of Catalysis, 2007. **246**(2): p. 428-433.
- [37] Lopez, D.E., J.G. Goodwin, Jr., and D.A. Bruce, *Transesterification of triacetin with methanol on Nafion (R) acid resins*. Journal of Catalysis, 2007. **245**(2): p. 381-391.

- [38] Lopez, D.E., J.G. Goodwin, Jr., D.A. Bruce, and S. Furuta, *Esterification and transesterification using modified-zirconia catalysts*. Applied Catalysis A-General, 2008. **339**(1): p. 76-83.
- [39] Chen, X., Z. Xu, and T. Okuhara, *Liquid phase esterification of acrylic acid with 1-butanol catalyzed by solid acid catalysts*. Applied Catalysis A-General, 1999. **180**(1-2): p. 261-269.
- [40] Heidekum, A., M.A. Harmer, and W.F. Hoelderich, *Addition of carboxylic acids to cyclic olefins catalyzed by strong acidic ion-exchange resins*. Journal of Catalysis, 1999. **181**(2): p. 217-222.
- [41] Liu, Y.J., E. Lotero, and J.G. Goodwin, Jr., *Effect of carbon chain length on esterification of carboxylic acids with methanol using acid catalysis*. Journal of Catalysis, 2006. **243**(2): p. 221-228.
- [42] Liu, Y.J., E. Lotero, and J.G. Goodwin, Jr., *Effect of water on sulfuric acid catalyzed esterification*. Journal of Molecular Catalysis A-Chemical, 2006. **245**(1-2): p. 132-140.
- [43] Ray, A.K., Z. Ziyang, and K. Hidajat, *Determination of adsorption and kinetic parameters for methyl tert-butyl ether synthesis from tert-butyl alcohol and methanol*. Journal of Catalysis, 2001. **200**(2): p. 209-221.
- [44] Wu, K.C. and Y.W. Chen, *An efficient two-phase reaction of ethyl acetate production in modified ZSM-5 zeolites*. Applied Catalysis A: General, 2004. **257**(1): p. 33-42.
- [45] Zhao, Z.H., *Studies on esterification reaction over aluminophosphate and silicoaluminophosphate molecular sieves*. Journal of Molecular Catalysis A: Chemical, 2001. **168**(1-2): p. 147-152.
- [46] Koster, R., B. Van der Linden, and E. Poels, *The mechanism of the gas-phase esterification of acetic acid and ethanol over MCM-41*. Journal of Catalysis, 2001. **204**(2): p. 333-338.
- [47] Ma, Y., Q.L. Wang, H. Yan, X. Ji, and Q. Qiu, *Zeolite-catalyzed esterification I. Synthesis of acetates, benzoates and phthalates*. Applied Catalysis A: General, 1996. **139**(1-2): p. 51-57.
- [48] Chu, W., X. Yang, X. Ye, and Y. Wu, *Vapor phase esterification catalyzed by immobilized dodecatungstosilicic acid (SiW₁₂) on activated carbon*. Applied Catalysis A: General, 1996. **145**(1-2): p. 125-140.
- [49] Mbaraka, I.K., D.R. Radu, V.S.Y. Lin, and B.H. Shanks, *Organosulfonic acid-functionalized mesoporous silicas for the esterification of fatty acid*. Journal of Catalysis, 2003. **219**(2): p. 329-336.

- [50] Perez-Pariente, J., I. Diaz, F. Mohino, and E. Sastre, *Selective synthesis of fatty monoglycerides by using functionalised mesoporous catalysts*. Applied Catalysis A: General, 2003. **254**(2): p. 173-188.
- [51] Verhoef, M.J., P.J. Kooyman, J.A. Peters, and H. Van Bekkum, *A study on the stability of MCM-41-supported heteropoly acids under liquid- and gas-phase esterification conditions*. Microporous and Mesoporous Materials, 1999. **27**(2-3): p. 365-371.
- [52] Hino, M. and K. Arata, *Synthesis of solid superacid catalyst with acid strength of $H_0 < -16.04$* Journal of the Chemical Society, Chemical Communications, 1980(18): p. 851-852.
- [53] Arata, K., H. Matsushashi, M. Hino, and H. Nakamura, *Synthesis of solid superacids and their activities for reactions of alkanes*. Catalysis Today, 2003. **81**(1): p. 17-30.
- [54] Suwannakarn, K., E. Lotero, J.G. Goodwin, Jr., and C.Q. Lu, *Stability of sulfated zirconia and the nature of the catalytically active species in the transesterification of triglycerides*. Journal of Catalysis, 2008. **255**(2): p. 279-286.
- [55] Ardizzone, S., C.L. Bianchi, V. Ragaini, and B. Vercelli, *SO₄-ZrO₂ catalysts for the esterification of benzoic acid to methylbenzoate*. Catalysis Letters, 1999. **62**(1): p. 59-65.
- [56] Furuta, S., H. Matsushashi, and K. Arata, *Catalytic action of sulfated tin oxide for etherification and esterification in comparison with sulfated zirconia*. Applied Catalysis A-General, 2004. **269**(1-2): p. 187-191.
- [57] Hino, M., S. Kobayashi, and K. Arata, *Reactions of butane and isobutane catalyzed by zirconium oxide treated with sulfate ion. Solid superacid catalyst [7]*. Journal of the American Chemical Society, 1979. **101**(21): p. 6439-6441.
- [58] Wakasugi, K., T. Misaki, K. Yamada, and Y. Tanabe, *Diphenylammonium triflate (DPAT): Efficient catalyst for esterification of carboxylic acids and for transesterification of carboxylic esters with nearly equimolar amounts of alcohols*. Tetrahedron Letters, 2000. **41**(27): p. 5249-5252.
- [59] Zong, M.H., Z.Q. Duan, W.Y. Lou, T.J. Smith, and H. Wu, *Preparation of a sugar catalyst and its use for highly efficient production of biodiesel*. Green Chemistry, 2007. **9**(5): p. 434-437.
- [60] Liu, K.S., *Preparation of fatty acid methyl esters for gas-chromatographic analysis of lipids in biological materials*. Journal of the American Oil Chemists' Society, 1994. **71**(11): p. 1179-1187.
- [61] Freedman, B., E.H. Pryde, and T.L. Mounts, *Variables affecting the yields of fatty esters from transesterified vegetable oils*. Journal of the American Oil Chemists' Society, 1983. **61**(10): p. 1638-1643.

- [62] Kulkarni, M.G., R. Gopinath, L.C. Meher, and A.K. Dalai, *Solid acid catalyzed biodiesel production by simultaneous esterification and transesterification*. Green Chemistry, 2006. **8**(12): p. 1056-1062.
- [63] Yow, C.J. and K.Y. Liew, *Hydrolysis of palm oil catalyzed by macroporous cation-exchanged resin*. Journal of the American Oil Chemists Society, 1999. **76**(4): p. 529-533.
- [64] Bozek-Winkler, E. and J. Gmehling, *Transesterification of methyl acetate and n-butanol catalyzed by Amberlyst 15*. Industrial & Engineering Chemistry Research, 2006. **45**(20): p. 6648-6654.
- [65] Hua, W.M. and J. Sommer, *Hydroisomerization of n-butane over sulfated zirconia catalysts promoted by alumina and platinum*. Applied Catalysis A-General, 2002. **227**(1-2): p. 279-286.
- [66] Yori, J.C., C.R. Vera, and J.M. Parera, *n-butane isomerization on tungsten oxide supported on zirconia*. Applied Catalysis A-General, 1997. **163**(1-2): p. 165-175.
- [67] Chen, X., C. Chen, N. Xu, and C.Y. Mou, *Catalytic activity of Al₂O₃/WO₃/ZrO₂ strong solid acid catalyst for n-butane isomerization*. Chinese Journal of Catalysis, 2003. **24**(12): p. 924-928.
- [68] Iglesia, E., D.G. Barton, S.L. Soled, S. Miseo, J.E. Baumgartner, W.E. Gates, G.A. Fuentes, and G.D. Meitzner, *Selective isomerization of alkanes on supported tungsten oxide acids*, in *Studies in Surface Science and Catalysis*. 1996. p. 533-542.
- [69] Barton, D.G., S.L. Soled, G.D. Meitzner, G.A. Fuentes, and E. Iglesia, *Structural and catalytic characterization of solid acids based on zirconia modified by tungsten oxide*. Journal of Catalysis, 1999. **181**(1): p. 57-72.
- [70] Barton, D.G., M. Shtein, R.D. Wilson, S.L. Soled, and E. Iglesia, *Structure and electronic properties of solid acids based on tungsten oxide nanostructures*. Journal of Physical Chemistry B, 1999. **103**(4): p. 630-640.
- [71] Barton, D.G., S.L. Soled, and E. Iglesia, *Solid acid catalysts based on supported tungsten oxides*. Topics in Catalysis, 1998. **6**(1-4): p. 87-99.
- [72] Di Gregorio, F. and V. Keller, *Activation and isomerization of hydrocarbons over WO₃/ZrO₂ catalysts - I. Preparation, characterization, and X-ray photoelectron spectroscopy studies*. Journal of Catalysis, 2004. **225**(1): p. 45-55.
- [73] Santiesteban, J.G., J.C. Vartuli, S. Han, R.D. Bastian, and C.D. Chang, *Influence of the preparative method on the activity of highly acidic WO₃/ZrO₂ and the relative acid activity compared with zeolites*. Journal of Catalysis, 1997. **168**(2): p. 431-441.

- [74] Boyse, R.A. and E.I. Ko, *Crystallization Behavior of Tungstate on Zirconia and Its Relationship to Acidic Properties*. Journal of Catalysis, 1997. **171**(1): p. 191-207.
- [75] Occhiuzzi, M., D. Cordischi, D. Gazzoli, M. Valigi, and P.C.n. Heydorn, *WO_x/ZrO₂ catalysts: Part 4. Redox properties as investigated by redox cycles, XPS and EPR*. Applied Catalysis A: General, 2004. **269**(1-2): p. 169-177.
- [76] Ward, D.A. and E.I. Ko, *One-Step Synthesis and Characterization of Zirconia-Sulfate Aerogels as Solid Superacids*. Journal of Catalysis, 1994. **150**(1): p. 18-33.
- [77] Wachs, I.E., *Recent conceptual advances in the catalysis science of mixed metal oxide catalytic materials*. Catalysis Today, 2005. **100**(1-2): p. 79-94.
- [78] Lebarbier, V., G. Clet, and M. Houalla, *Relations between structure, acidity, and activity of WO_x/TiO₂: Influence of the initial state of the support, titanium oxyhydroxide, or titanium oxide*. Journal of Physical Chemistry B, 2006. **110**(45): p. 22608-22617.
- [79] Wongmaneevil, P., B. Jongsomjit, and P. Praserttham, *Influence of calcination treatment on the activity of tungstated zirconia catalysts towards esterification*. Catalysis Communications, 2009. **10**(7): p. 1079-1084.
- [80] Kongwudthiti, S., P. Praserttham, P. Silveston, and M. Inoue, *Influence of synthesis conditions on the preparation of zirconia powder by the glycothermal method*. Ceramics International, 2003. **29**(7): p. 807-814.
- [81] Kob, N., R.S. Drago, and V. Young, *Preparation, characterization, and acidity of a silica gel/Tungsten oxide solid acid*. Inorganic Chemistry, 1997. **36**(22): p. 5127-5131.
- [82] Harmer, M.A., W.E. Farneth, and Q. Sun, *High surface area nafion resin/silica nanocomposites: A new class of solid acid catalyst*. Journal of the American Chemical Society, 1996. **118**(33): p. 7708-7715.
- [83] Zimmermann, Y. and S. Spange, *Solvent influence on the catalytic activity and surface polarity of inorganic solid acids*. Journal of Physical Chemistry B, 2002. **106**(48): p. 12524-12530.
- [84] Patil, T.A., D.N. Butala, T.S. Raghunathan, and H.S. Shankar, *Thermal hydrolysis of vegetable-oils and fats. 1. Reaction-kinetics*. Industrial & Engineering Chemistry Research, 1988. **27**(5): p. 727-735.
- [85] Patil, T.A., T.S. Raghunathan, and H.S. Shankar, *Thermal hydrolysis of vegetable-oils and fats. 2. Hydrolysis in continuous stirred tank reactor*. Industrial & Engineering Chemistry Research, 1988. **27**(5): p. 735-739.

- [86] Pinto, J.S.S. and F.M. Lancas, *Hydrolysis of corn oil using subcritical water*. Journal of the Brazilian Chemical Society, 2006. **17**(1): p. 85-89.
- [87] Li, L.S., Y. Yoshinaga, and T. Okuhara, *Unusual acceleration of acid-catalyzed reactions by water in the presence of Mo/Zr mixed oxides calcined at high temperatures*. Physical Chemistry Chemical Physics, 2002. **4**(24): p. 6129-6136.
- [88] Ackelsberg, O.J., *Fat splitting*. Journal of the American Chemical Society, 1958. **35**: p. 635-640.
- [89] King, J.W., R.L. Holliday, and G.R. List, *Hydrolysis of soybean oil in a subcritical water flow reactor*. Green Chemistry, 1999. **1**(6): p. 261-264.
- [90] Namdev, P.D., T.A. Patil, T.S. Raghunathan, and H.S. Shankar, *Thermal hydrolysis of vegetable-oils and fats. 3. An analysis of design alternatives*. Industrial & Engineering Chemistry Research, 1988. **27**(5): p. 739-743.
- [91] Edwards, A.L., *Hydrolysis Methods*. Journal of the American Chemical Society, 1954. **31**: p. 542-544.
- [92] Hartman, L., *Kinetics of the Twitchell hydrolysis*. Nature, 1951. **167**: p. 1190-1199.
- [93] Holliday, R.L., J.W. King, and G.R. List, *Hydrolysis of vegetable oils in sub- and supercritical water*. Industrial & Engineering Chemistry Research, 1997. **36**(3): p. 932-935.
- [94] Sturzenegger, A. and H. Sturm, *Hydrolysis of fats at high temperatures*. Ind. Eng. Chem., 1951. **43**: p. 510-515.
- [95] Corma, A., S. Iborra, S. Miquel, and J. Primo, *Catalysts for the production of fine chemicals - Production of food emulsifiers, monoglycerides, by glycerolysis of fats with solid base catalysts*. Journal of Catalysis, 1998. **173**(2): p. 315-321.
- [96] Liu, Y., E. Lotero, J.G. Goodwin, Jr., and X. Mo, *Transesterification of poultry fat with methanol using Mg-Al hydrotalcite derived catalysts*. Applied Catalysis A-General, 2007. **331**: p. 138-148.
- [97] Roy, J.R.V. and A.O. Converse, *Biomass Hydrolysis with Sulfur Dioxide and Water in the Region of the Critical Point*. 1985, Amsterdam, The Netherlands: Elsevier Science Publishers.
- [98] Tanabe, K., *Surface and catalytic properties of ZrO₂*. Materials Chemistry and Physics, 1985. **13**(3-4): p. 347-364.

- [99] Moquin, P.H.L., F. Temelli, H. Sovova, and M.D.A. Saldana, *Kinetic modeling of glycerolysis-hydrolysis of canola oil in supercritical carbon dioxide media using equilibrium data*. Journal of Supercritical Fluids, 2006. **37**(3): p. 417-424.
- [100] Boocock, D.G.B., S.K. Konar, V. Mao, and H. Sidi, *Fast one-phase oil-rich processes for the preparation of vegetable oil methyl esters*. Biomass & Bioenergy, 1996. **11**(1): p. 43-50.
- [101] Boocock, D.G.B., S.K. Konar, V. Mao, C. Lee, and S. Buligan, *Fast formation of high-purity methyl esters from vegetable oils*. Journal of the American Oil Chemists Society, 1998. **75**(9): p. 1167-1172.
- [102] Ngaosuwan, K., E. Lotero, K. Suwannakarn, J.G. Goodwin, Jr., and P. Praserttham, *Hydrolysis of triglycerides using solid acid catalysts*. Industrial & Engineering Chemistry Research, 2009. **48**(10): p. 4757-4767.
- [103] Moquin, P.H.L. and F. Temelli, *Kinetic modeling of hydrolysis of canola oil in supercritical media*. Journal of Supercritical Fluids, 2008. **45**(1): p. 94-101.
- [104] Mao, V., S.K. Konar, and D.G.B. Boocock, *The pseudo-single-phase, base-catalyzed transesterification of soybean oil*. Journal of the American Oil Chemists Society, 2004. **81**(8): p. 803-808.
- [105] Kusdiana, D. and S. Saka, *Two-step preparation for catalyst-free biodiesel fuel production - Hydrolysis and methyl esterification*. Applied Biochemistry and Biotechnology, 2004. **113-116**: p. 781-791.
- [106] Meher, L.C., D.V. Sagar, and S.N. Naik, *Technical aspects of biodiesel production by transesterification - a review*. Renewable & Sustainable Energy Reviews, 2006. **10**(3): p. 248-268.
- [107] Martin, G.A., *A quantitative approach to the ensemble model of catalysis by metals*. Catalysis Review Science and Engineering, 1988. **30**(4): p. 519-562.
- [108] Nijhuis, T.A., A.E.W. Beers, F. Kapteijn, and J.A. Moulijn, *Water removal by reactive stripping for a solid-acid catalyzed esterification in a monolithic reactor*. Chemical Engineering Science, 2002. **57**(9): p. 1627-1632.
- [109] Bender, M.L., *Mechanism of catalysis of nucleophilic reactions of carboxylic acid derivatives*. Chemical Review, 1960. **60**(1): p. 53-113.
- [110] Ivanovskaya, M.I. and E.V. Frolova, *Nature and conditions of formation of structural defects in zirconium (IV) oxide in the course of its preparation from zirconium hydroxide*. Russian Journal of General Chemistry, 2007. **77**(4): p. 524-531.
- [111] Hino, M. and K. Arata, *Synthesis of solid superacid of tungsten oxide supported on zirconia and its catalytic action for reactions of butane and*

- pentane*. Journal of the Chemical Society, Chemical Communications, 1988. **18**(18): p. 1259-1260.
- [112] Kongwudthiti, S., P. Praserttham, W. Tanakulrungsank, and M. Inoue, *The influence of Si-O-Zr bonds on the crystal-growth inhibition of zirconia prepared by the glycothermal method*. Journal of Materials Processing Technology, 2003. **136**(1-3): p. 186-189.
- [113] Cortes-Jacome, M.A., C. Angeles-Chavez, X. Bokhimi, and J.A. Toledo-Antonio, *Generation of WO₃-ZrO₂ catalysts from solid solutions of tungsten in zirconia*. Journal of Solid State Chemistry, 2006. **179**(8): p. 2663-2673.
- [114] Benaissa, M., J.G. Santiesteban, G. Daz, C.D. Chang, and M. Jose-Yacaman, *Interaction of Sulfate Groups with the Surface of Zirconia: An HRTEM Characterization Study*. Journal of Catalysis, 1996. **161**(2): p. 694-703.
- [115] Reddy, B.M., P.M. Sreekanth, and P. Lakshmanan, *Sulfated zirconia as an efficient catalyst for organic synthesis and transformation reactions*. Journal of Molecular Catalysis A: Chemical, 2005. **237**(1-2): p. 93-100.
- [116] Reddy, B.M., M.K. Patil, G.K. Reddy, B.T. Reddy, and K.N. Rao, *Selective tert-butylation of phenol over molybdate- and tungstate-promoted zirconia catalysts*. Applied Catalysis A: General, 2007. **332**(2): p. 183-191.
- [117] Ross-Medgaarden, E.I., W.V. Knowles, T. Kim, M.S. Wong, W. Zhou, C.J. Kiely, and I.E. Wachs, *New insights into the nature of the acidic catalytic active sites present in ZrO₂-supported tungsten oxide catalysts*. Journal of Catalysis, 2008. **256**(1): p. 108-125.
- [118] Wachs, I.E., T. Kim, and E.I. Ross, *Catalysis science of the solid acidity of model supported tungsten oxide catalysts*. Catalysis Today, 2006. **116**(2): p. 162-168.
- [119] Morterra, C., E. Giamello, L. Orio, and M. Volante, *Formation and reactivity of Zr³⁺ centers at the surface of vacuum-activated monoclinic zirconia*. Journal of Physical Chemistry, 1990. **94**(7): p. 3111-3116.
- [120] Liu, H., L. Feng, X. Zhang, and Q. Xue, *ESR characterization of ZrO₂ nanopowder*. Journal of Physical Chemistry, 1995. **99**(1): p. 332-334.
- [121] Frolova, E.V. and M.I. Ivanovskaya, *The origin of defects formation in nanosized zirconia*. Materials Science and Engineering C, 2006. **26**(5-7): p. 1106-1110.
- [122] Zhao, Q., X. Wang, and T. Cai, *The study of surface properties of ZrO₂*. Applied Surface Science, 2004. **225**(1-4): p. 7-13.
- [123] Zhu, J., J.G. van Ommen, and L. Lefferts, *Effect of surface OH groups on catalytic performance of yttrium-stabilized ZrO₂ in partial oxidation of CH₄ to syngas*. Catalysis Today, 2006. **117**(1-3): p. 163-167.

- [124] Sarkar, D., D. Mohapatra, S. Ray, S. Bhattacharyya, S. Adak, and N. Mitra, *Synthesis and characterization of sol-gel derived ZrO₂ doped Al₂O₃ nanopowder*. *Ceramics International*, 2007. **33**(7): p. 1275-1282.
- [125] Matos, J.M.E., F. MAnjos Jr., L. S.Cavalcante, V.Santos, S. H. Leal, L. S. Santos Jr., M. R. M. C.Santos, and E. Longo, *Reflux synthesis and hydrothermal processing of ZrO₂ nanopowders at low temperature*. *Materials Chemistry and Physics*, 2009. **117**(2-3): p. 455-459.
- [126] Scheithauer, M., R.K. Grasselli, and H. Knozinger, *Genesis and structure of WO_x/ZrO₂ solid acid catalysts*. *Langmuir*, 1998. **14**(11): p. 3019-3029.
- [127] Ross-Medgaarden, E.I. and I.E. Wachs, *Structural determination of bulk and surface tungsten oxides with UV-vis diffuse reflectance spectroscopy and raman spectroscopy*. *Journal of Physical Chemistry C*, 2007. **111**(41): p. 15089-15099.
- [128] Martinez, A., G. Prieto, M.A. Arribas, P. Concepcion, and J.F. Sanchez-Royo, *Influence of the preparative route on the properties of WO_x-ZrO₂ catalysts: A detailed structural, spectroscopic, and catalytic study*. *Journal of Catalysis*, 2007. **248**(2): p. 288-302.
- [129] Ngaosuwan, K., X. Mo, J.G. Goodwin, Jr., and P. Praserthdam, *Reaction kinetics and mechanisms for hydrolysis and transesterification of triglycerides on tungstated zirconia*. *Topics in Catalysis* (in press), 2009.
- [130] Afanasiev, P., C. Geantet, M. Breyse, G. Coudurier, and J.C. Vedrine, *Influence of preparation method on the acidity of MoO₃(WO₃)/ZrO₂ catalysts*. *Journal of the Chemical Society, Faraday Transactions*, 1994. **90**(1): p. 193-202.
- [131] Scheithauer, M., T.K. Cheung, R.E. Jentoft, R.K. Grasselli, B.C. Gates, and H. Knozinger, *Characterization of WO_x/ZrO₂ by vibrational spectroscopy and n-pentane isomerization catalysis*. *Journal of Catalysis*, 1998. **180**(1): p. 1-13.
- [132] Park, Y.M., D.W. Lee, D.K. Kim, J.S. Lee, and K.Y. Lee, *The heterogeneous catalyst system for the continuous conversion of free fatty acids in used vegetable oils for the production of biodiesel*. *Catalysis Today*, 2008. **131**(1-4): p. 238-243.
- [133] Praserthdam, S. and B. Jongsomjit, *Observation on different turnover number in two-phase acid-catalyzed esterification of dilute acetic acid and 1-heptanol*. *Catalysis Letters*, 2009. **130**(3-4): p. 583-587.



APPENDICES

ศูนย์วิทยทรัพยากร
จุฬาลงกรณ์มหาวิทยาลัย

APPENDIX A

PREPARATION OF ZIRCONIA SUPPORT

The preparation of zirconia support by solvothermal method

The equipment for the synthesis of zirconia consists of an autoclave reactor as shown in Figure A.1. Thermocouple is attached to the reagent in the autoclave. Amount of zirconium tetra-*n*-butoxide 80 wt% solution in 1-butanol (starting material) was 25 g. Organic solvent (1,4-butanediol) of 100 mL was filled in the test tube and 30 mL in the gap between test tube and autoclave wall. A temperature program controller was connected to a thermocouple attached to the autoclave. Electrical furnace supplied the required heat to the autoclave for the reaction.

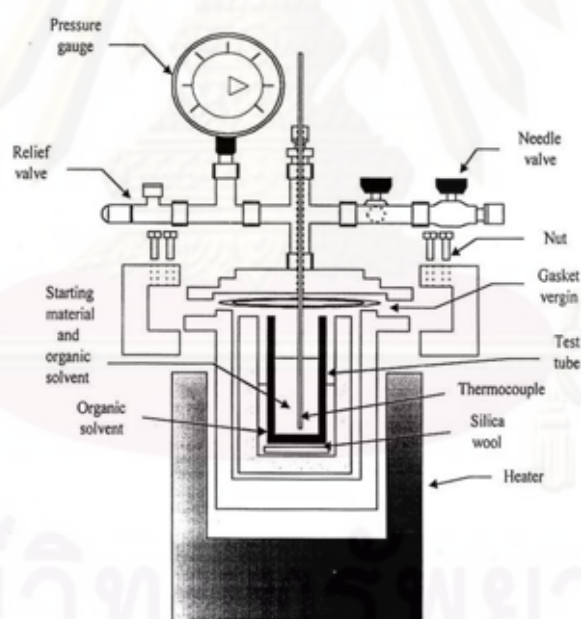


Figure A.1 Autoclave reactor.

Nitrogen was set with a pressure regulator (0-150 bar) and needle valves were used to release gas from autoclave. The diagram of the reaction equipment for the synthesis of catalyst is shown in Figure A.2

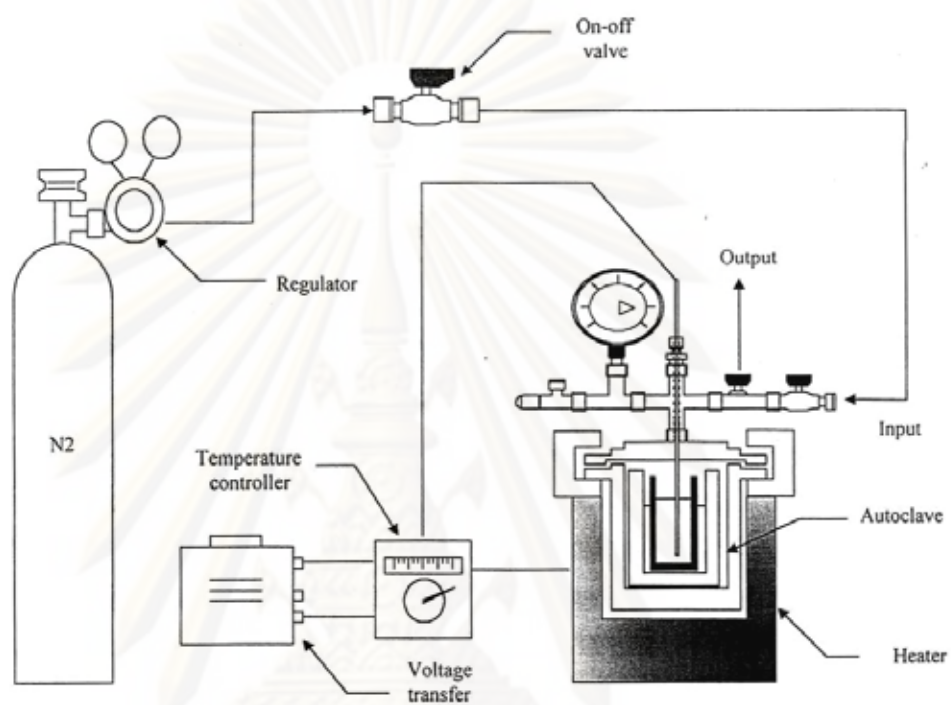


Figure A.2 Diagram of the reaction equipment for the synthesis of catalyst.

APPENDIX B

CALCULATION FOR CATALYST PREPARATION

The calculation for the preparation of tungstated zirconia

Preparation of WZ-NT and WZ-H2 with 15 wt% of tungsten loading by the incipient wetness impregnation method is shown as follow:

Reagent : Tungsten (VI) chloride (WCl_6) Molecular wieght = 396.56
 Support: Zirconia sythesized by solvothermal namely Z-NT
 Support: The reductive thermal treatment of zirconia support namely Z-H₂.

Calculation:

15 wt% WZ

Based on 100 g of catalyst used, the composition of the catalyst will be follows:

Tungsten = 15 g
 Zirconia support = 100 – 15 = 85 g

For 2 g of zirconia

Tungsten required = 2 x (15/85) = 0.353 g

Tungsten 0.353 g was prepared from WCl_6 and molecular weight of W is 183.56

$$\begin{aligned} WCl_6 \text{ required} &= \frac{\text{MW of } WCl_6 \times W \text{ required}}{\text{MW of W}} \\ &= \frac{396.56 \times 0.353}{183.56} \\ &= 0.763 \text{ g} \end{aligned}$$

The de-ionized water was added to obtain an aqueous solution of WCl_6 until equal pore volume of 15 wt% WZ.

APPENDIX C

CALCULATION FOR CRYSTALLITE SIZE

The calculation crystallite size by Debye-Scherrer equation

The crystallite size was calculated from the half-height width of the diffraction peak of XRD pattern using the Debye-Scherrer equation.

From Scherrer equation:

$$D = \frac{K\lambda}{\beta \cos \theta} \quad (\text{C.1})$$

Where D = Crystallite size, Å

K = Crystallite–shape factor (= 0.9)

λ = X-ray wavelength (= 1.5418 Å for CuK $_{\alpha}$)

θ = Observed peak angle, degree

β = X-ray diffraction broadening, radian

The X-ray diffraction broadening (β) is the pure width of power diffraction free from all broadening due to the experimental equipment. α -Alumina is used as a standard sample to observe the instrumental broadening since its crystallite size is larger than 2000 Å. The X-ray diffraction broadening (β) can be obtained by using Warren's formula.

From Warren's formula:

$$\beta = \sqrt{B_M^2 - B_S^2} \quad (\text{C.2})$$

Where B_M = the measure peak width in radians at half peak height.

B_S = the corresponding width of the standard material.

APPENDIX D

CONDITION OF GAS CHROMATOGRAPHY

The condition of Gas Chromatography (GC) analysis for this study

Hewlett-Packard 6890 GC model with an on-column automatic injector, an EC-5 column (30m x 0.25 mm x 0.25 μ m), and an FID detector was used to analyze the catalytic performance for hydrolysis and transesterification of TCp. To achieve complete separation, the column temperature program consisted of 3 min at 40°C, a ramp of 40°C/min to 180°C (hold for 5 min), and a ramp of 15°C/min to 270°C (hold for 3 min) as summarized in Table D.1

Table D.1 GC analysis condition of hydrolysis and transesterification of TCp.

Gas Chromatography	Hewlett-Packard 6890
Detector	FID
Column	EC-5 column
Make up gas	He (UHP grade) with constant make up mode
H ₂ flow (mL/min)	60
Air flow (mL/min)	210
Inlet temperature (°C)	Track oven
Inlet pressure (psi)	45.5
Detector temperature (°C)	250
Column temperature	
Initial temperature (°C)	40
Holding time (min)	5
1 st ramp rate (°C/min)	30
1 st target temperature (°C)	180
Holding time (min)	3
Final temperature (°C)	270
2 nd ramp rate (°C)	15
Holding time (min)	5

The catalytic activity measurement for esterification of dilute acetic acid and 1-heptanol, samples were diluted with 2-propanol (10 mL) to stop reaction and perform in a single phase, and then analyzed by GC (Shimadzu) equipped with a flame ionization detector and Chrompack SE52 column as presented in Table D.2.

Table D.2 GC analysis condition of esterification of dilute acetic acid and 1-heptanol.

Gas Chromatography	Shimadzu GC-14B
Detector	FID
Column	Chrompack SE52
Carrier gas	He (UHP grade)
Carrier gas flow rate (mL/min)	30
Injector temperature (°C)	255
Detector temperature (°C)	280
Column temperature	
Initial temperature (°C)	50
Holding time (min)	3
Ramp rate (°C/min)	10
Final temperature (°C)	210
Holding time (min)	9

APPENDIX E

CALCULATION FOR CATALYTIC PERFORMANCE

The catalytic performance for hydrolysis and transesterification was evaluated in terms of % TCp conversion, % HCp yield, MeCp yield, % DCp yield, % MCp yield, and % GL yield.

$$\% \text{ TCp conversion} = \frac{\text{initial mol of TCp at time 0} - \text{mol of TCp at time t}}{\text{initial mol of TCp at time 0}} \times 100\%$$

$$\% \text{ HCp yield} = \frac{\text{mol of HCp produced at time t}}{\text{initial mol of TCp at time 0}} \times 100\%$$

$$\% \text{ MeCp yield} = \frac{\text{mol of MeCp produced at time t}}{\text{initial mol of TCp at time 0}} \times 100\%$$

$$\% \text{ DCp yield} = \frac{\text{mol of DCp produced at time t}}{\text{initial mol of TCp at time 0}} \times 100\%$$

$$\% \text{ MCp yield} = \frac{\text{mol of MCp produced at time t}}{\text{initial mol of TCp at time 0}} \times 100\%$$

$$\% \text{ GL yield} = \frac{\text{mol of GL produced at time t}}{\text{initial mol of TCp at time 0}} \times 100\%$$

The catalytic performance for esterification of dilute acetic acid and 1-heptanol was evaluated in terms of % Acetic acid conversion.

$$\% \text{ Acetic acid conversion} = \frac{\text{initial acetic acid conc.} - \text{acetic acid conc. at time (t)}}{\text{initial acetic acid conc.}} \times 100$$

APPENDIX F

CALIBRATION CURVE

The calibration curve of reactant and product for this study

The calibration curve for hydrolysis and transesterification are including of TCp, HCp, MeCp, DCp, MCp, and GL.

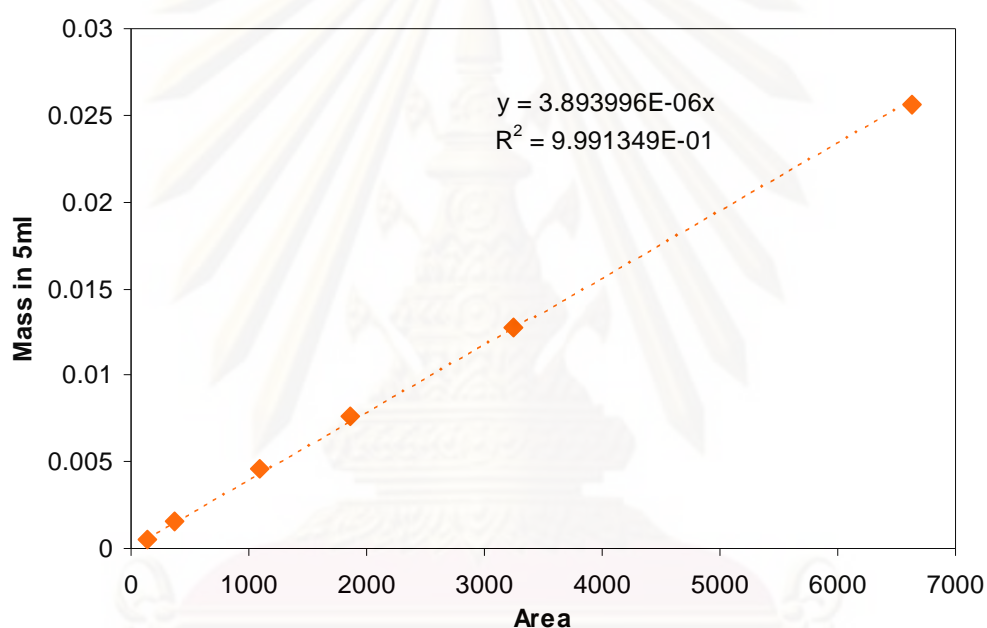


Figure F.1 The calibration curve of TCp.

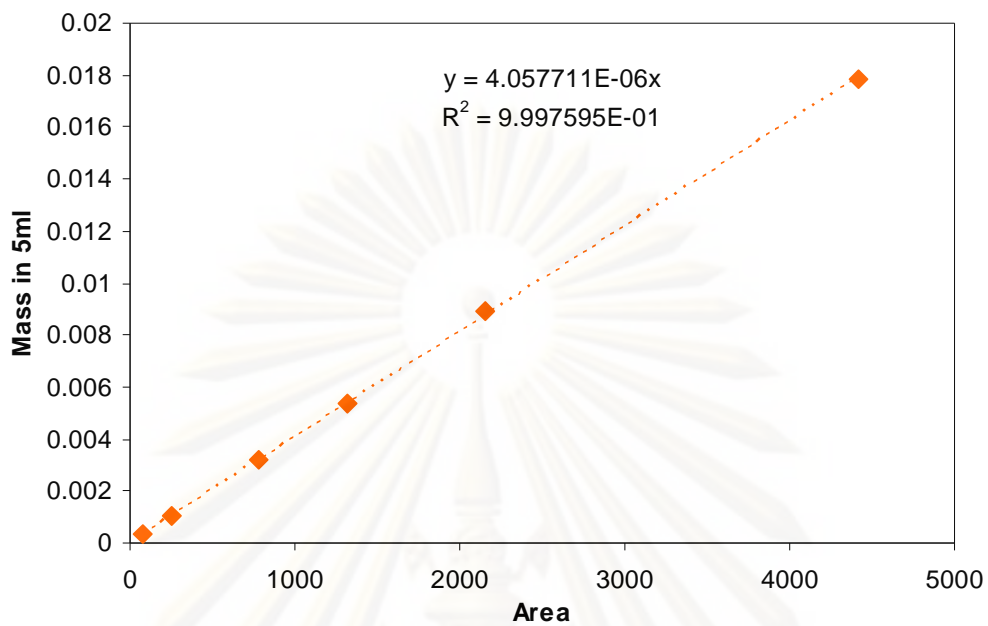


Figure F.2 The calibration curve of HCp.

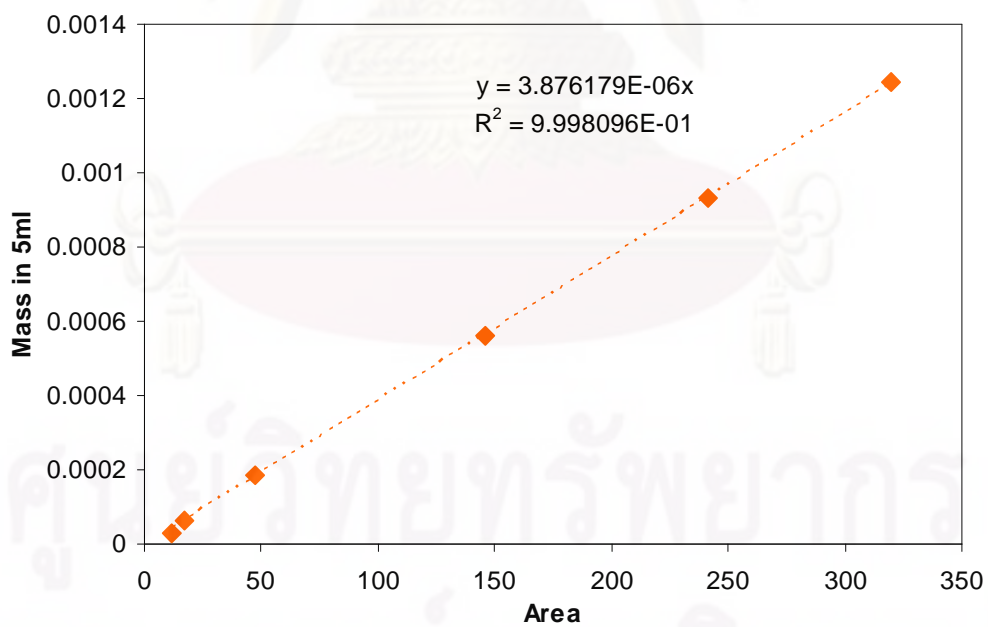


Figure F.3 The calibration curve of MeCp.

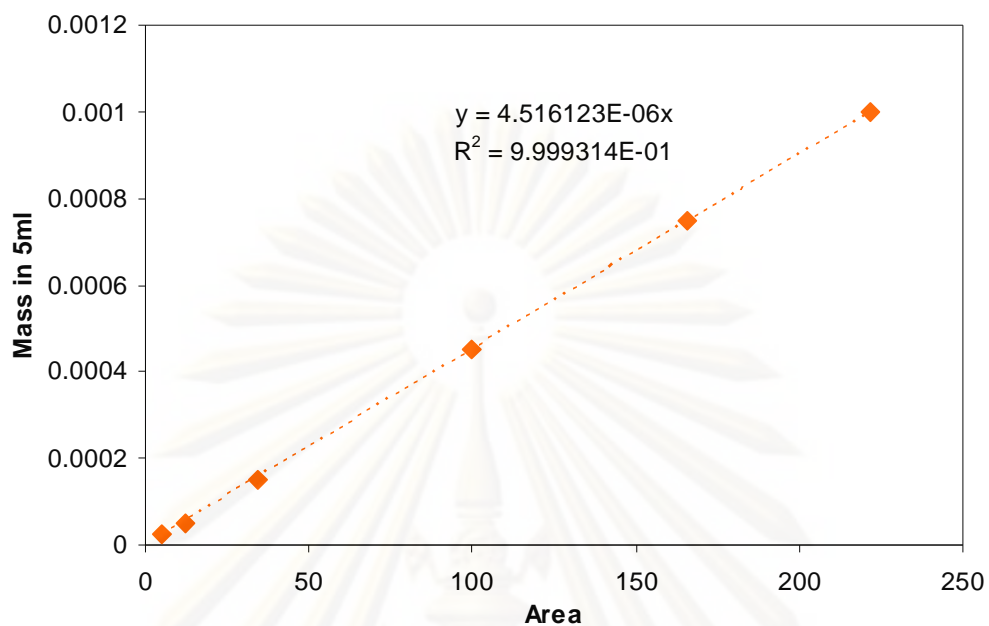


Figure F.4 The calibration curve of DCp.

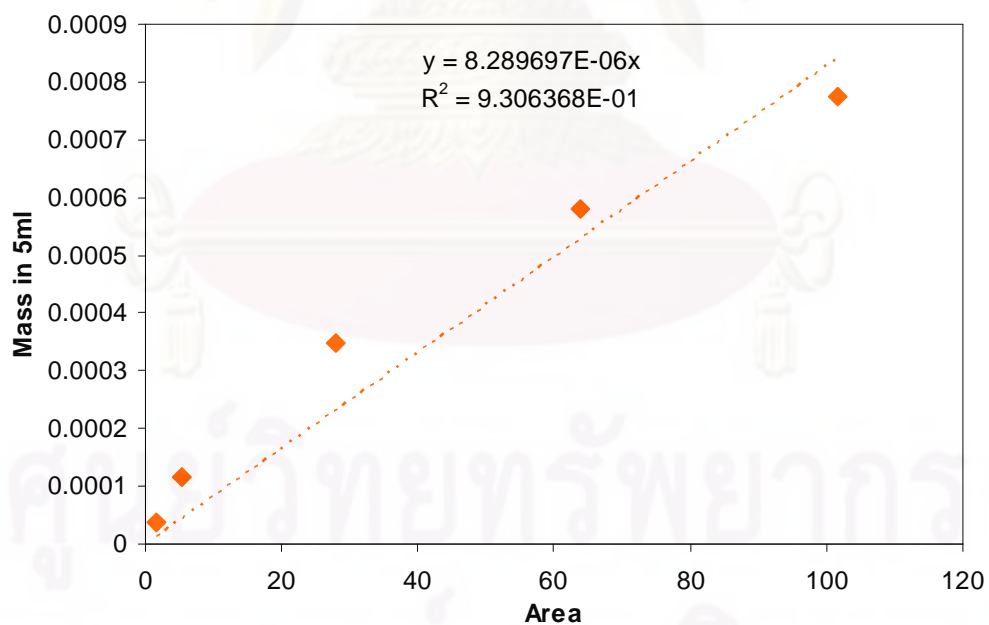


Figure F.5 The calibration curve of MCp.

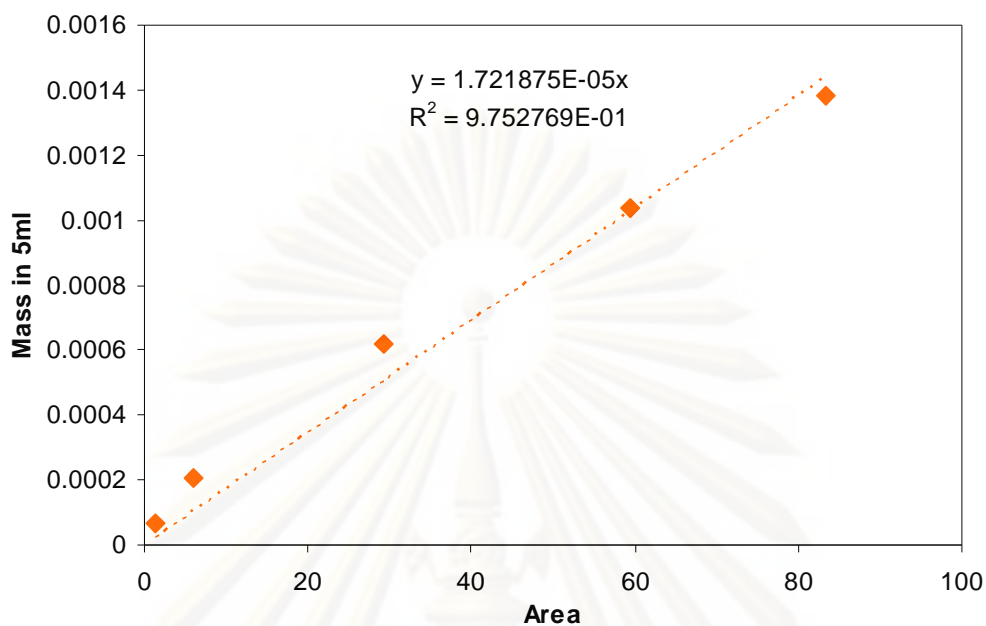
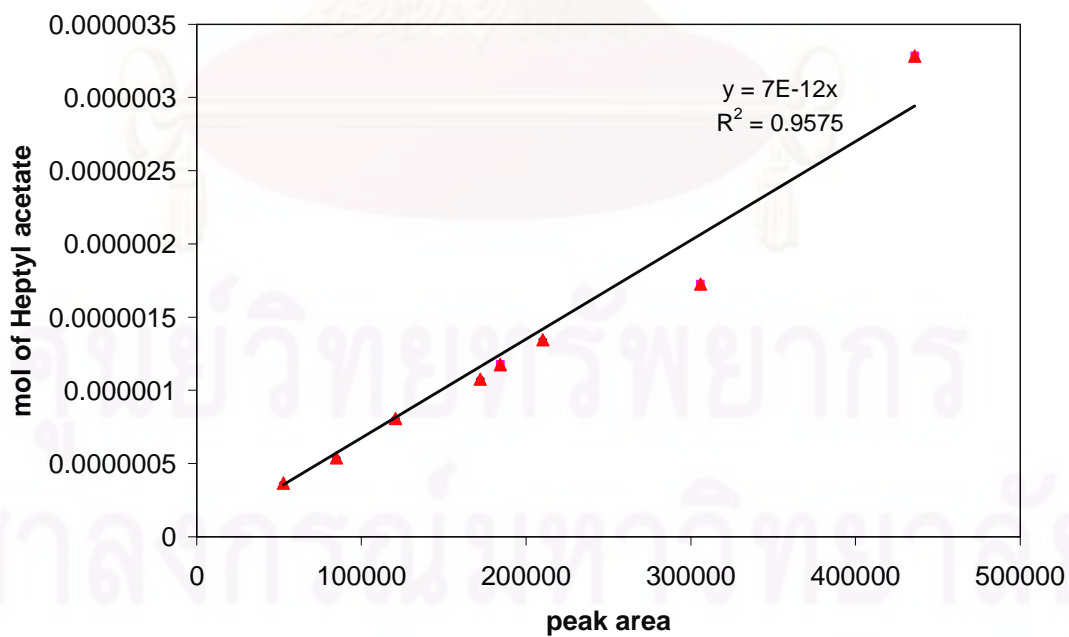


Figure F.6 The calibration curve of GL.

The calibration curve of heptyl acetate was used to calculate the catalytic performance for esterification of dilute acetic acid and 1-heptanol.



APPENDIX G

LIST OF PUBLICATIONS

1. Kanokwan Ngaosuwan, Edgar Lotero, Kaewta Suwannakarn, James G. Goodwin Jr., and Piyasan Prasertdam, Hydrolysis of Triglycerides Using Solid Acid Catalysts, *Ind. Eng. Chem. Res.*, (2009), 48, 4757–4767.
2. Kanokwan Ngaosuwan, Xunhua Mo, James G. Goodwin Jr., and Piyasan Prasertdam, Reaction Kinetics and Mechanisms for Hydrolysis and Transesterification of Triglycerides on Tungstated Zirconia, *Topics in Catalysis*, (in press).
3. Kanokwan Ngaosuwan, Bunjerd Jongsomjit, and Piyasan Prasertdam, The Role of Zirconia Surface on Catalytic Activity of Tungstated Zirconia via Two-phase Esterification of Acetic acid and 1-Heptanol, *Catal. Lett.*, (2009), Published online Nov, 03.

VITAE

Miss Kanokwan Ngaosuwan was born on 1st August 1977, in Uthaithani, Thailand, She received her Bachelor degree of Engineering with Chemical Engineering from Suranaree University of Technology, Nakornratchasima, Thailand in March, 1998 and her Master degree of Engineering with Chemical Engineering from Kasetsart University, Bangkok, Thailand in March 2001. She has been working at Rajamangala University of Technology Krungthep as a faculty in Chemical Engineering Department from November 2004 until present. Since June 1, 2006, she has been studying for her Doctoral degree of Engineering from Department of Chemical Engineering, Chulalongkorn Univerisity.



ศูนย์วิทยทรัพยากร
จุฬาลงกรณ์มหาวิทยาลัย